2010

Paleolimnological Reconstruction of Hydrologic Change in the Slave River and Great Slave Lake During the Past Millennium

Matthew Ennis
Wilfrid Laurier University

Your file Votre référence
ISBN: 978-0-494-75370-5
Our file Notre référence
ISBN: 978-0-494-75370-5

Paleolimnological reconstruction of hydrologic change in the Slave River and Great Slave Lake during the past millennium

By

Matthew Ennis

Honours Bachelor of Science, Wilfrid Laurier University, 2007

THESIS
Submitted to the Department of Geography and Environmental Studies
in partial fulfillment of the requirements
for the Master of Science degree
Wilfrid Laurier University
Waterloo, Ontario, Canada
2010

Abstract

The Slave River Delta (SRD), NWT, represents a pivotal node in the upper Mackenzie Basin watershed and is a productive northern wetland landscape with a rich natural and cultural heritage. Concerns over environmental consequences of natural and anthropogenic-driven decline in river discharge as well as climate variability have prompted hydroecological studies to improve understanding of how this ecosystem functions over time and space. However, long-term natural hydrological variability of the Slave River system is not well documented and needs to be further developed. In order to provide a temporal context for understanding and evaluating the impacts of climate variability and change and other stressors on Slave River discharge, multi-proxy paleolimnological analyses have been conducted to reconstruct a long-term record of hydrologic variability in the Slave River system. Study sites include two small closed-drainage lakes (GSL1, SD34) located near a former elevated strandline of Great Slave Lake and another lake (SR1) located upstream on an island in the Slave River.

Multi-proxy analysis of lake sediment cores collected from SD34, GSL1 and SR1 provided a ~1200-year record of water level variation for the Slave River and Great Slave Lake. Sediment composition and elemental and stable isotope geochemistry proved to be sensitive indicators of hydrologic change within the study basins. Interpretation of C/N ratios and $\delta^{13}C_{org}$ values from SD34, GSL1 and SR1 additionally indicated that conventional, straightforward interpretation of these commonly applied paleolimnological measurements is not always appropriate.

Prior to the onset of the last millennium, during the Early Medieval period (MP), high C/N ratios, low $\delta^{18}O_{lw}$, high $\delta^{13}C_{org}$ and inorganic sediment indicated open-drainage

conditions caused by riverine inundation of both study lakes. River inundation of SD34 and GSL1 was attributed to Slave River discharge dominated by a large flashy spring freshet and high ice-jam flood frequency.

The percent organic carbon, organic nitrogen, $\delta^{15}N$, C/N ratios, $\delta^{18}O_{lw}$ values and $\delta^{13}C_{org}$ values appear to indicate isolation of SD34 and GSL1 from the Slave River at ~1000 AD and ~1150 AD, respectively. However, reduced ice-jam flood frequency in the SRD precedes a similar change in the upstream Peace-Athabasca Delta (PAD) by ~400 years. A change in the distributary network of the SRD and low Slave River discharge may account for the ~400 year offset and explain why SD34 and GSL1 became isolated from ice-jam flooding during the Middle MP, when ice-jam flood frequency was high in the PAD.

The interval of low Slave River discharge suggested by SD34 and GSL1 sediment records appeared to end at ~1300 AD with the re-emergence of open-drainage conditions in SD34 indicated by high $\delta^{13}C_{org}$ values. Open-drainage conditions at SD34 spanned the Late MP and were attributed to high Slave River discharge that is consistent with an interval of high North Saskatchewan River discharge.

The SR1 C/N record indicated that high Late MP Slave River discharge continued throughout the Little Ice Age (LIA). High LIA Slave River discharge was attributed to a delay in snowmelt-generated runoff that sustained higher summer river discharge as a result of a shift to cooler climate conditions. High $\delta^{13}C_{org}$ values in the GSL1 record indicated open-drainage conditions in GSL1 throughout the LIA and $\delta^{18}O_{lw}$ values that were similar to modern Great Slave Lake (GSL) $\delta^{18}O_{lw}$ values suggested that the open-drainage conditions were the result of GSL inundation. Therefore, increased Slave River discharge appears to have caused high GSL water levels during the LIA, similar to that observed upstream in Lake Athabasca. High GSL water levels inundated GSL1 and likely occupied the strandline visible in the landscape to the south of the SRD.

At the beginning of the 20th century, the SR1, SD34 and GSL1 sediment records indicate closed-drainage conditions were established. Closed-drainage conditions at each study lake were attributed to a decline in water level within the Slave River system at the end of the LIA A 20th century decline in discharge parallels a shift to a warmer climate regime that has been shown to cause an earlier, more rapid melt of the spring snowpack in the headwaters of the Peace and Athabasca rivers. The sediment records of the three study lakes indicated that water levels within the Slave River system have declined from the high levels that characterized the LIA, falling to levels possibly similar to the MP. However, high $\delta^{18}O_{lw}$ values at GSL1, throughout the 20th century that are unique within the ~1200 record may suggest that present hydrological conditions at this site are unprecedented in the last ~1200 years.

These findings establish a link between hydrologic conditions within the Slave River system and those upstream in the PAD and Lake Athabasca. Sediment records from SD34, GSL1 and SR1 demonstrated that in the past ~400 years, the hydrology of the Slave River system responded similarly to the PAD in response to shifting climate regimes. This indicates that hydrologic change upstream in the headwaters of the Slave River has historically translated downstream to the SRD and GSL. Furthermore, these results show that water levels in the upper Mackenzie River system have varied considerably in the last ~1200 years and that they have been in decline over the last 200 years – a decline that is likely to continue given expected trajectories in river discharge.

Acknowledgements

I would like to thank my advisor Dr. Brent Wolfe for his time, patience, support and guidance which have been given from start to finish. Your passion for this work is contagious and has made the writing process much easier. I would also like to thank Brent for allowing me the opportunity to participate in field work outside the scope of my own project I would like to sincerely thank my co-advisor Dr. John Johnston for his time, patience and enthusiasm. Thank you for helping me think outside the box and for bringing a different perspective to the table that was always appreciated.

I am thankful to the following people for providing me with help and support during lab work and all other components of the thesis process: Dr. Brent Wolfe, Dr. John Johnston, Dr.Thomas Edwards, Dr. Roland Hall, Johan Wiklund, Bill Mark, Bronwyn Brock, Michelle Tai, Paige Harms, Caleb Light, Stephanie Lyons, Erin Dobson, Kevin Turner, Nick Sidhu and the rest of the MBD/NHL group. I would like to thank the following organizations for providing funding for fieldwork and analytical support: NSERC Northern Research Chair Program, Northern Scientific Training Program and the Polar Continental Shelf Program.

I would like to thank my family for all their support and encouragement. A special thank you to Suzanne Hatch for being there for me throughout the whole Masters process with continued support and encouragement. As well, an additional thank you to Caleb Light, Eric Thuss, Erin Dobson, Eric Sadowski and Andrea Kenward for "Wednesday Lunch Beers".

Table of Contents

List of Tables

List of Figures

Chapter 1- *Introduction*

1.1 Introduction

The Slave River Delta (SRD) (Figure 1) is located on the southeast shore of Great Slave Lake (GSL) at the terminus of the Slave River. The SRD is a productive northern wetland landscape, home to a variety of unique plant and animal assemblages (Milburn et al., 1999). Deltaic landscapes such as the SRD are ecologically significant because they are more productive than other components of northern river systems (Milburn et al., 1999). The SRD is also of great cultural importance to the Deninu Ku'e First Nation community of Fort Resolution who utilize natural resources in the delta to support and maintain traditional lifestyles (Wolfe et al., 2007a).

The Slave River is part of the upper Mackenzie River system and is sourced predominantly by the Peace and Athabasca rivers. There are several potential stressors on the Peace-Athabasca-Slave river system. The Peace River was regulated in 1968 by the construction of the WAC Bennett Dam at Hudson's Hope, British Columbia. Additionally, growing energy demand has led to increased interest in hydroelectric development on the Slave River near Fort Smith (Hannaford, 2008). Increasing water withdrawal from the Athabasca River for oil sands production has recently put additional stress on the river system (Campbell and Spitzer, 2007). As well, climate change in recent years has caused the recession of alpine glaciers and a decline of snowpacks (Schindler and Donahue, 2006). This has resulted in a reduction in source water entering alpine-sourced rivers systems such as the Peace-Athabasca-Slave river system. All of these factors potentially influence the flow of water in the Slave River, but how these changes in river discharge may affect the SRD is not fully understood.

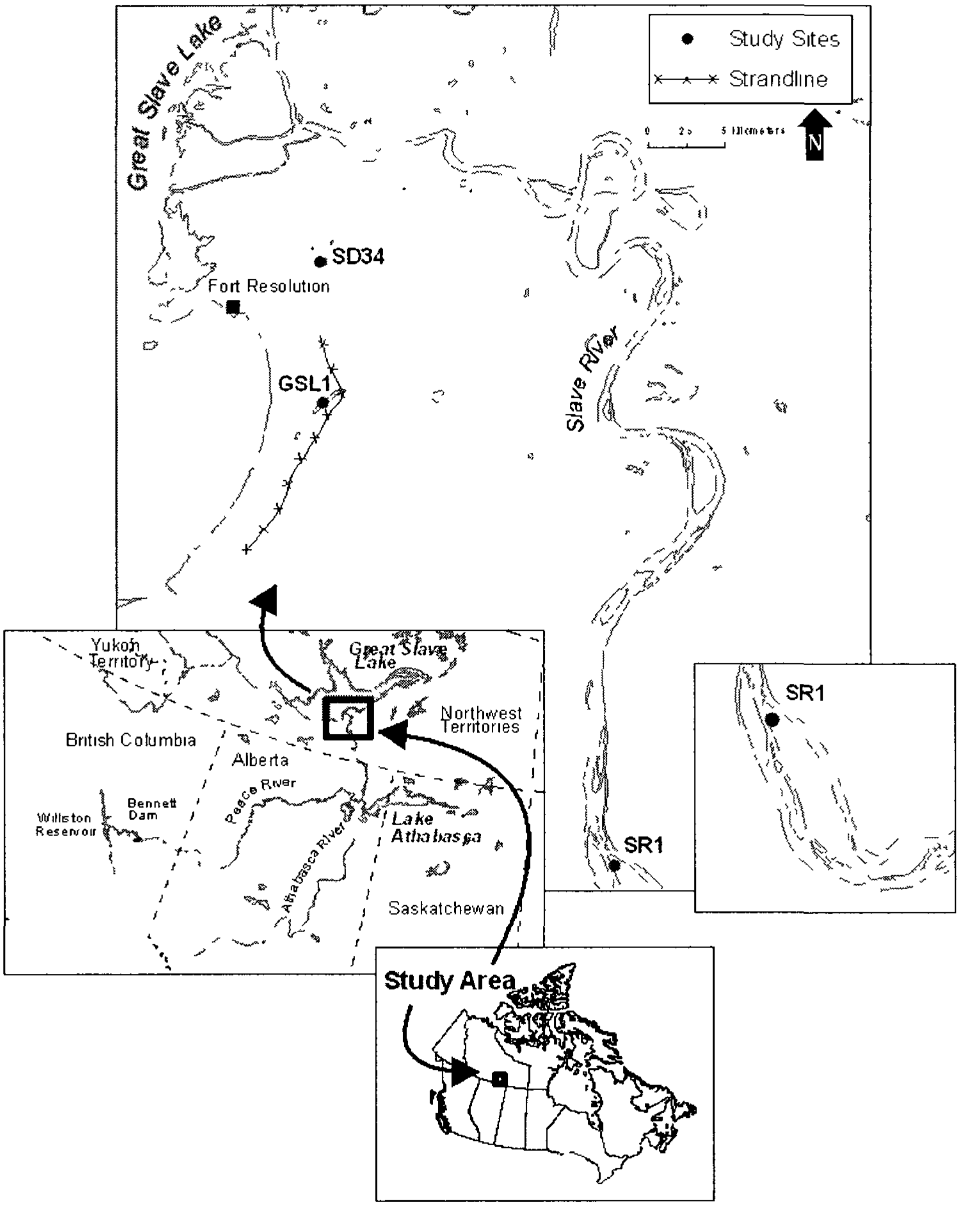

Figure 1 Slave River Delta and study lakes SR1, SD34 and GSL1 A former strandline of GSL visible in the landscape during the 2007 field season is also highlighted

The ability to predict future evolution of northern rivers is difficult because of a lack of long-term river and climate data for Canada's North (Rouse et al., 1997; Schindler and Donahue, 2006). The paucity of river gauging stations and short duration of available records provide limited insight into natural variability in discharge of northern river systems. Studies by Dery and Wood (2005) and Dery et al. (2009) have shown that hydrologic trends inferred from short-term records are susceptible to drastic change (reversal of trend) in response to fluctuating discharge over short periods of time. Longer hydrologic records than those available are then required to strengthen understanding of natural variability within northern river systems such as the Slave River. Long-term records of hydrologic variability within northern river systems would provide the knowledge required to make informed water resource management decisions (Sear and Arnell, 2006).

Extensive studies in the Peace-Athabasca Delta (PAD), upstream from the SRD by Wolfe et al. (2005, 2006, 2008a,b) have demonstrated the effectiveness of using multi-proxy paleolimnological reconstruction as a tool for developing long-term hydrologic records to supplement sparse discharge data for a northern river system. Wolfe et al. (2005, 2006, 2008a,b) analyzed sediment cores from several PAD lakes in response to reports of less frequent and extensive spring flooding, declining lake levels and loss of wildlife habitat since the regulation of the Peace River (at the WAC Bennett Dam). These studies aimed to distinguish the effects of multiple stressors on the hydrological regime of a northern river system and to provide temporal context for the evaluation of causes affecting contemporary hydrological change. Results have indicated that the drying of PAD lakes can occur at a variety of time scales in the absence of spring river flooding.

Some lakes may last decades without the input of river water and others may dry up within years (Wolfe at al., 2005; Peters et al., 2006). Wolfe et al. (2006, 2008a) also indicate that river flooding over the last several centuries has oscillated between multi-decadal intervals of both high and low flood frequency, suggesting significant natural variability in spring river flood frequency. As well, the most recent interval of low flood frequency in the PAD began several decades before the construction of the WAC Bennett Dam (Wolfe et al., 2006). Wolfe et al. (2008a,b) suggesting that changes in headwater climate and local geomorphic changes in Athabasca River flow appear to be the dominant drivers of river discharge and flooding in the PAD.

Using reconstructions of winter temperature and growth season relative humidity in the Columbia Icefield based on isotope analysis of tree-ring records, Edwards et al. (2008) described past climate of the eastern Rocky Mountains in the headwaters of the Athabasca River. During the past millennium, the upper Mackenzie River system has been characterized by a three-phase climate history, which includes the Medieval Period (MP) (AD ~1000 to ~1530), Little Ice Age (LIA) (AD ~1530 to ~1890) and 20th century. The climate of the MP consisted of relatively warm winters and higher relative humidity during the growth season and the LIA was characterized by a transition to colder temperatures and low growth season relative humidity (Edwards et al., 2008). Since the end of the LIA, temperature and relative humidity have increased and the climate reconstruction suggests that conditions may be returning to those similar to the early millennium.

Wolfe et al. (2008a), Sinnatamby et al. (2010) and Johnston et al. (2010) have demonstrated significant variability in discharge within the Peace-Athabasca river system over the last 1000 years in response to the changing climate patterns in the eastern Rocky Mountains outlined by Edwards et al. (2008). For instance, water levels in Lake Athabasca increased from a low at the onset of the millennium (MP) to a high during the LIA (Wolfe et al., 2008a; Sinnatamby et al., 2010; Johnston et al., 2010). Lake level variation over this period has been influenced by changes in summer discharge through the Peace-Athabasca river system. During the MP, warmer temperatures caused an earlier spring melt in headwater regions and a "flashy" spring freshet, which resulted in frequent, high-magnitude ice-jam flood events but low summer discharge and low Lake Athabasca water levels (Figure 2). During the LIA, colder temperatures delayed the spring melt in the Peace-Athabasca headwater regions, resulting in sustained high summer discharge that raised Lake Athabasca water levels ~2.3 m above contemporary levels (Wolfe et al., 2008a; Sinnatamby et al., 2010; Johnston et al., 2010) (Figure 2).

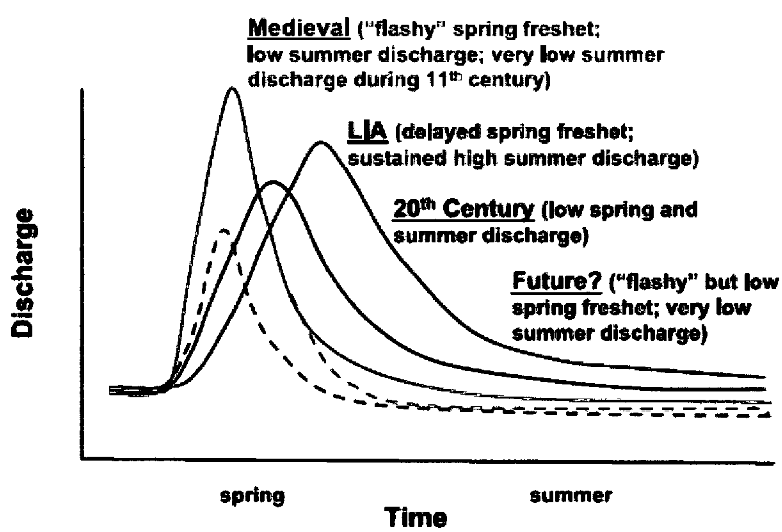

Figure 2. Reconstructed and projected hydrographs for rivers draining the hydrographic apex of North America (Wolfe et al., 2008a).

Since the end of the LIA (~1900 AD), river discharge in the Peace-Athabasca river system has been in decline causing Lake Athabasca water levels to decrease (Wolfe et al., 2008a). If current trends of decreasing discharge persist, summer discharge in the Peace-Athabasca river system may fall below the low levels reconstructed for the 11^{th} century (Figure 2). Lake Athabasca and GSL are both natural reservoirs in the same river system and their water levels have been shown to respond comparably during wet and dry years (Bennett, 1970). As a result, it is likely that in the past millennium GSL has experienced periods of high and low water level similar to those documented by Wolfe et al. (2008a), Sinnatamby et al. (2010), and Johnston et al. (2010) for Lake Athabasca. Evidence of fluctuating Great Slave Lake water levels similar to Lake Athabasca would provide new insight into the natural forcing factors that contribute to variability in Slave River discharge.

While there has been extensive study upstream in the PAD and Lake Athabasca, a long-term record of Slave River hydrologic variability is lacking. Using multi-proxy paleolimnological methods, Brock et al. (2010) were able to supplement the 47-year gauged record of the Slave River by generating an 80-year record of flood frequency for an SRD lake. The 80-year record indicates flood frequency was lowest prior to upstream river regulation and that the onset of river regulation coincided with a period of increased flood frequency. Changes in flood frequency at the SRD, as determined by Brock et al. (2010), paralleled those observed in the flood frequency records developed by Wolfe et al. (2006) for the PAD, suggesting climate is the dominant driver of change in runoff regime for both the SRD and PAD. However, the Brock et al. (2010) record is still relatively short and does not address long-term hydrologic variability in the Slave River system. A long-term record of hydrologic variability of the SRD would not only provide new insight to the relationship between the PAD and SRD (two large important wetland systems in the upper Mackenzie River Basin), but more importantly, would provide understanding of the Slave River system's response to a variable climate. Such knowledge is critical in establishing a historical context of natural hydrologic variability within the Slave River system A context of natural variability coupled with an understanding of the relationship between climate and river discharge is critical for making informed management decisions. The importance of informed management of the Slave River system may be amplified in the near future as discharge through the system is expected to decline as a result of declining glacier melt contributions and snow pack runoff in headwater regions (Barnett et al., 2005, Lapp et al., 2005, Rood et al., 2005).

1.2 Objectives

The objective of this study is to establish a long-term hydrologic record for the Slave River and gain a better understanding of the relationship between climate variation over the past 1200 years and Slave River hydrology. Such a record would extend beyond the instrumental records (47 years) of the Slave River and the flood frequency record established by Brock et al. (2010) (~80 years). Research questions that multi-proxy geochemical analyses will address include: 1) How has Slave River discharge changed over the past millennium and what is its relationship to climate? 2) How does variation in Slave River discharge compare to paleohydrological records of the upstream PAD? and 3) Does the postulated strandline south of the SRD observed during field study in March 2007 (Figure 3) correspond to a GSL high-stand during the LIA similar to the high-stand of Lake Athabasca documented by Sinnatamby et al. (2010) and Johnston et al. (2010)? Information gained here regarding the relationships between climate and discharge as well as the Slave River and PAD can be used to inform water resource management within the upper Mackenzie River basin.

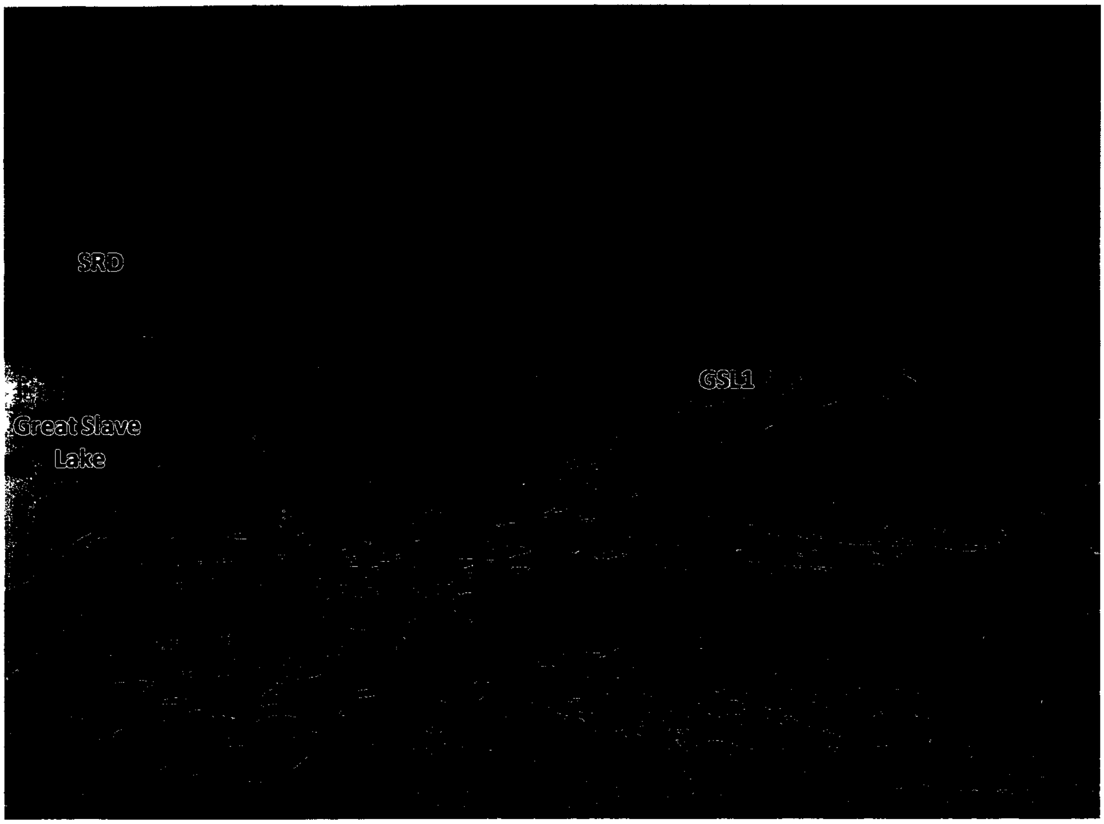

Figure 3. Possible strandline of Great Slave Lake is shown by dashed line. The relict river channel GSL1 terminating at the potential shoreline is also indicated (photo taken March 2007, facing north).

Chapter 2 – *Study Site*

2.1 Slave River-Great Slave Lake System

The Slave River flows through relict deltaic and alluvial sediments, deposited after the retreat of the Keewatin Ice Sheet. The Slave River and GSL are located within former Glacial Lake McConnell. Outflow and glacial isostatic adjustment resulted in Lake McConnell draining by 8300 BP (Vanderburgh and Smith, 1988) leaving present-day Lake Athabasca, GSL and Great Bear Lake as remnants of the second largest glacial lake in North America. Observations of the landscape surrounding GSL have indicated that lake water levels have declined more then 90 m from early post-glacial conditions (Rawson, 1950). Since the draining of Glacial Lake McConnell, sediment carried by the Slave River has been deposited in the southern arm of GSL forming the SRD. Since 1180 ^{14}C yr BP, progradation of the delta has occurred at an average rate of 10 m per year, and the relict delta now covers an area of ~8300 km^2 (Vanderburgh and Smith., 1988). Currently, only about 5% of the SRD is actively prograding and at a much slower rate than the historical average (Vanderburgh and Smith, 1988).

The Slave River flows for 420 km north from its origin at the confluence of the Peace River and Rivière des Rochers in the Peace-Athabasca Delta (PAD). The channel remains relatively straight for the majority of its length, but as it nears the SRD, meander bends and island bar complexes become more prevalent (Figure 1). The Peace River contributes ~66% of the flow to the Slave River (English et al., 1997) with the bulk of remaining water input supplied by the Athabasca River and Lake Athabasca. The Slave

River terminates at the SRD, and accounts for the majority of annual water input to GSL, a primary source of water for the Mackenzie River.

The Peace-Athabasca-Slave system drains approximately 615,000 km^2 and discharges at an annual rate of ~3,400 m^3/s into GSL (Prowse et al., 2002), accounting for ~75% of total inflow to the lake (Gibson et al., 2006a). GSL occupies ~27,200 km^2 with a maximum length of 440 km and width of 160 km and has a total volume of ~$1.58x10^{12}$ m^3 (Rawson, 1950). The mean water level of GSL (from 1939-99) is approximately 166.60 ± 0.22 masl. However, there is considerable variability in lake level, both annually and interannually, with an historical annual range of ~1.2 m (Gibson, 2006b). The water balance of GSL is dominated by river flow, accounting for 95% of the input and 93% of the output. As a result, the water level of GSL is subject to both seasonal and annual fluctuations driven predominantly by variation in Slave River discharge (Rawson, 1950). Maximum water levels occur in late May and early June corresponding to peak river flow and minimum levels occur in April when Slave River discharge is lowest (Gibson et al., 2006b). Fluctuations of inflow to the Slave River from headwater regions in the eastern Rocky Mountains have been shown to influence the instrumental (~past 50 years) water balance of GSL (Gibson et al., 2006b). High (low) water levels within GSL correspond to increased (decreased) discharge through the Peace-Athabasca-Slave system (Gibson et al., 2006a). This indicates that a longer record of GSL water level change would be useful for identifying climatic and hydrologic variability within the upper Mackenzie River system (including the SRD).

The SRD contains a variety of small lakes and wetlands, spanning a range of hydrological settings. SRD lakes were classified based on the dominant process affecting their water balances during the 2003 thaw season (Brock et al., 2007). SRD lakes were classified as evaporation-, flood- or exchange-dominated. Evaporation-dominated lakes have water balances controlled by snowmelt in the spring followed by evaporation and precipitation during the summer months and are generally not affected by river flooding during the spring melt. The water balance of exchange-dominated lakes is variable throughout the thaw season and depends mainly on the strength of seiche events on GSL or Slave River inflow. Flood-dominated lakes have water balances that are largely controlled by river flooding during the spring break-up. Spring break-up flooding is important in a northern delta such as the SRD because it provides water to lakes otherwise isolated from the main drainage network of the Slave River (Brock et al., 2007, 2008; Sokal et al., 2008). The pulses of water from spring break-up flooding replenish water levels and introduce sediment to lake beds (Milburn et al., 1999; Rouse et al., 2007). The occurrence and magnitude of flooding in the SRD depends predominantly on the amount of Slave River discharge during the spring breakup (Brock et al., 2008). Because Slave River discharge is dependent on snow accumulation and rate of melt in its source regions, changes in upstream hydrologic conditions can have significant influence downstream in the lakes of the SRD (Brock et al., 2008).

2.2 Study Basins

Multi-proxy paleolimnological analyses were conducted on sediment cores retrieved from three study basins: SR1 (Figure 1, 4, 5), GSL1 (Figure 1, 6) and SD34 (Figure 1, 7) to gain insight into multi-centennial hydrologic change in the Slave River system. SR1 was chosen because it is located upstream from the SRD and was expected to provide a record of Slave River water level outside of the active delta and SD34 was chosen because it was anticipated to record high Slave River water levels within the contemporary delta. GSL1 is located outside of the active delta, adjacent to a strandline south of the SRD (Figure 3) and was chosen because it was expected to provide a record of high GSL water levels. All three basins are currently isolated from hydrological influence of the Slave River and GSL.

2 2 1 SR1 (60° 48'09 7'' N, 113° 13'33 9'' W)

SR1 is a small basin (~100 m in length) that at the time of coring (March 24, 2007) was ~90 cm deep (Figure 4, 5). This basin is located on a large island (~10 km long and ~1.5 km wide) on the Slave River, ~60 km upstream from the SRD. The island has no evidence of recent flooding and the basin is surrounded by mature spruce forest, with no evidence of inflow or outflow channels (Figure 4, 5). It is expected that SR1 would only experience flooding during periods of Slave River discharge higher than the present.

Figure 4. SR1 (March 2007, facing north).

Figure 5. SR1 (March 2007, facing north).

2.2.2 SD34 (61° 11'41" N, 113° 33'49" W)

SD34 (Figure 6) is located in the relict region of the SRD, ~6 km northeast of Fort Resolution. The lake is kidney-shaped with a maximum length of ~600 m and is less than 2 m at its deepest point. The lake appears to be located at an elevation of ~159 metres above sea level (masl) (Figure 7). SD34 contains no inflow or outflow channels. Presently, the lake is isolated from the Slave River and its distributaries and is not flooded by river water during the spring break-up, even during large spring break-up floods like that of 2005 (Brock et al., 2008). SD34 was classified as an evaporation-dominated basin by Brock et al. (2007).

Figure 6. SD34 (May 2005, facing east)

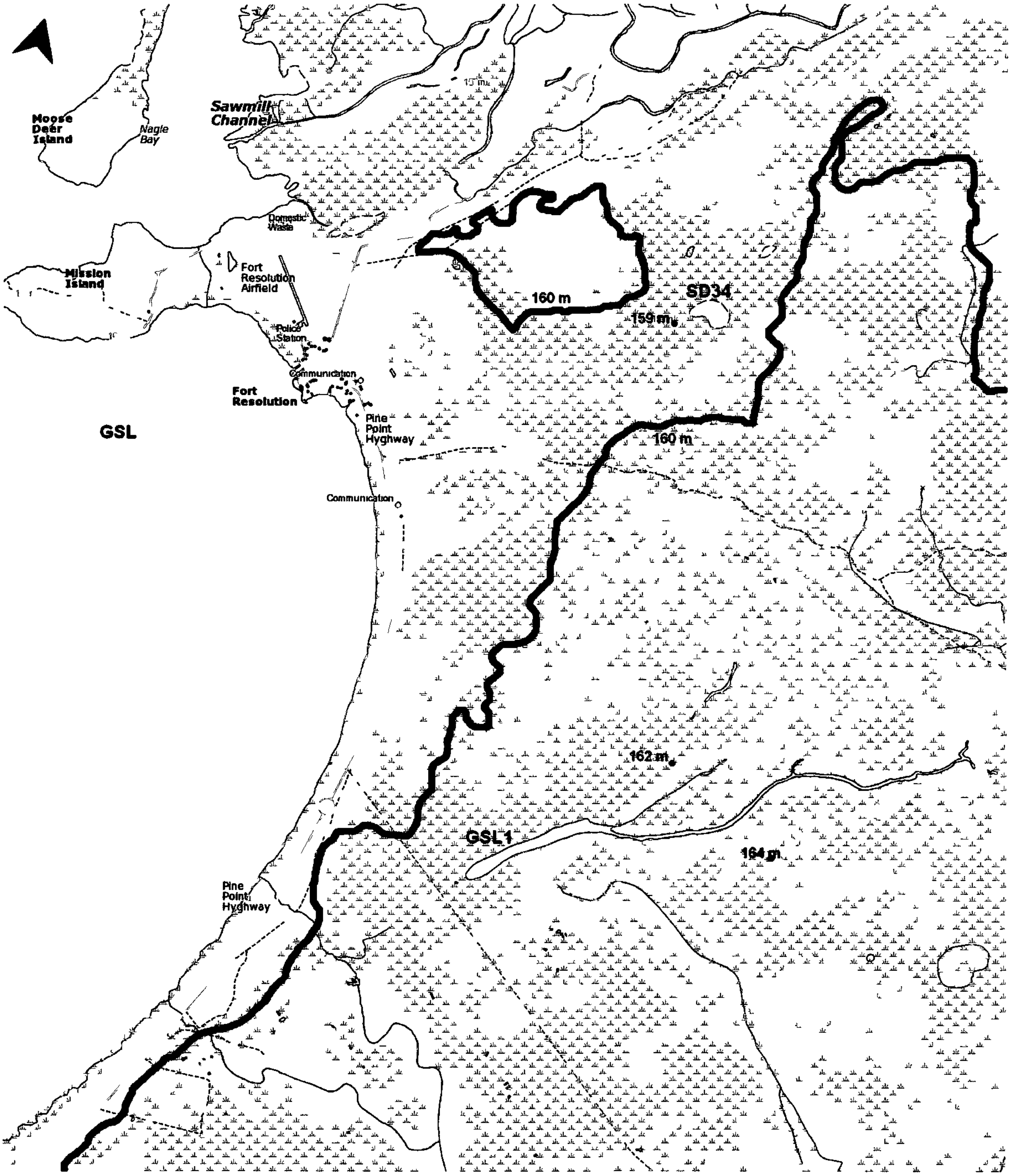

Figure 7. Topographic map of SRD area including GSL1 and SD34 (Atlas of Canada, 2006). 160 m contour lines are indicated by thick black line, spot elevations in close proximity to GSL1 and SD34 are also highlighted. Elevation of GSL1 is approximated to be between 161 masl to 163 masl based on spot elevations in the vicinity of the lake and the proximity of the lake to 160 masl contour line. Elevation of SD34 is approximated to be 159 masl based on its location between two 160 masl contour lines and its close proximity to a 159 masl spot elevation.

2.2.3 GSL1 (61° 11'41'' N, 113° 33'49'' W)

GSL1 is the terminal end of a relict river channel that was likely a former distributary channel of the Slave River (Figure 8). It is located ~2.5 km east of the current GSL shoreline and ~8 km southeast of Fort Resolution (Figure 1). The main body of the basin is shallow (< 2 m deep) and has a length of ~2 km and width of ~150 m. The elevation of GSL1 appears to be between ~161-163 masl (Figure 7), ~3.6-5.6 m higher in elevation than the highest gauged GSL water level (157.23 masl) (Gibson, 2006b). Currently, the lake is located outside the range of contemporary river flooding (see Brock et al., 2008). However, a possible former strandline of GSL observed near this site during field study in March 2007 suggests the area may have been flooded during a high-stand of GSL (Figure 9). The strandline is marked by a change in the spatial distribution of lakes and the termination of several relict river channels (such as GSL1) (Figure 9). A greater concentration of lakes likely indicates poorer drainage on the GSL side of the strandline.

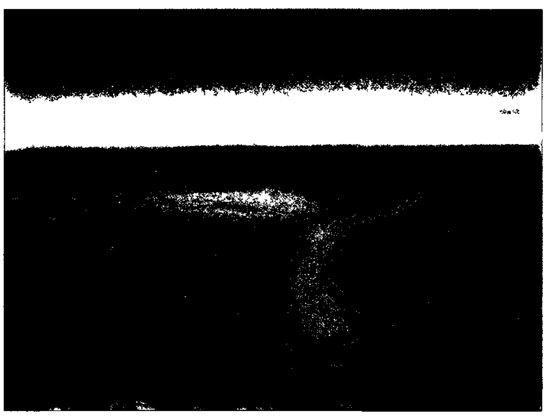

Figure 8. GSL1 (March 2007, facing northeast).

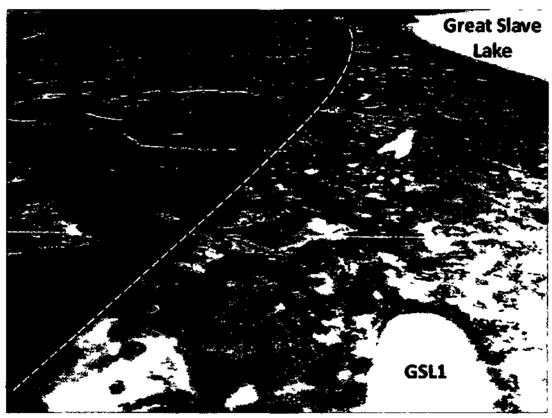

Figure 9. GSL strandline (March 2007, facing south).

Chapter 3 – *Field and Laboratory Methods*

3.1 Retrieval of Sediment Cores

Lake sediment cores were collected for each study lake (SD34, GSL1 and SR1) through lake ice in March 2007 using gravity and Russian peat corers. Gravity cores were collected using a Glew gravity corer, driving a tube (open at both top and bottom) vertically into the lake sediment using gravity (Glew et al., 1989). The cores were then sectioned into 0.5-cm intervals at the field station. The Russian peat coring process involved the use of a chamber corer. In the closed position, the chamber corer was driven vertically into the sediment with drive rods. While maintaining its vertical orientation, the corer was then rotated capturing the sediment within the chamber and the Russian peat corer was then removed (Glew et al., 2001). Russian cores were then sectioned into 0.5-cm intervals in the laboratory at Wilfrid Laurier University. The combination of gravity and Russian cores is effective for providing a sedimentary record for the recent past because the gravity core preserves the integrity of the uppermost sediment sequence and the Russian corer can penetrate more deeply than the gravity corer, extending the sediment record.

Several cores were taken from each study lake (Table 1 and 2). Gravity cores were denoted KB and Russian cores were denoted RC. Depths and names of all cores taken are presented in Table 1. For SR1, the KB-2 core was used for analysis because it had a more defined sediment-water interface than KB-1, indicating that the uppermost sediments had been less disturbed during the core retrieval process. For SD34, the KB-2 core had a better defined sediment-water interface than KB-1 and was used for analysis. Two RC cores were also taken from SD34. SD34 RC-2 was used for analysis because it appeared to have preserved a greater amount of the uppermost sediment than RC-1. One of each core type was taken from GSL1 and as a result KB-1 and RC-1 cores were used for analysis. Russian cores from SD34 (SD34 RC-2) and GSL1 (GSL1 RC-1) were aligned to their corresponding gravity cores (SD34 KB-2 and GSL1 KB-1) using percent organic matter values. Once aligned, the Russian core depths were adjusted to account for missing surface sediment.

Table 1 Summary of gravity cores

Study Lake	Coring Date (2007)	Gravity Core Name	KB Core Depth (cm)
SR1	March 24	SR1 KB-1	54.0
SR1	March 24	SR1 KB-2	39.5
SD34	March 24	SD34 KB-1	36 5
SD34	March 24	SD34 KB-2	38.0
GSL1	March 25	GSL1 KB-1	26.5

Table 2 Summary of Russian cores

Study Lake	Russian Core Name	RC Core Depth (Field Measurement) (cm)	RC Core Depth (Adjusted in Lab) (cm)
SR1	SR1 RC-1	4 - 100	Not analyzed
SD34	SD34 RC-1	7 - 54	Not analyzed
SD34	SD34 RC-2	0 - 66	4 5 - 75.5
GSL1	GSL1 RC-1	0 - 95	0 5 - 100

3.2 Laboratory Methods

3.2.1 Loss-on-Ignition Analysis

Loss-on-ignition (LOI) is frequently used to determine moisture content, bulk organic matter content and inorganic content of lake sediment (Dean, 1974; Heiri et al, 2001). Organic content profiles are of greatest interest to this study as they can potentially reveal patterns and trends in lake productivity, organic matter diagenesis and terrestrial organic matter and inorganic matter inputs over time. Additionally, in order to establish a continuous stratigraphic record for SD34 and GSL1, LOI results were used to align the gravity and Russian cores.

LOI was conducted at 0.5-cm intervals on samples from SR1 KB-2 (0 cm to 39.5 cm), SD34 KB-2 (0 cm to 38.0 cm), SD34 RC-2 (4.5-cm to 75.5-cm), GSL1 KB-1 (0 cm to 26.5 cm) and GSL1 RC-1 (0.5 cm to 43.5 cm). Wet sediment samples from each interval (approximately 0.5 grams) were weighed before and after heating at 90°C, 550°C and 950°C. The weight loss during each temperature stage was measured and provides an estimate of the water content (1), organic matter content (2), mineral content (3) and carbonate content (4) of the sediment samples.

(1) Water content, $LOI_{90} = ((WW - DW_{90}/WW)*100$
(2) Organic matter content, $LOI_{550} = ((DW_{90} - DW_{550})/DW_{90})*100$
(3) Mineral matter content, $LOI_{950} = ((DW_{90} - DW_{950})/DW_{90})*100$
(4) Carbonate content, $\%CaCO_3 = (LOI_{950}/0.44)$

*WW wet weight of sample, before heating to 90°C
DW dry weight of sample, after heating to 90°C
(Heiri et al., 2001).

3.2.2 Sediment Chronology

A ^{210}Pb-based sediment chronology was developed for each study lake. Total ^{210}Pb activity is a measure of both unsupported ^{210}Pb, the result of atmospheric fallout, and supported ^{210}Pb, which occurs naturally within the sediment column as the result of in situ ^{226}Ra decay (Appleby, 2001). Supported ^{210}Pb, in equilibrium with ^{226}Ra, can be subtracted from the total ^{210}Pb inventory, and the amount of unsupported ^{210}Pb can then be determined. The unsupported ^{210}Pb value for each sediment interval can be used to determine the sediment age using the radioactive decay of ^{210}Pb (22.26 yrs), to produce a chronology for the core over the period of time that unsupported ^{210}Pb is present (~150 years) (Appleby, 2001). The Constant Rate of Supply (CRS) model (Appleby, 2001) assumes a constant flux of ^{210}Pb to the sediment, independent of changes in sedimentation rates, was used to establish the core chronologies.

The peak activity of ^{137}Cs, usually reported as 1963, can also provide a stratigraphic marker for sediment chronologies (Appleby, 2001) and was measured using gamma spectrometry. ^{137}Cs values may peak at 1963 in stratigraphic records because this was when peak fallout occurred from above ground nuclear bomb testing, which released ^{137}Cs into the atmosphere.

^{210}Pb and ^{137}Cs analysis were conducted on SR1 KB-2, SD34 KB-2 and GSL1 KB-1 because gravity cores preserve integrity of the uppermost sediment sequence. Preparation for dating required packing freeze-dried lake sediment samples into plastic tubes. Samples taken at 1-cm intervals (from 0-cm to 40-cm for SR1 KB-2, 0-cm to 36.5-cm for SD34 KB-2 and 0.5-cm to 26.5-cm for GSL1 KB-1) were prepared for each study lake. After packing, the sediment in the tube was sealed with epoxy and submitted to the

University of Waterloo Environmental Change Laboratory (WATER) for ^{210}Pb and ^{137}Cs analysis. Gamma spectrometry was used to measure the radioisotope activity needed for the development of the sediment chronologies. Values from samples measured in the gamma spectrometer were coupled with interpolated values to calculate CRS dates for every sample where unsupported ^{210}Pb was present in SR1 KB-2, SD34 KB-2 and GSL1 KB-1. The depth of supported ^{210}Pb was interpreted to be reached where ^{210}Pb values became relatively constant.

In order to constrain sediment chronologies of Russian cores that extend well below the ^{210}Pb chronology, radiocarbon dating ^{14}C was attempted. Radiocarbon (^{14}C) has a half-life of 5,568 years and is most often applied for age-dating up to 40,000 years. Lake sediments usually contain telmatic and limnic plant and animal debris that can be collected and dated in order to obtain age control on sedimentary sequences (Björk and Wohlfarth, 2001). For this study, plant macrofossils extracted from SD34 RC-2 at 45-cm and 54-cm core depth were radiocarbon-dated to constrain the sediment chronology below the ^{210}Pb dated interval.

3.2.3 Analysis of Organic Carbon and Nitrogen Content and Stable Isotope Composition

Organic carbon and nitrogen content and stable isotope composition were analysed to reconstruct nutrient dynamics related to hydrologic variability in each study lake. Geochemical characterization of organic matter within lake sediment can reveal organic matter source and supply, cycling of nutrients, and lake productivity throughout time and thus is useful for reconstructing past environmental conditions within lakes (Meyers, 1997; Meyers and Teranes, 2000). The content and isotopic composition of organic carbon and nitrogen may also be strongly linked to hydrological processes as they have been successfully used in combination with other proxies to reconstruct long-term hydroecological change within the upper Mackenzie River Basin (Wolfe et al., 2008b; Brock et al , 2010; Johnston et al., 2010).

Percent total organic carbon (%C_{org}) describes the abundance of organic matter in lake sediments (Meyers and Teranes, 2001). However, only ~50% of lake sediment organic matter is composed of carbon, making the total organic matter roughly double the %C_{org} value (Meyers and Teranes, 2001). The %C_{org} value is a more sensitive proxy than total organic matter (determined through LOI) because total organic matter content can be inflated by variable amounts of volatile non-carbon components (Meyers and Teranes, 2001). Changes in %C_{org} within a sediment core can be associated with changes in primary productivity, making it a useful proxy for inferring paleoenvironmental change (Meyers and Teranes, 2001).

Total nitrogen content (%N) includes the measurement of both inorganic and organic nitrogen in lake sediment (Talbot, 2001). Nitrogen is an important nutrient for organic productivity. Additionally, nitrogen can act as the limiting nutrient for organic productivity in lakes, meaning changes in lake organic matter production and composition can be influenced by the source and cycling of nitrogen (Talbot, 2001). However, determination of bulk nitrogen by an elemental analyzer does not separate organic and inorganic nitrogen. Inorganic nitrogen typically represents a small fraction of total nitrogen in lake sediments, but can represent a larger proportion of total nitrogen in sediment with low organic content (Meyers, 1997). In such cases, the inorganic fraction can artificially depress the C/N ratio (Meyers, 1997).

Expressing lake sediment %C_{org} and %N values as a ratio (C/N) can indicate the relative contribution of organic matter from terrestrial (allochthonous) or aquatic (autochthonous) sources (Meyers and Teranes, 2001). Typically, organic matter that is aquatic in origin has C/N ratios that are low (4-10), whereas organic matter derived from (cellulose-rich, protein-poor) vascular land plants have high C/N ratios of >20 (Meyers and Teranes, 2001). However, algal growth under nitrogen-limiting conditions has been shown to cause elevated C/N values in highly productive basins (Meyers and Teranes, 2001).

The carbon isotope composition in the organic matter of lake sediments is an important proxy for assessing organic matter sources, reconstructing past productivity, and identifying changes in availability of nutrients in surface waters (Meyers and Teranes, 2001). Stable carbon isotope composition of lake sediment organic matter ($\delta^{13}C_{org}$) represents the $^{13}C/^{12}C$ ratio and provides an archive of catchment and within-lake processes (Meyers and Teranes, 2001). The carbon isotope composition of aquatic plants is primarily determined by the $\delta^{13}C$ of the dissolved inorganic carbon source ($\delta^{13}C_{DIC}$). Processes controlling the $\delta^{13}C_{DIC}$ composition include the source and supply of inorganic carbon (e.g., from catchment runoff), ^{13}C-enrichment from preferential uptake of ^{12}C by phytoplankton during photosynthesis, isotopic exchange with atmospheric CO_2, recycling of ^{13}C-depleted CO_2 from respiration/decay of water column and bottom sediment organic matter, and uptake of bicarbonate ($HCO_3^-{}_{(aq)}$) at elevated pH (Wolfe et al., 2000). Conventional interpretations typically attribute positive shifts in $\delta^{13}C_{org}$ to increases in aquatic productivity (McKenzie, 1985; Schelske and Hodell, 1991, 1995;

Meyers and Lallier-Verges, 1999). However, stratigraphic shifts in lake sediment $\delta^{13}C_{org}$ may also result from hydrologically-driven changes (Wolfe et al., 1999, 2000)

Nitrogen isotope composition ($\delta^{15}N$) is commonly used as an indicator of ecosystem productivity, nutrient availability, and the source of organic matter (Meyers, 1997; Talbot, 2001). Using $\delta^{15}N$ values to identify the source of organic matter is based on the difference between $^{15}N/^{14}N$ ratios of inorganic nitrogen available to plants in water and on land (Meyers and Teranes, 2001). A $\delta^{15}N$ signature depends predominantly on its source. Atmospheric N_2 fixed by blue-green algae produce a signature that is lower (0‰) than non-nitrogen fixing algae (7-10‰) (Meyers and Teranes, 2001). Despite this, interpretation of sedimentary $\delta^{15}N$ records is made more difficult than those of carbon, by the complicated dynamics of nitrogen biogeochemical cycling (Fogel and Cifuentes, 1993; Bernasconi et al., 1997; Hodell and Schelske, 1998; Brenner at al., 1999; Talbot, 2001)

In order to prepare sediment for organic carbon and nitrogen content and stable isotope analysis, samples taken at 0.5-cm intervals from SR1 KB-2 (0 cm – 40 cm), SD34 KB-2 (0 cm – 36.5 cm), SD34 RC-2 (4.5 cm – 75 cm), GSL1 KB-1 (0 cm – 26.5 cm) and GSL1 RC-1 (20 cm – 100 cm) were treated with a 10% HCl wash to dissolve carbonate and rinsed with deionized water to a neutral pH. Samples were then freeze-dried and dry-sieved through a 500-µm mesh to to remove coarse organic matter that may be of terrestrial origin. Organic carbon and nitrogen elemental and stable isotope compositions were measured on the fine fraction using a Continuous Flow Isotope Ratio Mass Spectrometer (CF-IRMS) at the University of Waterloo Environmental Isotope Laboratory (UW-EIL). Elemental organic carbon and nitrogen results are expressed in percent weight. Stable isotope results are expressed as deviations in per mil (‰) from a standard material. The organic carbon stable isotope composition ($\delta^{13}C$) is measured against Vienna Peedee Belemnite (VPDB) and the nitrogen stable isotope composition ($\delta^{15}N$) is measured against atmospheric nitrogen (AIR). Analytical uncertainties of $\%C_{org}$, %N, $\delta^{13}C$ and $\delta^{15}N$ for SR1 KB-2 are ±0.10%, ± 0.01%, ± 0.08‰ and ±0.01‰, respectively. Analytical uncertainties of $\%C_{org}$, %N, $\delta^{13}C$ and $\delta^{15}N$ for SD34 KB-2 and RC-2 (combined) are ±0.50%, ± 0.04%, ± 0.12‰ and ±0.11‰, respectively. Analytical uncertainties of $\%C_{org}$, %N, $\delta^{13}C$ and $\delta^{15}N$ for GSL1 KB-1 and RC-1 (combined) are ±0.50%, ± 0.10%, ± 0.05‰ and ±0.40‰, respectively. All analytical uncertainties are based on sample replicates.

3.2.4 Cellulose Oxygen Isotope Analyses

Oxygen isotope analysis of aquatic plant cellulose extracted from lake sediments can be used to reconstruct lake water oxygen isotope composition, a useful tracer of past hydrological conditions (Edwards and McAndrews, 1989; Edwards, 1993; Wolfe et al., 2001, 2007b). Cellulose is a bio-molecule that exists in the cell walls of plants and some algae and is preserved in sediments as algal cells within zooplankton fecal pellets, or as amorphous organic matter (Edwards, 1993). Aquatic cellulose incorporates the oxygen isotope composition of the lake water from which it is formed. The cellulose $\delta^{18}O$ can be used to reconstruct lake water oxygen-isotope history under the assumption that oxygen isotope fractionation between the lake water and cellulose is constant ($\alpha_{cell-lw} = 1.028$) and is independent of temperature and plant species (Wolfe et al., 2001).

Sediment from SD34 RC-2, GSL1 KB-1 and GSL1 RC-1 were analyzed for cellulose oxygen isotope composition Sediment from SR1 was not analyzed because it was determined that analysis of organic carbon and nitrogen content and stable isotope composition was sufficient for reconstructing past hydrological conditions. SD34 RC-2 was sampled at 0.5-cm resolution (4.5 cm – 75 cm) and GSL1 KB-1 (0 cm – 26.5 cm) and GSL1 RC-1 (27 cm – 100 cm) was sampled at 3.0-cm resolution. Cellulose extraction involved several steps (Wolfe et al., 2001, 2007b). Acid-washing to remove carbonate and sieving to separate coarse and fine fractions (see Analysis of Organic Carbon and Nitrogen Content and Stable Isotope Composition) were performed first. Solvent extraction, bleaching, and alkaline hydrolysis were performed on the fine fraction to remove non-cellulose organic material. Next, removal of iron and manganese oxyhydroxides was completed through hydroxylamine leaching, followed by heavy-liquid density separation using sodium polytungstate to separate the cellulose fraction from the minerogenic residue. Cellulose oxygen isotope composition was measured using standard methods (Wolfe et al., 2007b) by CF-IRMS at the UW-EIL. Oxygen isotope results were expressed as δ–values, which represent deviations in per mil (‰) from the Vienna-Standard Mean Ocean Water (VSMOW) standard for oxygen. Analytical uncertainties for SD34 RC-2, GSL1 KB-1 and GSL1 RC-1 were ±0.19‰, ±0.72‰, and ±0.43‰, respectively, based on sample replicates.

Chapter 4 - *Results and Interpretation*

4.1 SR1

4.1.1 Core Description

Visual observations of the SR1 KB-2 sediment core prior to field sectioning revealed two distinct units. The lower unit extended from the base of the core (39.5-cm depth) to 30.5-cm depth and consisted of inorganic-rich, light grey, silty clay sediment. No plant fibres were observed in these lower strata and LOI revealed high percent mineral matter (78.0% to 90.0%) and low organic matter content (8.1% to 18.7%) below 30.5-cm depth (Figure 10). At 30.5-cm depth there was an abrupt contact where sediment changed from light grey silty clay to dark brown organic sediment (Figure 10). A similar silty clay - organic contact was observed in the longer Russian core collected from SR1 (SR1 RC-1). The silty clay interval of the Russian core extended from the contact to the base of the core, indicating that this interval extended at least 57 cm below the base of SR1 KB-2. However, the Russian core was not used for analysis because SR1 KB-2 captured the sediment contact and the uppermost sediments extending to the sediment-water interface were obtained.

The upper strata in SR1 KB-2 consisted of dark brown organic sediment and extended from 30.5 cm – 0 cm. Organic matter content increased towards the top of the core from 19.1% to 30.1% and was higher than in the lower unit. The increase in organic content (Figure 10) was coupled with an increase in visible plant fibres towards the top of the core.

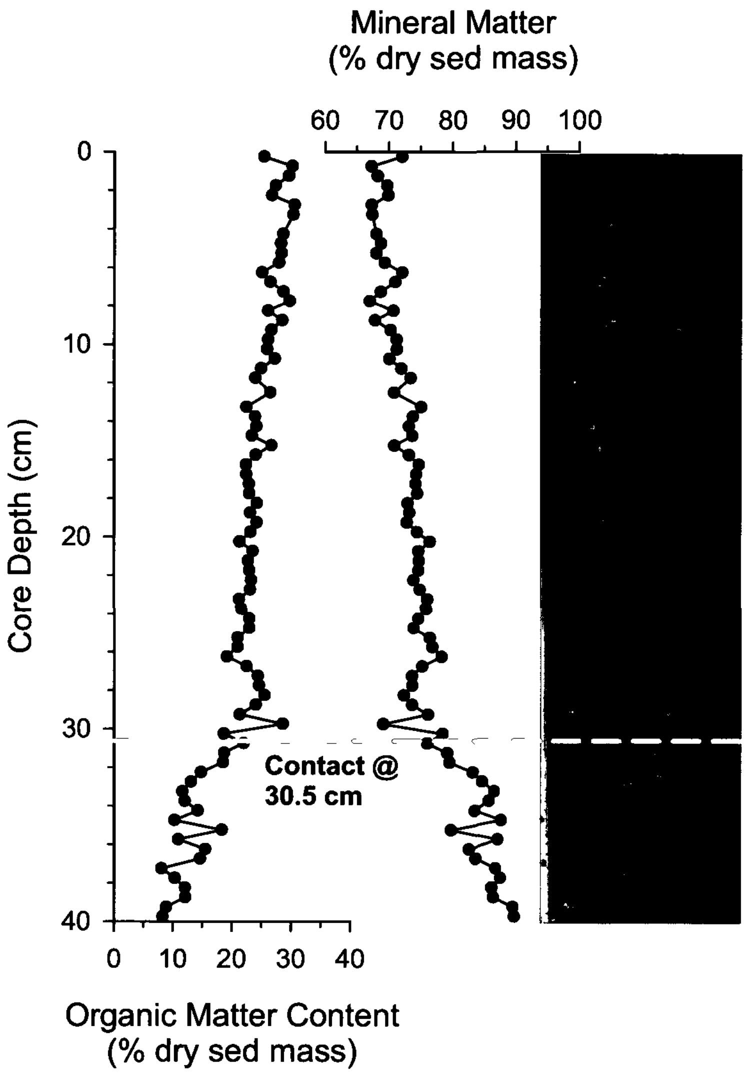

Figure 10. Organic matter content and mineral matter values from LOI analysis on SR1 KB-2. An image of SR1 RC-2 is scaled to fit the core depth of SR1 KB-2 in order to highlight the sediment contact at 30.5-cm core depth.

4.1.2 Sediment Core Chronology

Total ^{210}Pb activity for SR1 KB-2 ranged from 0.023 Bq/g to 0.134 Bq/g. Total ^{210}Pb activity peaked at 3.25-cm midpoint core depth (0.130 Bq/g) and then generally declined from 3.25-cm (0.101 Bq/g) to 15.25-cm (0.040 Bq/g) midpoint core depth (Figure 11a). From 15.25-cm to 39.25-cm, values became relatively constant, ranging from 0.023 Bq/g to 0.059 Bq/g. It was estimated that background (i.e., supported) ^{210}Pb levels were reached at approximately 15.25-cm midpoint depth (0.040 Bq/g) where total ^{210}Pb activity becomes relatively constant. This resulted in a basal Constant Rate of Supply (CRS) ^{210}Pb date of ~1792 AD at the 15.25-cm depth horizon (Figure 11a, b). SR1 KB-2 exhibited a well-defined ^{137}Cs peak that corresponded to a CRS ^{210}Pb date ~1963 AD at the 9.75-cm midpoint depth horizon (Figure 11a, b). The dating of the ^{137}Cs peak to ~1963 AD corresponds to the maximum ^{137}Cs fallout due to above-ground nuclear bomb testing. The dating of the ^{137}Cs peak to ~1963 AD and a ^{210}Pb background value of 0.040 Bq/g, similar to values determined for cores from the upstream PAD (Wolfe et al., 2005, 2008b) suggests that modeled CRS dates for SR1 KB-2 are robust. The mean sampling resolution for SR1 KB-2 for the CRS modeled dates is ~15.4 years per cm.

Sediment core chronology below unsupported ^{210}Pb levels in SR1 KB-2 was extrapolated using a linear regression of the cumulative dry mass and CRS modeled ^{210}Pb dates through the 0-cm to 14.25-cm interval. The 0-cm to 15.25-cm interval (where supported levels of ^{210}Pb were estimated to be reached) was not used to extrapolate dates down-core because samples from 14.75-cm and 15.25-cm midpoint depth spanned time intervals (~34 and 102 years, respectively) that were significantly larger than the average interval for CRS modeled dates above 14.25-cm midpoint depth (~3.0 years) and were most likely the result of the large peak in ^{210}Pb concentration observed at 15.25-cm depth. These values are likely over-estimated and were deemed less reliable. This resulted in a date of ~1784 AD at the observed sediment contact at 30.5 cm and a basal date of ~1546 AD (39.25-cm midpoint depth) for SR1 KB-2 (Figure 11b). Below the 30.5 cm horizon, there is marked change in the average resolution of extrapolated dates from 8.3 yrs/cm to 25.4 yrs/cm. A decrease in the resolution of extrapolated dates indicates a slower sedimentation rate below the sediment contact at 30.5-cm (Figure 11b). Because the extrapolation is based on CRS values from the organic sediment above the contact, there is less confidence in the chronology below the contact.

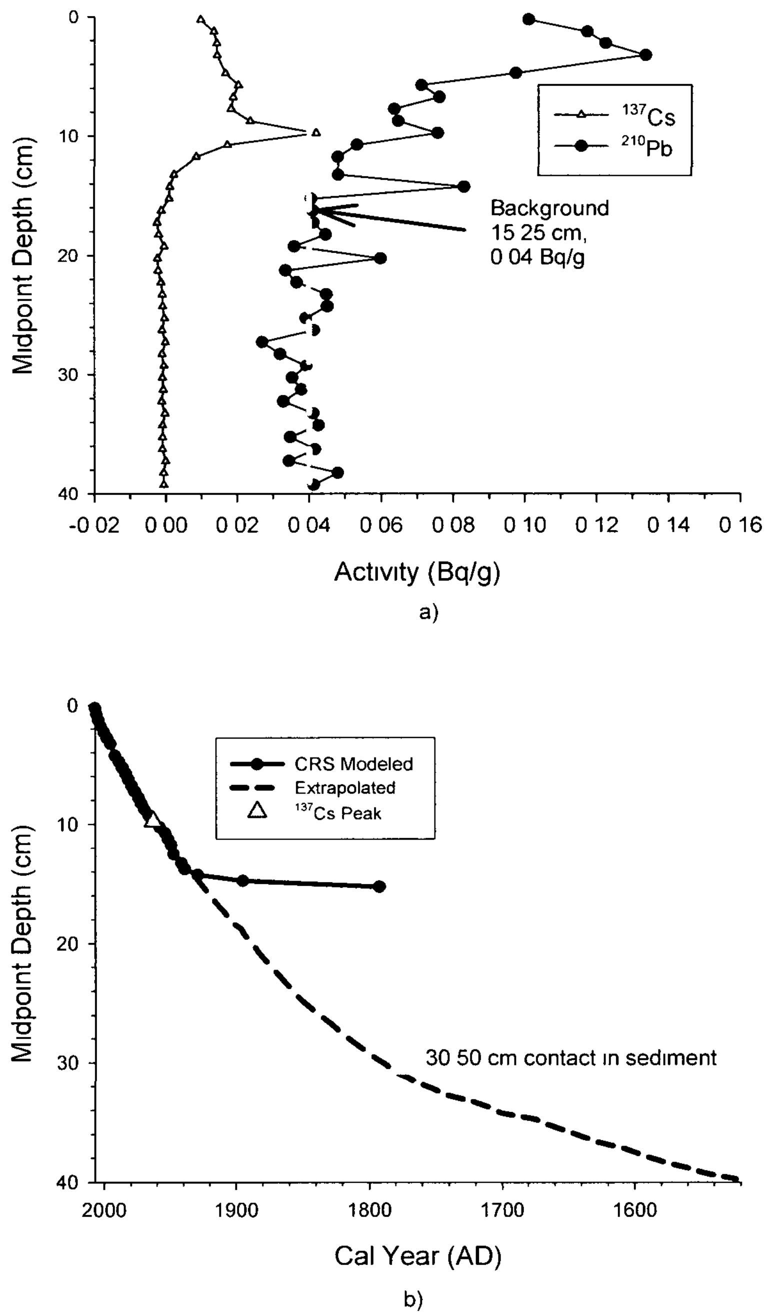

Figure 11 a) Activity profiles of ^{210}Pb and ^{137}Cs in Bq/g for SR1 KB-2 Dashed grey line denotes background levels of supported ^{210}Pb b) SR1 sediment core chronology based on the Constant Rate of Supply (CRS) model, extrapolated down core for KB-2 using a linear regression of cumulative dry mass and CRS dates through the 0 cm to 14 75-cm interval

4.1.3 Geochemical Stratigraphy

Assessment of the Inorganic Nitrogen Fraction: Correction for C/N Ratios

Evaluation of inorganic nitrogen is important because, if present, it can depress calculation of C/N ratios and lead to incorrect interpretations of this important metric. Talbot (2001) suggested that inorganic nitrogen can be detected by plotting percent nitrogen (on the y-axis) versus percent organic carbon (on the x-axis) and determining the y-intercept of the regression line. If the y-intercept of the regression line passes through the y-axis at a positive value, percent nitrogen is present in excess of percent organic carbon and the positive y-intercept value can be used as an estimate to correct for the presence of inorganic nitrogen. Because of the significant change in sediment composition at the visible contact in SR1 KB-2, values from above and below the contact were plotted separately to assess the presence of inorganic nitrogen. Above the visible contact (~1784 AD to ~2007 AD), the linear regression intercepts the x-axis indicating that organic carbon is present in excess of nitrogen and that bulk nitrogen values from this interval do not need correction. In contrast, below the visible sediment contact (~1546 AD to ~1784 AD), the linear regression intercepts the y-axis at 0.030% (Figure 11). The 95% confidence interval for ~1546 AD to ~1784 AD is relatively narrow and closely follows the regression line (Figure 12). Therefore, a correction factor of 0.030% was applied to bulk N values from this interval. The correction resulted in increases to C/N ratios below the contact ranging in value from 0.6 to 1.8. The entire corrected geochemical record is shown in Figure 13.

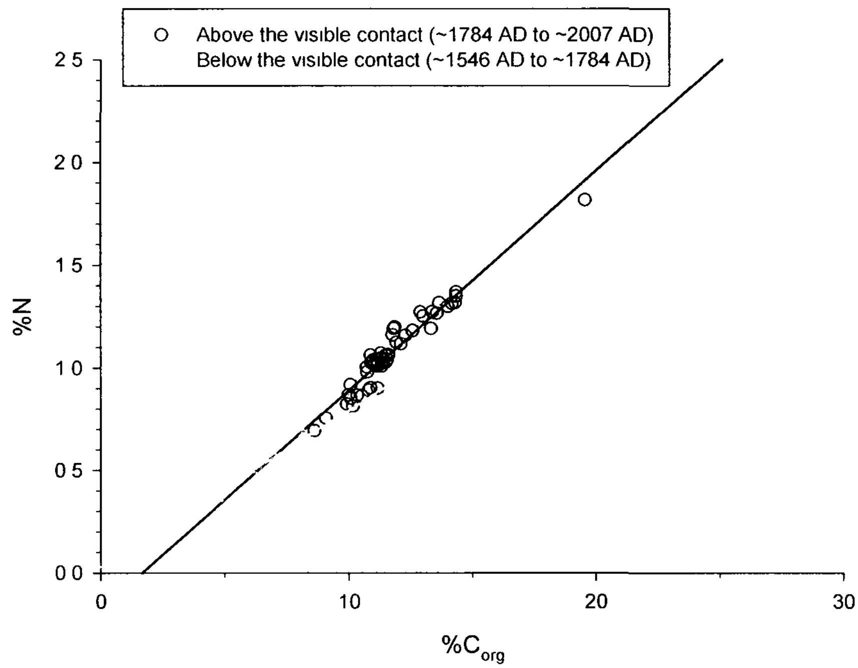

Figure 12 Percent nitrogen and percent organic carbon cross-plot of SR1 KB-2 Solid lines denote linear regression lines Note that for the interval below the visible contact (~1546 AD to ~1784 AD), the linear regression line intersects the y-axis The value of the y-intercept indicates the average amount of inorganic nitrogen for this interval (Talbot, 2001) Dotted lines denote the 95% confidence intervals for above and below the visible contact

Geochemical Results and Interpretation

Organic content and carbon and nitrogen elemental and stable isotope analysis have been used to identify four stratigraphic zones in the SR1 KB-2 sediment core (Figure 13). These zones were determined based on observed changes in the geochemical proxies. The transition from Zone 1 to 2 is based on changes in organic carbon, organic nitrogen, $\delta^{13}C_{org}$ and $\delta^{15}N$. The visible contact in the sediment was not used to establish Zone 2 because changes in most parameters occurred above this horizon. Zone 3 was established at changes in the trends of $\delta^{13}C_{org}$, $\delta^{15}N$ and C/N ratio and Zone 4 was based on a change in $\delta^{13}C_{org}$. These zones are described and interpreted below.

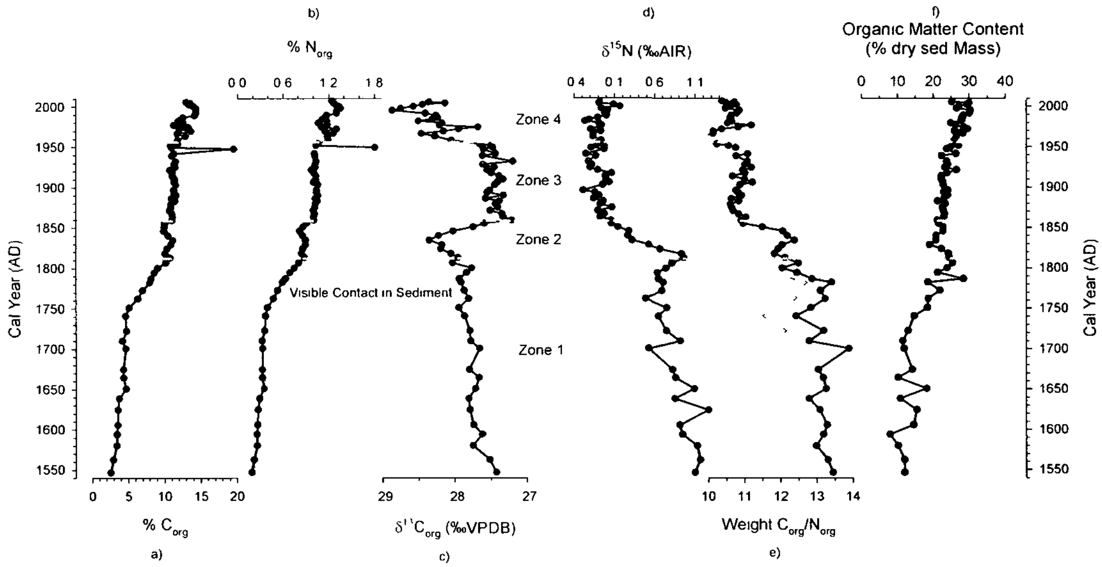

Figure 13 Geochemical records for SR1 KB-2 showing a) organic carbon content, b) organic nitrogen content (light grey line denotes uncorrected values), c) $\delta^{13}C_{org}$, d) $\delta^{15}N$, e) C/N (dark grey line denotes values before N correction) and f) organic matter content Dashed lines distinguish different stratigraphic zones

Zone 1 (~1546 AD to ~1818 AD)

In Zone 1, organic matter content was relatively variable in comparison to higher in the core, and gradually increased from 8.1% to 28.6%. The organic carbon and nitrogen contents in Zone 1 were the lowest in the record ranging from 2.6% to 10.2% and 0.22% to 0.81%, respectively. Values showed little variability and increased slightly within the zone. $\delta^{13}C_{org}$ values ranged narrowly and declined within Zone 1 from -28.0‰ to -27.4‰. $\delta^{15}N$ values ranged from 0.5‰ to 1.3‰ and were considerably more variable than $\delta^{15}N$ values in other zones. $\delta^{15}N$ values decreased slightly within Zone 1, but represented some of the highest values in the record. After correcting for the presence of inorganic nitrogen, the C/N ratios ranged from 11.4 to 13.9 and were among the most variable and highest in the record. C/N ratios increased gradually throughout Zone 1. The visible stratigraphic contact (30.5 cm) observed in the sediment was located near the top of Zone 1.

The high C/N ratios observed in Zone 1 may be associated with an allochthonous source of organic matter because they are slightly higher (>11) than values that are typically aquatic in origin (4-10) (Meyers and Teranes, 2001). High $\delta^{15}N$ values may also suggest a terrestrial supply of organic material as values in Zone 1 (0.5‰ to 1.3‰) are similar to the $\delta^{15}N$ signature of land plants (~0.5‰) (Meyers and Teranes, 2001). If the source of organic material to SR1 is indeed allochthonous, organic matter content, organic carbon content, organic nitrogen content and $\delta^{13}C_{org}$ values are representative of organic material from outside the basin and therefore, cannot be used as indicators of aquatic productivity within Zone 1.

Zone 2 (~1818 AD to ~1863 AD)

In Zone 2, organic matter content ranged from 19.1% to 24.4%. Values showed little variability and remained relatively constant within the zone. The organic carbon and nitrogen contents ranged narrowly from 10.1% to 11.2% and 0.82% to 0.90%, respectively. $\delta^{13}C_{org}$ values ranged from -28.4‰ to -27.7‰ in Zone 2 with little variability (similar to Zone 1). $\delta^{13}C_{org}$ values decreased steadily (from -27.9‰ to -28.3‰) until ~1848 AD at a rate (-0.22‰/year) greater than that of Zone 1 (-0.0024‰/year). From ~1848 AD to the top of Zone 2, $\delta^{13}C_{org}$ values increased steadily from -28.3‰ to -27.7‰. $\delta^{15}N$ values ranged from 0.06‰ to 0.96‰ showing little variability. With the onset of Zone 2, $\delta^{15}N$ values declined at a faster rate than Zone 1 (from 0.96‰ to 0.15‰). C/N ratios ranged from 11.5 to 12.4, remaining relatively high, similar to Zone 1. Values were less variable than Zone 1, and remained relatively constant until ~1851 AD, after which values decreased to the top of the zone (from 12.4 to 11.5).

High C/N ratios until ~1851 AD had a similar range (11.8 to 12.4) to Zone 1 (11.4 to 12.6) suggesting the dominant source of organic material in Zone 2 remained allochthonous. However, after ~1851, C/N ratios decreased to the top of the zone. Values became closer (11.5) to those of aquatic origin (4-10) (Meyers and Teranes, 2001) suggesting a possible shift in the dominant source of organic material from allochthonous to autochthonous. A shift in organic material source in Zone 2 may also be supported by decreasing $\delta^{15}N$ values throughout the zone. $\delta^{15}N$ values that approach zero by the top of Zone 2 are similar to values produced by nitrogen-fixing algae (~0‰) and may suggest increased aquatic productivity towards the top of Zone 2 (Meyers and Teranes, 2001). $\delta^{13}C_{org}$ values that increase towards the top of Zone 2 also support an increase in aquatic productivity as increasing $\delta^{13}C_{org}$ values are commonly associated with greater in-lake productivity (Schelske and Hodell, 1991; Hodell and Schelske, 1998; Meyers and Teranes, 2001). As well, in Zone 2, organic matter content, organic carbon content and organic nitrogen content were consistently higher than observed in Zone 1, consistent with an increase in aquatic productivity

Zone 3 (~1863 AD to ~1953 AD)

In Zone 3, organic matter content ranged from 21.2% to 26.7%. Values showed little variability (similar to Zone 2) and increased throughout the entire zone. Organic carbon and organic nitrogen content narrowly ranged between 10.1% to 11.8% and 0.9% to

1.2%, respectively, remaining relatively constant throughout Zone 3 Outlying values were observed at ~1956 AD (19.5% for %C_{org} and 1 8% for %N_{org}). $\delta^{13}C_{org}$ values in Zone 3 ranged from -27.6‰ to -27.2‰ and are considerably more variable than the lower two zones. $\delta^{13}C_{org}$ values fluctuate throughout the zone and are the highest values in the sediment core. $\delta^{15}N$ values ranged from -0.28‰ to 0.07‰ and were more variable than Zone 2. $\delta^{15}N$ values remained relatively constant throughout the zone. C/N ratios ranged narrowly from 10.6 to 11.2 and were lower than the lower two zones. Values remained constant throughout Zone 3.

In Zone 3, lower C/N ratios than the previous two zones (10.6 to 11.2) represent values similar to organic matter that is aquatic in origin (4-10) (Meyers and Teranes, 2001). This suggests that the dominant source of organic matter deposition in SR1 throughout Zone 3 is autochthonous. Autochthonous deposition of organic matter is supported by low $\delta^{15}N$ values (close to 0‰) throughout the zone. These values are similar to those produced by nitrogen-fixing algae and suggest nitrogen-limiting conditions within SR1 as a result of high primary productivity, similar to studies elsewhere (Brenner et al., 1999; Talbot and Laerdal, 2000). Additionally, $\delta^{13}C_{org}$ values in Zone 3 are the highest in the SR1 record. Trends of increasing $\delta^{13}C_{org}$ values are conventionally interpreted as an indicator of increased aquatic productivity (Schelske and Hodell, 1991; Hodell and Schelske, 1998; Meyers and Teranes, 2001). High values in organic matter content, organic carbon content and organic nitrogen content are consistent with deposition of organic material from high aquatic productivity; however these values may also represent a reduced flux of inorganic sediment to SR1.

Zone 4 (~1953 AD to ~2007 AD)

In Zone 4, organic matter content ranged from 25.1% to 30.5%. Values ranged narrowly, gradually increasing to the top of the core. Organic carbon and nitrogen content were relatively variable and increased from 11.7% to 14.3% and 1.1% to 1.4%, respectively. These values were the highest in the stratigraphic record. $\delta^{13}C_{org}$ values ranged from -28.9‰ to -27.7‰ and were the most variable in the $\delta^{13}C_{org}$ record. Values gradually decreased towards the top of Zone 4 from -27.7‰ to -28.4‰. $\delta^{15}N$ values in Zone 4 ranged from -0.30‰ to 0.20‰ and were similarly variable as in Zone 3. Values increased very gradually from -0.06‰ to -0.09‰ to the top of the record. C/N values ranged from 9.9 to 11.2 and showed little variability. Values decreased at the base of Zone 4 (from 10.2 to 9.9) and then increased from 9.9 to 11.1 until ~1979 AD. C/N ratios ranged narrowly between 10.4 and 10.9 from ~1979 AD to the top of the core.

Throughout Zone 4, C/N ratios remained close to 10, indicating that the dominant source of organic matter had not changed from Zone 3 and remained autochthonous. Similarly, $\delta^{15}N$ values remained close to zero (-0.3‰ to 0.2‰) suggesting that nitrogen remained limited throughout Zone 4. Continued autochthonous deposition of organic matter and high aquatic productivity are consistent with continued high organic matter content, high organic carbon content and high organic nitrogen content at the top of the core. However, applying conventional interpretation of productivity-driven changes in $\delta^{13}C_{DIC}$ to decreasing $\delta^{13}C_{org}$ values within Zone 4 is inconsistent with high productivity indicated by all other parameters. This suggests that other factors may have caused a change in the $\delta^{13}C_{org}$ values.

4.2 SD34

4.2.1 Core Description

In order to maximize length and integrity of the SD34 sediment record, SD34 KB-2 and SD34 RC-2 were aligned and analyzed. Results from LOI analysis indicated that alignment could be achieved by shifting the SD34 RC-2 record down so that the top was positioned at 4.5-cm core depth (Figure 14). Between 39.0-cm and 12.5-cm, the organic matter content profiles diverge slightly, offset by as much as ~10 % (Figure 14). The offset in organic content between SD34 KB-2 and RC-2 could be related to the slightly different coring locations. The overlap indicates that SD34 RC-2 was missing the uppermost 4.5 cm of sediment and that it spanned 75.5 cm to 4.5 cm.

Visual observations of SD34 RC-2 revealed an abrupt contact in the sediment core at 62.5-cm depth, which was not observed in the shorter KB-2 gravity core (Figure 13). From the base of the core to 62.5 cm, the sediment was light brown silty clay, lacking any distinguishable plant material. Similar to the basal sediment of SR1 KB-2, sediment below 62.5-cm core depth in SD34 RC-2 was very dense and had the lowest percent organic matter values in the core (5.4% to 17.6%) (Figure 14). From 62.5 cm to 4.5 cm in SD34 RC-2, sediment was darker brown and composed of organic-rich material including many visible plant fibres (Figure 13). Organic matter content values were considerably higher through this interval and increased from 20.3% to 66.5% to the top of the core (Figure 14). The entire length of SD34 KB-2 was composed of dark brown sediment similar to SD34 RC-2. There was an increase in organic matter content (from 30.0% to 85.0%) towards the top of the core similar to the upper sediment of SD34 RC-2. However, there are two very low organic matter content values at 1 cm (16.9%) and 0.5

cm (27.9%) core depth in SD34 KB-2 (Figure 14) that are not accompanied by any observable sedimentary evidence of change.

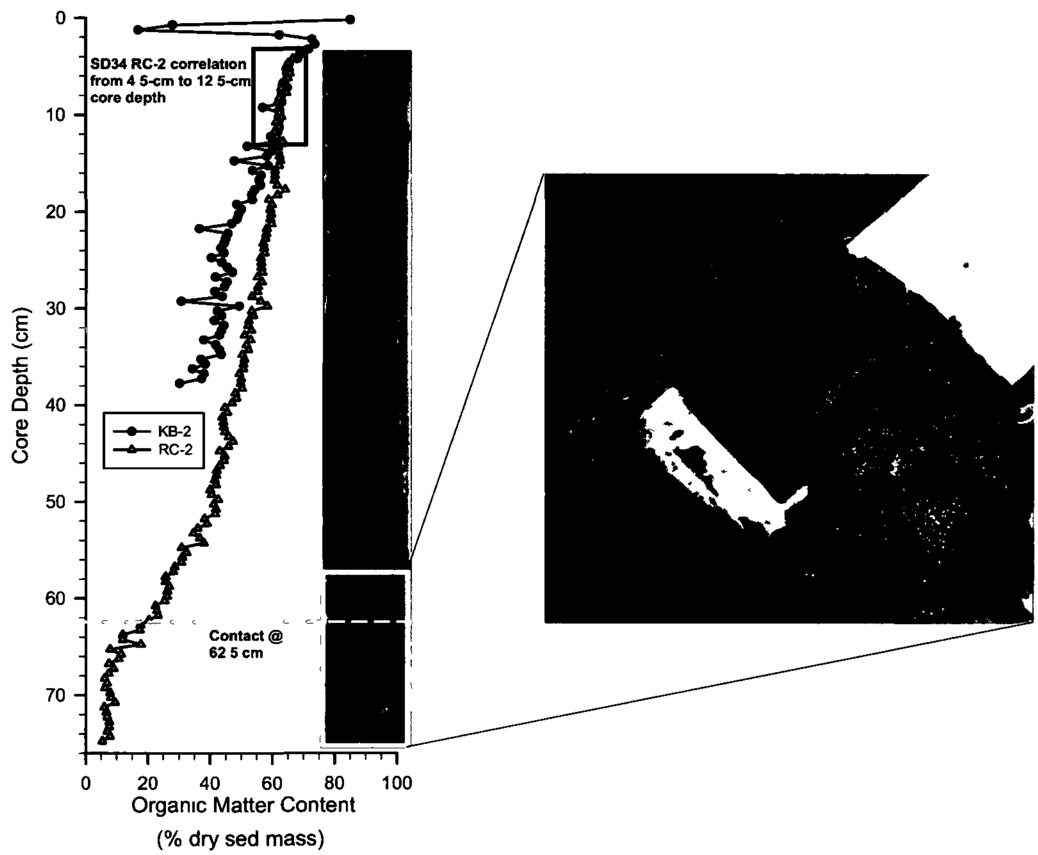

Figure 14 Correlation between SD34 RC-2 and SD34 KB2 using organic matter content values from LOI analysis. Top of SD34 RC-2 overlaps SD34 KB-2 at 4.5-cm core depth. An image of SD34 RC-2 core prior to sectioning is scaled to fit the core depth axis. A second image shows the contact close up. Dashed line denotes visible sediment contact at ~62.5-cm core depth.

4.2.2 Sediment Core Chronology

Total ^{210}Pb activity for SD34 KB-2 (38 cm to 0 cm) ranged from 0.015 Bq/g to 0.325 Bq/g and the ^{210}Pb activity profile generally declined from 0 cm to 15.25 cm (Figure 15a). Below 15.25-cm midpoint depth, ^{210}Pb activity became relatively constant ranging between 0.015 Bq/g and 0.044 Bq/g. Supported ^{210}Pb levels were estimated to be reached at approximately 15.25-cm midpoint depth (0.030 Bq/g). This resulted in a basal Constant Rate of Supply (CRS) ^{210}Pb date of ~1856 AD at 15.25-cm midpoint depth, providing a mean sampling resolution of 5.0 years from 0 cm to 15.25 cm (Figure 15b). Despite a broad but relatively well-defined ^{137}Cs peak at 7.25-cm midpoint depth, this occurs at a CRS ^{210}Pb date of ~1980 AD, ~17 years after peak fallout from above-ground nuclear bomb testing. This suggests diffusion of ^{137}Cs has modified the peak position in the sediment profile of SD34 KB-2. Diffusion of ^{137}Cs can occur in sediment with high organic matter content such as SD34 KB-2 (Figure 14) (Longmore, 1982; Foster et al., 2006). Diffusion has also been invoked as a process possibly influencing ^{137}Cs activity profiles in paleolimnological studies from the upstream PAD (Hall et al., 2004).

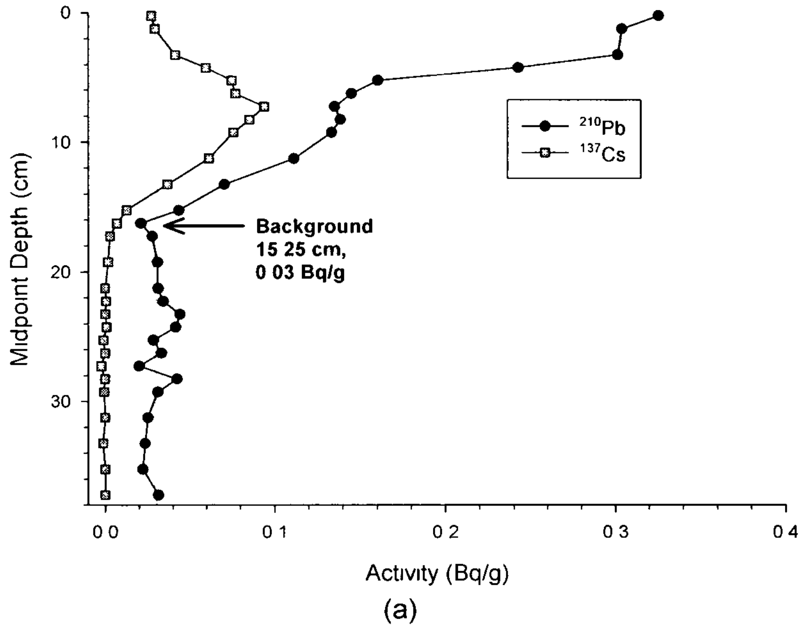

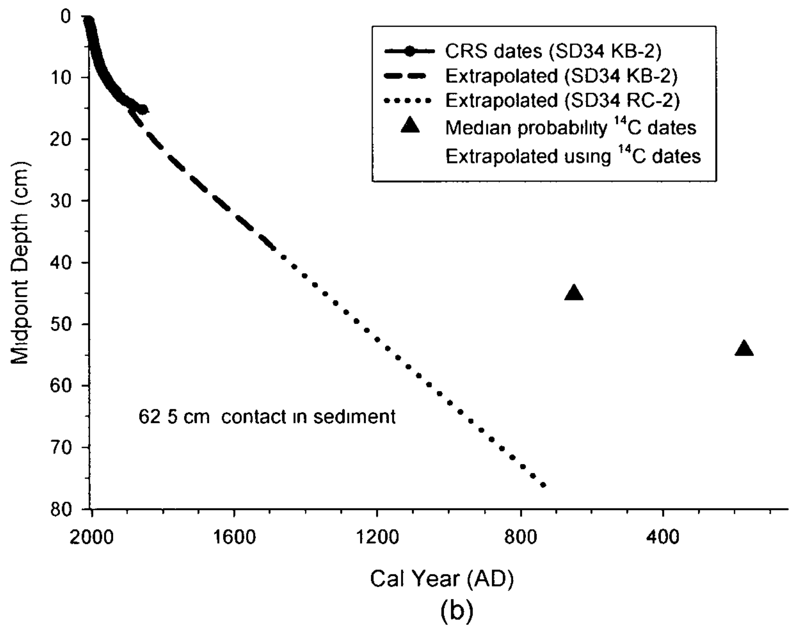

Figure 15 a) Activity profiles of ^{210}Pb and ^{137}Cs in Bq/g for SD34 KB-2, dashed grey line denotes background levels of supported ^{210}Pb b) SD34 sediment core chronology based on the Constant Rate of Supply (CRS) model, extrapolated down core for both KB-2 and RC-2 Median probability ^{14}C dates of two seed samples are indicated

Sediment chronology below unsupported ^{210}Pb levels in SD34 KB-2 (14.75 cm to 38 cm) was extrapolated using a linear regression of the cumulative dry mass and CRS modeled ^{210}Pb dates through the 0 cm to 14.25 cm interval, resulting in a basal date of ~1496 AD for SD34 KB-2 at 37.75-cm midpoint depth (Figure 15b). Samples from 0 cm to 14.25 cm midpoint depth were used and not 0 cm to 15.25 cm (where supported levels of ^{210}Pb were estimated to be reached) as samples from 14.75 cm to 15.25 cm spanned relatively large time intervals (~23-58 years) that were likely over estimated and deemed less reliable (Figure 15b). The chronology of SD34 was extended to include SD34 RC-2 (37.75-cm to 75 25-cm midpoint depth) using a linear regression of extrapolated dates through the 14.75-cm to 37.75-cm interval of SD34 KB-2. This yielded a date of ~998 AD for the observed sediment contact at 62.5 cm and a basal core date of ~762 AD at 75.25-cm midpoint depth (Figure 15b) Based on this analysis, the sediment record for SD34 spans from ~762 AD to ~2007 AD (~1245 years) (Figure 15b). However, because the abrupt change in sediment characteristics below the contact is likely accompanied by a change in sedimentation rate, there is increased uncertainty in sediment age below 62.75-cm midpoint core depth.

Radiocarbon (^{14}C) dating of two macrofossil samples (seeds from the aquatic plant *Potamogeton*) from SD34 RC-2 taken from organic sediment above the 62.5-cm depth contact resulted in calibrated median probability ^{14}C dates of 649 AD (42.25-cm midpoint core depth) and 173 AD (54.25-cm midpoint core depth) (Table 3, Figure 15b). These dates are considerably older than the corresponding extrapolated ^{210}Pb dates (~815 years at 45.25 cm and ~1018 years at 54.25 cm depth) (Figure 15b). Constraining the SD34 ^{210}Pb chronology using these ^{14}C dates would require a sedimentation rate substantially slower (~0.023 cm/year) than the one based on ^{210}Pb extrapolation (0.061 cm/year). The sedimentation rate based on ^{210}Pb extrapolation (0 061 cm/year) is also similar to average sedimentation rates of other closed-drainage basins upstream in the PAD (0.069, 0.056, and 0.069 cm/year for PAD 5, 9 and Bustard Island North Pond, respectively; Wolfe et al., 2008a). Additionally, observations of the SD34 RC-2 core above the contact reveal no noticeable change in sediment appearance and no evidence of sediment loss due to erosion (Figure 14). Therefore, a marked change in sedimentation rate (~3 times slower) below 15.75-cm is unlikely. Thus, it was concluded that the samples used for radiocarbon (^{14}C) dating were significantly older than the sediment matrix. For this reason, the radiocarbon dates were dismissed and the extrapolated ^{210}Pb dates were determined to be most reliable for constructing the sediment core chronology

Table 3 Results of seed samples from SD34 RC-2 submitted for radiocarbon dating with 2 sigma standard deviations (95% probability) Radiocarbon dates were calibrated to calendar years before present using the program CALIB (version 6 0) (Stuiver and Reimer, 1993) with the calibration data set of Reimer et al (2004)

Lab Number	Material	$\delta^{13}C$ (‰)	Core Depth (cm)	Reported Age (^{14}C yr BP)	Calibrated Age (Year AD)	Relative Area under the distribution	Median Probability
Beta-259576	Potamogeton seed	-13 6	42 0 to 42 5	1380 +/- 40 BP	582-694, 704-705 and 748-765	0 971 0 002 0 027	649
Beta-259577	Potamogeton seed	-16 9	54 0 to 54 5	1840 +/- 40 BP	75-255 and 305-312	0 991 0 009	173

4.2.3 Geochemical Stratigraphy

Assessment of the Inorganic Nitrogen Fraction: Correction for C/N Ratios

Using methods outlined by Talbot (2001), percent nitrogen and percent organic carbon were plotted against each other to determine the quantity of inorganic nitrogen for SD34 KB-2 and RC-2. Because of the significant change in sediment composition at the visible contact in SD34 RC-2, values from above and below the contact were plotted separately. Above the visible contact (~998 AD to ~2007 AD), the linear regression intercepts the x-axis indicating that bulk nitrogen values from this interval do not need correction. In contrast, below the visible sediment contact (~762 AD to ~998 AD), the linear regression intercepts the y-axis at 0.041% (Figure 16). The 95% confidence interval for values below the visible contact is relatively narrow and closely follows the regression line (Figure 16). Therefore, a correction of 0.041% was applied to bulk nitrogen values from this interval. The correction resulted in increases to C/N ratios below the contact ranging in value from 0.7 to 1.7. The entire corrected geochemical record is shown in Figure 17.

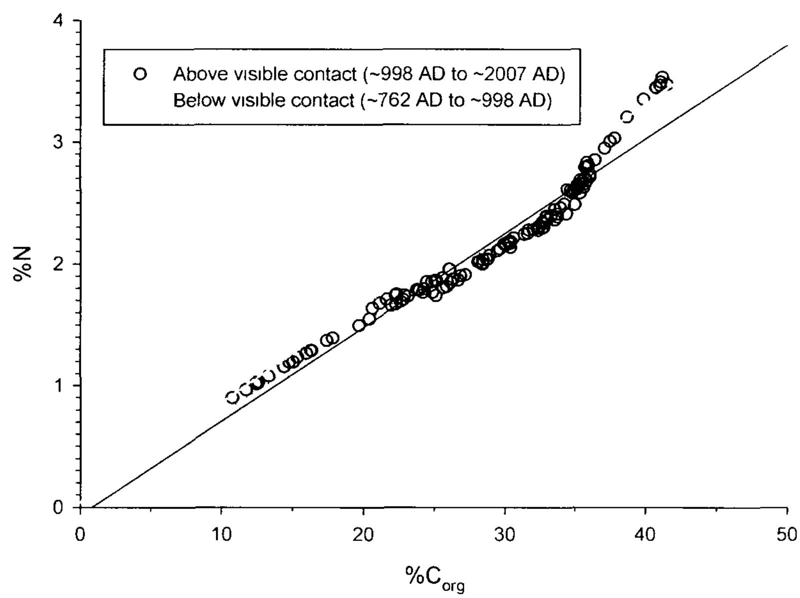

Figure 16 Percent nitrogen and percent organic carbon cross-plot of SD34 KB-2 and RC-2 Solid lines denote linear regression lines Note that for the interval below the visible contact (~762 AD to ~998 AD), the linear regression line intersects the y-axis The value of the y-intercept indicates the average amount of inorganic nitrogen for this interval (Talbot, 2001) Dotted lines denote the 95% confidence intervals for above and below the visible contact

Geochemical Results and Interpretation

Four stratigraphic zones in the SD34 sediment record (KB-2 and RC-2 cores) have been identified using organic carbon and nitrogen content and elemental and stable isotope analyses (Figure 17). These zones were established based on horizons of change in the geochemical proxies. The transition from Zone 1 to 2 is based on changes in organic matter content, organic carbon content, organic nitrogen content, $\delta^{13}C_{org}$ and the C/N ratio. These stratigraphic changes lie at the same horizon as the visible contact between silty clay sediment and organic sediment in SD34 RC-2. Zone 3 was established at an abrupt shift in $\delta^{13}C_{org}$ values and Zone 4 was established at another prominent shift in $\delta^{13}C_{org}$ values. The four zones are described and interpreted below.

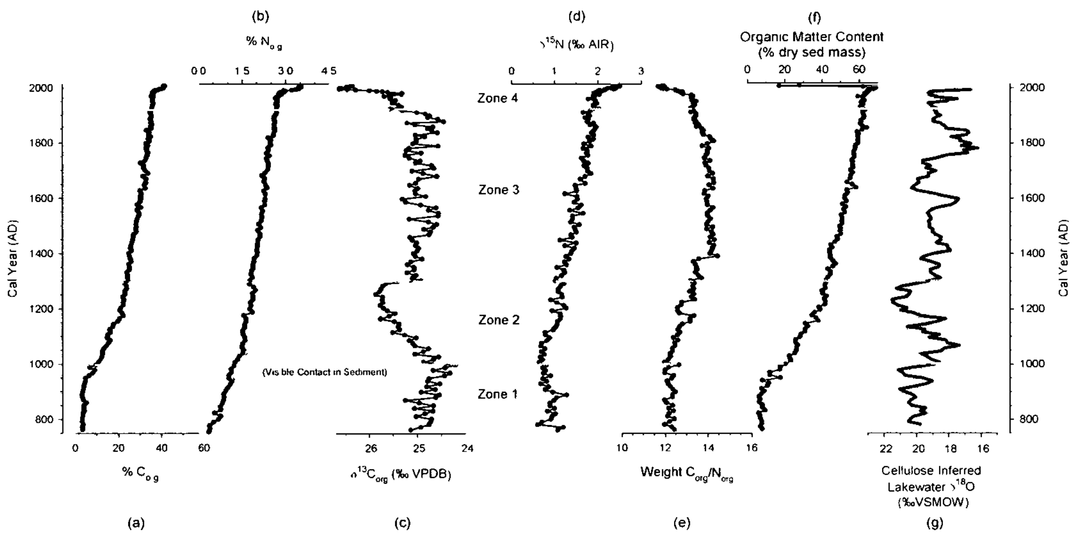

Figure 17 Geochemical records for SD34 showing a) percent organic carbon, b) percent organic nitrogen (light grey line denote uncorrected values), c) $\delta^{13}C_{org}$, d) $\delta^{15}N$, e) C/N (dark grey line denotes values before N correction), f) organic matter content, and g) cellulose-inferred lake water $\delta^{18}O$ Black line through $\delta^{18}O$ values is a 3-point running mean Dashed lines distinguish different stratigraphic zones SD34 KB-2 and RC-2 values are overlapped from 4 5 cm to 8 cm Plotted values through this interval are an average of KB-2 and RC-2 values

Zone 1 (~762 AD to ~998 AD)

In Zone 1, organic matter content narrowly ranged from 6.0% to 20.3% and were the lowest in the sedimentary record. Values were initially constant (narrowly ranging from 7.0% to 9.0%), and then gradually increased at ~909 AD from 9.0% to 20.3%. Similarly, organic carbon and nitrogen content in Zone 1 were the lowest in the record ranging from 3.0% to 9.6% and 0.3% to 1.3%, respectively. Both parameters gradually increased up-core. Zone 1 included some of the highest $\delta^{13}C_{org}$ values in the record ranging from -25.9‰ to -24.2‰. Values in Zone 1 had a relatively narrow range in comparison to values higher in the core and exhibited a gradual increase towards the top of the zone (from -25.3‰ to -24.2‰). $\delta^{15}N$ values ranged from 0.6‰ to 1.3‰ and were the lowest in the entire record. The C/N ratios ranged from 12.0 to 12.6 and were relatively constant throughout Zone 1. Cellulose-inferred lake water $\delta^{18}O$ values ($\delta^{18}O_{lw}$) ranged from -22.0‰ to -17.7‰ and were highly variable throughout Zone 1. $\delta^{18}O_{lw}$ values in Zone 1 were among the lowest in the record.

C/N ratios in Zone 1 were higher than values of organic material aquatic in origin (4-10), suggesting that the organic material deposited on the lake bed was predominantly allochthonous (Meyers and Teranes, 2001). $\delta^{15}N$ values in Zone 1 may also indicate a terrestrial supply of organic material as values (0.6‰ to 1.3‰) are similar to the $\delta^{15}N$ signature of land plants (~0.5‰) (Meyers and Teranes, 2001). $\delta^{13}C$ values in Zone 1 were among the highest in the SD34 sediment record. Conventionally, elevated $\delta^{13}C$ values are associated with elevated aquatic productivity (Schelske and Hodell, 1991; Hodell and Schelske, 1998; Meyers and Teranes, 2001). Elevated aquatic productivity is not consistent with physical observations of the sediment below the visible contact, low organic matter, low percent organic carbon and low percent organic nitrogen or with the interpretation of C/N ratios. Therefore, the $\delta^{13}C_{org}$ signature in Zone 1 is most likely reflecting the allochthonous source of organic material being deposited in SD34. An allochthonous source of organic material may have compromised the $\delta^{18}O_{lw}$ values in Zone 1. However, the raw cellulose values within Zone 1 range from 5.4 ‰ to 9.6 ‰ (Appendix E) and are significantly lower than those expected for terrestrial cellulose (>20‰) (e.g., Saurer at al., 1997). Therefore, the $\delta^{18}O_{lw}$ values in Zone 1 do not appear to be compromised by terrestrial organic material and likely reflect the $\delta^{18}O_{lw}$ signature of SD34.

Zone 2 (~998 AD to ~1292AD)

The transition from Zone 1 to 2 was characterized by changes in many parameters and is also associated with the visible sediment contact in SD34 RC-2. Organic matter content gradually increased within Zone 2 from 20.3% to 41.9%. Organic carbon content increased from 9.6% to 22.8% at a faster rate than Zone 1. In Zone 2, Organic nitrogen content increased from 1.3% to 1.7%, but at a slower rate than Zone 1. At the onset of Zone 2, $\delta^{13}C_{org}$ values abruptly reversed trend and gradually decreased from -24.8‰ to -25.9‰. $\delta^{13}C_{org}$ values through the ~1214 AD to ~1292 AD interval were among the lowest in the sediment record (between -25.9‰ and -25.7‰). $\delta^{15}N$ values gradually increased throughout Zone 2 from 0.7‰ to 1.1‰. C/N ratios ranged from 11.9 to 13.4 and increased throughout the zone. $\delta^{18}O_{lw}$ values ranged from -22.4‰ to -16.6‰ and were highly variable.

The increase in C/N ratios throughout Zone 2 could indicate that the source of the organic material is allochthonous. However, the change in sediment composition from inorganic to organic at the onset of Zone 2 coupled with increases in organic matter, organic carbon and organic nitrogen contents throughout the zone may alternatively suggest that deposition of organic matter in SD34 is associated with increased aquatic productivity. Teranes and Bernasconi (2000) have documented increases in productivity being accompanied by higher $\delta^{15}N$ values. Thus, increasing $\delta^{15}N$ values in Zone 2 may further indicate increased aquatic productivity above the visible sediment contact. Increased aquatic productivity contradicts the conventional C/N interpretation of relatively high C/N ratios reflecting allochthonous organic material deposition, indicating that elevated C/N values in Zone 2 may alternatively be the result of diagenetic alteration.

C/N ratios derived from algae can increase during sedimentation in lakes having high productivity due to active microbial denitrification of organic matter (Meyers and Teranes, 2001). Therefore, because of strong evidence from a variety of parameters, the organic material source for SD34 throughout Zone 2 is interpreted to be autochthonous despite increasing C/N ratios.

Conventional interpretation of $\delta^{13}C_{org}$ does not agree with the above interpretation of the other geochemical parameters. With the onset of Zone 2, $\delta^{13}C_{org}$ values began to decrease, a trend that is usually interpreted as a decline in productivity (Schelske and Hodell, 1991; Hodell and Schelske, 1998; Meyers and Teranes, 2001). As a result, the conventional interpretation of $\delta^{13}C_{org}$ is likely not appropriate for Zone 2. $\delta^{18}O_{lw}$ values in Zone 2 remained highly variable and difficult to interpret. However, low $\delta^{18}O_{lw}$ values at the onset of Zone 2 may indicate periods of low evaporative enrichment.

Zone 3 (~1292 AD to ~1918 AD)

In Zone 3, organic matter content gradually increased throughout the zone from 41.9% to 63.2%. Organic carbon and nitrogen contents ranged from 22.8% to 35.4% and 1.8% to 2.7%, respectively. Both sets of values gradually increased within Zone 3. $\delta^{13}C_{org}$ values ranged from -25.3‰ to -24.5‰ and were the most variable in the record. The transition from Zone 2 to 3 was associated with an abrupt +0.8‰ shift in $\delta^{13}C_{org}$ values (-25.7‰ to -24.9‰). Values remained high and variable for the duration of the zone. In Zone 3, $\delta^{15}N$ values increased from 1.2‰ to 1.8‰. C/N ratios ranged from 13.9 to 15.2 with little variability. From the onset of Zone 3 until ~1381 AD, C/N ratios were relatively constant (ranging from 13.9 to 14.4). There was an abrupt increase in C/N ratios (from 14.3 to 15.2) between ~1381 AD and ~1390 AD, followed by a gradual decrease in values (from 14.1 to 13.6) to the top of the zone. $\delta^{18}O_{lw}$ values ranged from -20.6‰ to -15.1‰ and were highly variable. Despite this, there was a noticeable oscillation in $\delta^{18}O_{lw}$ values within Zone 3. An interval of low values occurred between ~1607 AD and ~1736 AD with values generally ranging between -20.6‰ to -19.0‰. An interval of high $\delta^{18}O_{lw}$ values occurred between ~1745 AD and ~1837 AD ranging from -18.5‰ to -15.1‰, and included several of the highest $\delta^{18}O_{lw}$ values in the record.

C/N ratios in Zone 3 are higher (13.9 to 15.2) than those aquatic in origin (4-10). Similar to Zone 2, elevated values in Zone 3 may be explained by diagenetic alteration. C/N ratios produced by aquatic algae under highly productive conditions can increase during sedimentation due to active microbial denitrification of organic matter (Meyers and Teranes, 2001). High productivity in Zone 3 is suggested by elevated organic matter deposition as indicated by high organic matter, organic carbon and organic nitrogen contents. High aquatic productivity is further supported by increasing $\delta^{15}N$ values in Zone 3. Increased productivity can be accompanied by higher $\delta^{15}N$ values as observed by Meyers and Teranes (2000). $\delta^{18}O_{lw}$ values in Zone 3 were higher than Zones 1 and 2, possibly indicating that evaporative enrichment had increased.

Zone 4 (~1918 AD to ~2007 AD)

In Zone 4, organic matter content ranged from 59.1% to 84.9% with the exception of two outlier values (2004: 16.9%; 2006: 27.9%) that are very low. Similar changes are not observed at these horizons in any other proxy. Organic matter content increased throughout the zone from 63.2% to 84.9%. Organic carbon and nitrogen contents narrowly ranged from 35.4% to 41.0% and 2.7% to 3.5%, respectively. Values increased throughout Zone 4 with greater rates of increase occurring after ~1980 AD. $\delta^{13}C_{org}$ values ranged from -26.6‰ to -25.3‰ and are less variable than the previous zone. Values sharply decreased at the onset of Zone 4 from -25.3‰ to -26.3‰ to top of the record. $\delta^{15}N$ values gradually increased from 1.8‰ to 2.5‰. Similar to percent organic carbon and nitrogen values, $\delta^{15}N$ values exhibited a greater rate of increase after ~1980 AD. C/N values ranged from 11.7 to 13.9 with less variability than Zone 3 and remained relatively constant until ~1980 AD. C/N ratios declined after ~1980 AD from 13.6 to 11.8. $\delta^{18}O_{lw}$ values remained highly variable through this zone ranging from -19.9‰ to -15.8‰ and had no discernable pattern.

Relatively high C/N ratios (11.7 to 13.9) may suggest an allochthonous source of organic material for Zone 4. However, preferential loss of nitrogen from organic matter can cause C/N ratios derived from algae to increase (Meyers and Teranes, 2001). As a result, the high C/N ratios may be the result of microbial denitrification of organic matter in the lake sediment under highly productive conditions, similar to that observed by Sarazin et al. (1992). Bulk organic, organic carbon and organic nitrogen contents and $\delta^{15}N$ values in Zone 4 are all high, suggesting high productivity. C/N ratios after ~1980 AD decreased rapidly and are lower than values at the base of the zone. These values most likely represent C/N ratios that have not yet been altered by diagenetic effects inferred lower in the core. Similarly, percent organic matter, percent organic carbon and percent nitrogen all rapidly increase after ~1980 AD, possibly indicating that diagenesis has not altered the uppermost sediments.

The lowest $\delta^{13}C_{org}$ values occur at the top of Zone 4 with the greatest rates of decrease occurring after ~1980 AD, similar to other parameters measured for SD34. The shift to lower values at the onset of Zone 4 would conventionally correspond to decreased productivity, contradicting interpretations of the other geochemical variables. This would suggest that similar to Zone 1 and 2, the conventional interpretation of $\delta^{13}C_{org}$ values is not appropriate for Zone 4. As well, $\delta^{18}O_{lw}$ values continued to be highly variable. The range of values in Zone 4 is similar to Zone 3 making any interpretation of hydrologic change based on $\delta^{18}O_{lw}$ difficult.

4.3 GSL1

4.3.1 Core Description

To maximize the length and integrity of the GSL1 sediment record, GSL1 KB-1 and GSL1 RC-1 were aligned and analyzed. The organic matter content profile from GSL1 RC-1 (upper 43.5 cm) was shifted down by 0.5 cm to achieve the best observed overlap with the organic matter content profile of GSL1 KB-1 (0 cm to 26.5 cm) (Figure 18). This indicated that GSL1 RC-1 was only missing the uppermost 0.5 cm of sediment and the core spanned 0.5 cm to 100 cm of the GSL1 sediment profile (Figure 19). Therefore, overlapping the top of GSL1 RC-1 at 0.5 cm of GSL1 KB-1 generated a 100-cm-long sediment record.

The depth interval of 20 cm to 15 cm in GSL1 RC-1 included a large piece of plant material that corresponded with anomalously high and erratic percent organic matter content values (Figure 18). Thus, only GSL1 RC-1 samples below 20-cm depth and GSL1 KB1 samples from 26.5 cm to 0 cm were further analyzed for geochemical parameters. Percent organic carbon values from this continuous record are used to accompany visual observations of the sediment core because LOI (organic content) was only conducted on the uppermost 43.5 cm of GSL1 RC-1.

Visual observations of GSL1 RC-1 revealed a lithologic contact between 73 and 68-cm core depth that was gradational, in contrast to the abrupt contact visible in SR1 and SD34 (Figure 18). However, similar to the previously described cores, the gradational contact in GSL1 RC-1 separated two distinct stratigraphic units in the GSL1 sediment profile. The basal sediment (100-cm to 73-cm) was light brown silty clay and absent of plant material. Faintly visible laminations were observed throughout the lower strata (Figure 18) and a change in sediment particle size was observed from 92-cm to 88-cm where sediment was visibly coarser. These sediments are characterized by very low percent organic carbon values ranging from 1.2% to 4.6% (Figure 19). At 73-cm core depth, a gradual shift from light brown inorganic material to dark brown organic-rich material was observed. This observation was accompanied by an abrupt increase in percent organic carbon values from 4.6% to 25.8% through the 73 cm to 68 cm gradational contact (Figure 19). From 68 cm to 0 cm, sediment was dark brown and composed of organic-rich material including visible plant material that increased in abundance towards the top of the core (Figure 19). These sediments were characterized by high percent organic carbon values (30.6% to 45.2%) that increased towards the top of the core (Figure 19).

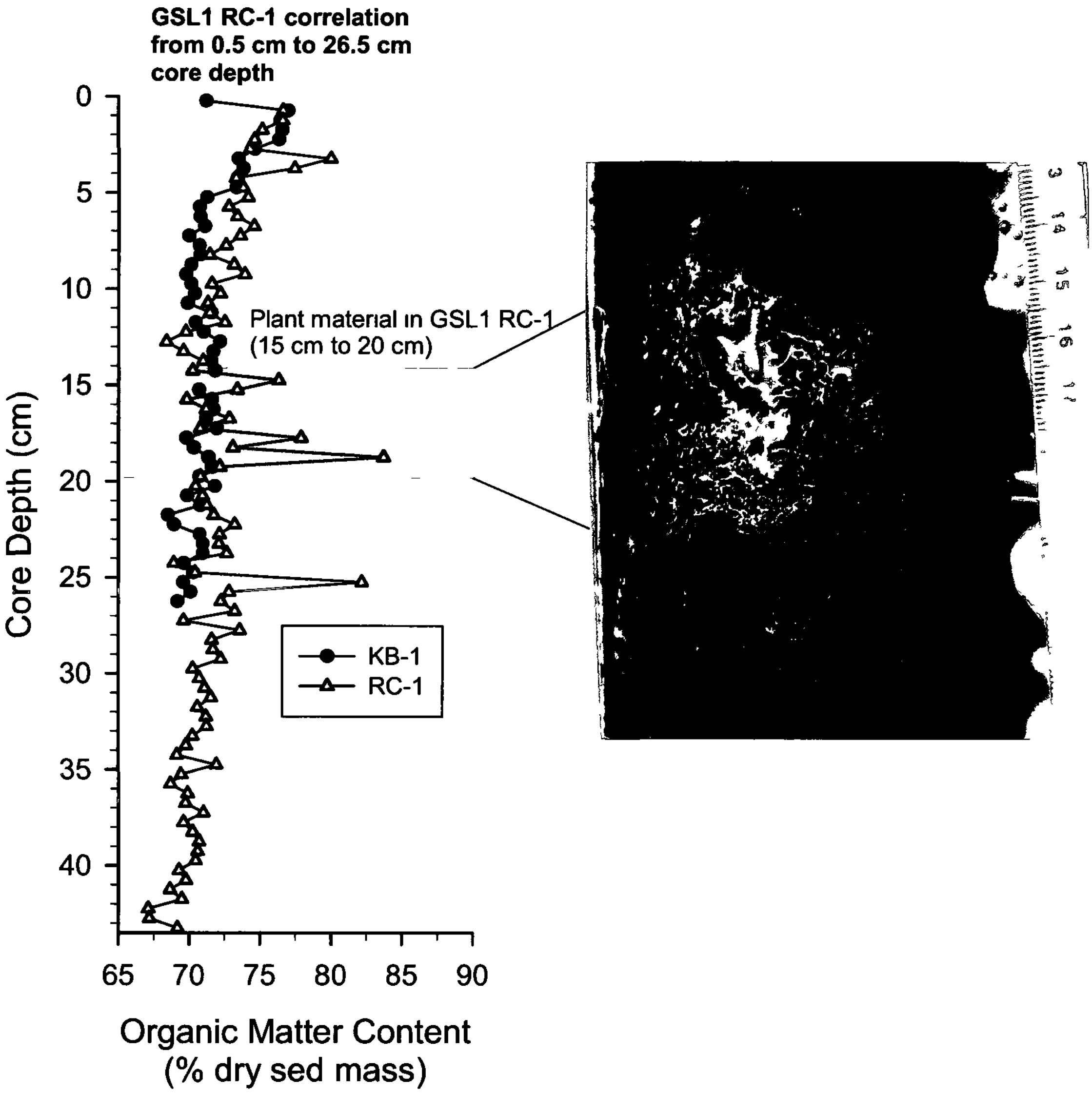

Figure 18. Correlation between GSL1 RC-1 and GSL1 KB-1 using organic matter content from LOI analysis. Top of GSL1 RC-1 overlaps GSL1 KB-1 at 0.5-cm core depth An image of a tuber which affected the percent organic content values within GSL1 RC-1 is shown at 15 cm to 20 cm

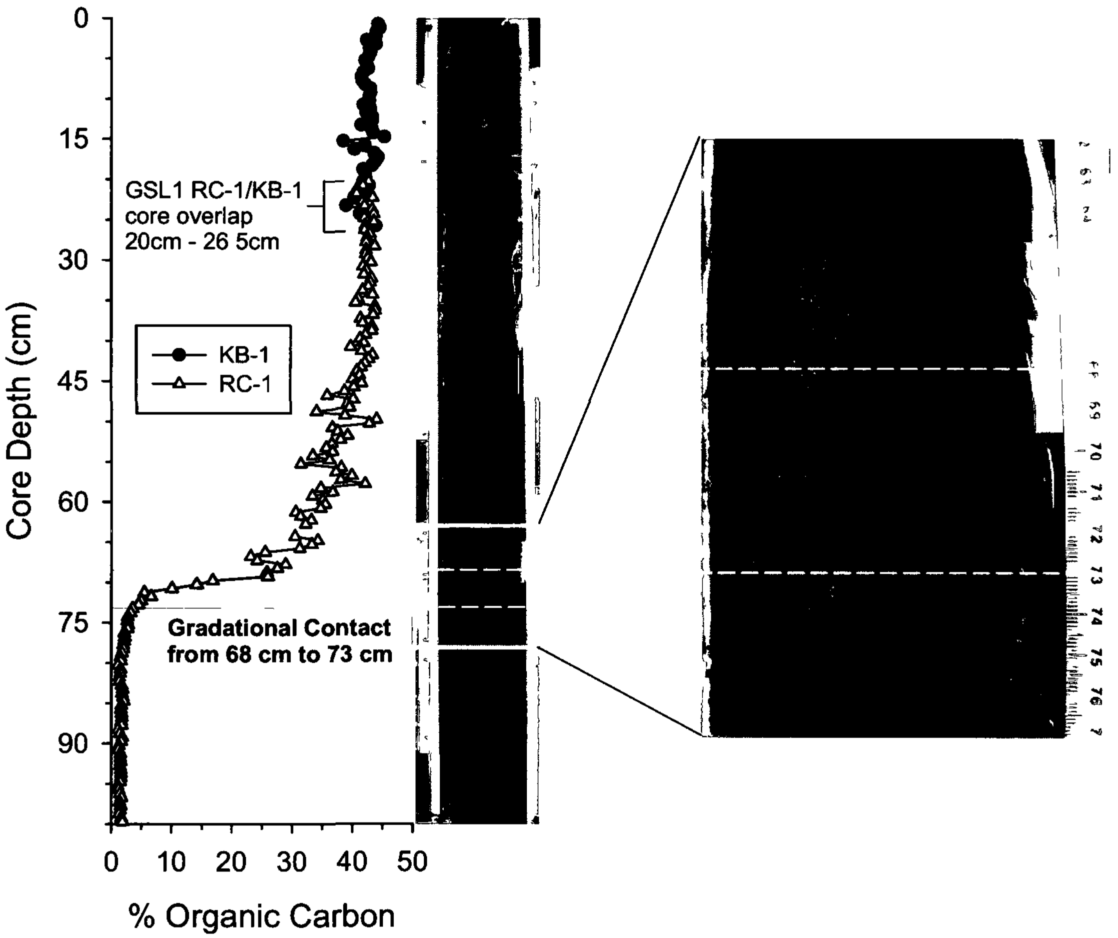

Figure 19 Organic carbon content for GSL1 KB-1 (26.5 cm to 0 cm) and GSL1 RC-1 (100 cm to 20 cm). The two cores are overlapped between the 20 cm to 26.5 cm interval. An image of GSL1 RC-1 prior to sectioning is scaled to fit the core depth axis. A second image shows the contact close up. Grey dashed lines denote visible gradational contact from 73 cm to 68 cm

4.3.2 Sediment Core Chronology

Total ^{210}Pb activity for GSL1 KB-1 ranged from 0.005 Bq/g to 0.260 Bq/g. Values declined from 0.250 Bq/g at 0-cm to 0.037 Bq/g at 11.75-cm midpoint core depth and become less variable between 12.25-cm and 26.25-cm midpoint core depth (ranging from 0.005 Bq/g to 0.023 Bq/g). Supported ^{210}Pb levels were estimated to be reached where ^{210}Pb activity becomes constant at ~12 25-cm midpoint depth (0.018 Bq/g) (Figure 20a). This resulted in a CRS ^{210}Pb date of ~1860 AD at 12.25-cm midpoint depth and provided a mean sampling resolution of 11.5 years through the 0-cm to 12.25-cm interval (Figure 20b). ^{137}Cs values from GSL1 KB-1 lacked a well-defined peak, and instead declined steadily from the top of the core to 12.25-cm midpoint depth (Figure 20a). The absence of a peak likely indicates diffusion of ^{137}Cs which occurs more frequently in organic-rich sediments (Longmore, 1982; Foster et al., 2006) such as those as the top of GSL1 KB-1 (Figure 18). Therefore, ^{137}Cs from GSL1 is unreliable for constraining the sediment core chronology.

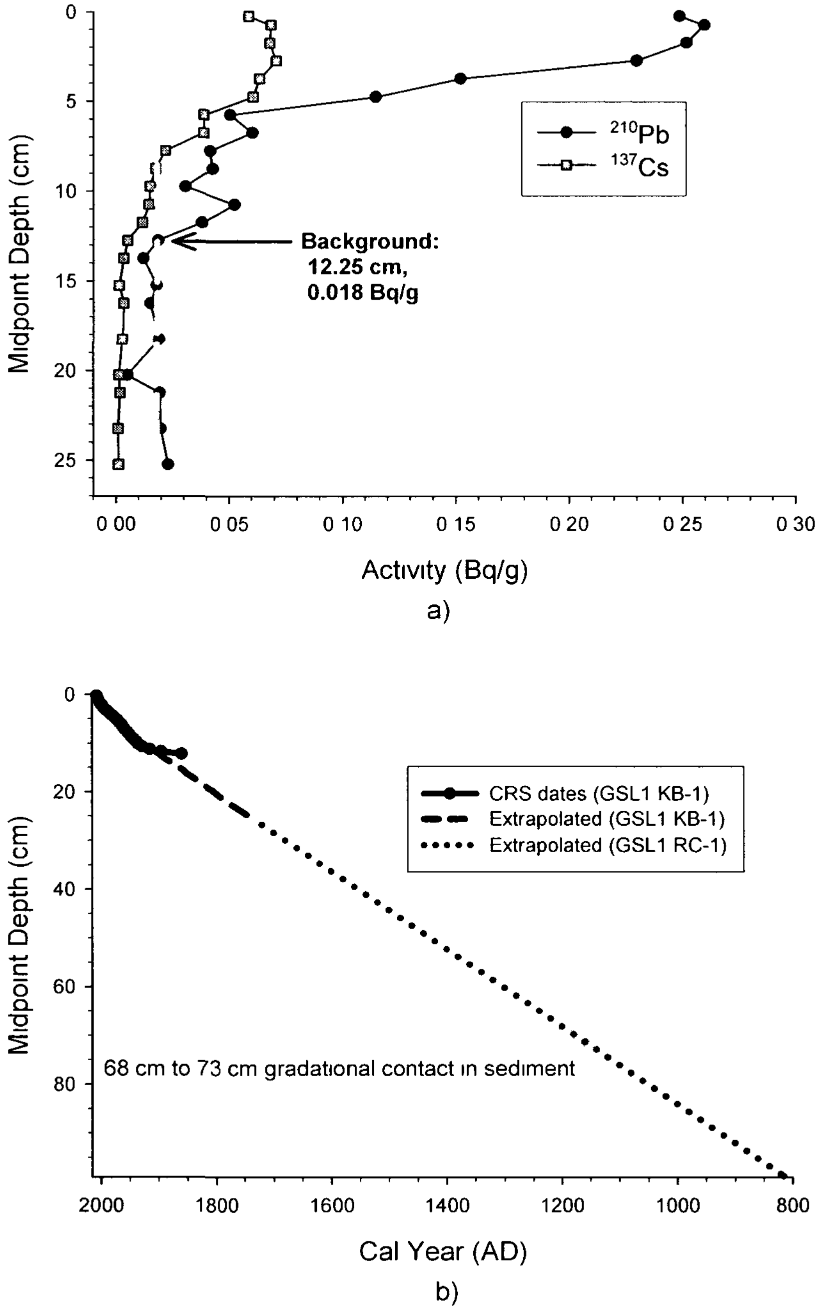

Figure 20 a) Activity profiles of ^{210}Pb and ^{137}Cs in Bq/g for GSL1 KB-1, Dashed grey line denotes supported ^{210}Pb b) GSL1 sediment core chronology based on the Constant Rate of Supply (CRS) model, extrapolated down-core for both KB-1 and RC-1

A linear regression of the cumulative dry mass and CRS modeled ^{210}Pb dates through the 0-cm to 11 25-cm interval of GSL1 KB-1 was used to extrapolate dates below unsupported ^{210}Pb levels in GSL1 KB-1. Dates were extrapolated from 11.25-cm depth to the bottom of the core and not from 12.25-cm where supported levels of ^{210}Pb were estimated to be reached, as calculated CRS dates for samples from 11.75 cm to 12.25 cm spanned relatively large time intervals (~21-35 years) that ware likely overestimated and were deemed to be less reliable Extrapolation resulted in a basal date of ~1728 AD for the gravity core at 26.25-cm midpoint depth (Figure 20b). Using a linear regression of extrapolated dates through the 11.25 cm to 26.75 cm interval of SD34 KB-1 and midpoint depth, the chronology of GSL1 was extended to include GSL1 RC-1 (26.75 cm to 99.75 cm) This yielded a dated interval of ~1142 AD to ~1199 AD for the gradational contact observed in the sediment core between 73-cm and 68-cm depth and a basal core date of ~803 AD at 99.75-cm midpoint depth (Figure 20b). Therefore, the sediment record for GSL1 spans from ~803 AD to ~2007 AD (~1204 years) (Figure 20b). However, similar to SR1 and SD34, the change in sediment characteristics below the contact is likely accompanied by a change in sedimentation rate, increasing the uncertainty in sediment age below 68 cm.

Radiocarbon (^{14}C) dating was not used to constrain the chronology of GSL1 because there were no plant macrofossils found in the core. Bulk samples were not submitted for ^{14}C dating because the presence of bitumen in the Peace and Athabasca river basins (upstream of the Slave River) has previously resulted in dates that are too old (e.g., Wolfe et al., 2006). Unreliable radiocarbon dates obtained for SD34 coupled with an absence of reliable dating material resulted in the decision to not attempt radiocarbon dating as a tool for constraining the ^{210}Pb-extrapolated sediment chronology.

4.3.3 Geochemical Stratigraphy

Assessment of the Inorganic Nitrogen Fraction: Correction for C/N Ratios

Because of the significant change in sediment composition at the gradational contact in GSL1 KB-1, percent nitrogen and percent organic carbon values from above, below and within the gradational contact were plotted separately. Above the visible contact (~1199 AD to ~2007 AD), the linear regression intercepts the x-axis indicating that organic carbon is present in excess of nitrogen and that bulk nitrogen values from this interval do not need correction. In contrast, within and below the visible sediment contact (~1155 AD to ~1199 AD and ~803 AD to ~1199 AD), linear regressions intercept the y-axis at 0.0409 % and 0.0165 %, respectively (Figure 21). Although these values are relatively small, the percent organic carbon and nitrogen values are also relatively small, making the correction factor meaningful. The 95% confidence intervals for ~1155 AD to ~1199 AD and ~803 AD to ~1199 AD are very narrow and closely follow the regression line (Figure 21). Therefore, corrections of 0.0409 % and 0.0165 % were applied to bulk N values from within and below the gradational contact, respectively. The correction resulted in increases to C/N ratios at the gradational contact ranging in value from 0.3 to 1.3 and below the gradational contact ranging from 0.5 to 3.7. The entire corrected geochemical record is shown in Figure 22.

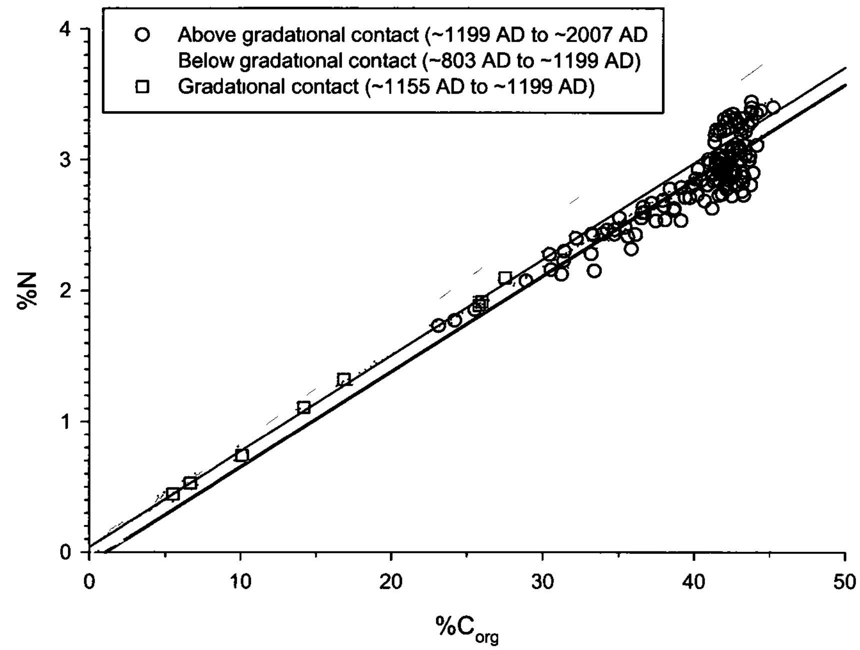

Figure 21 Percent nitrogen and percent organic carbon cross-plot of GSL1 KB and RC-1. Solid lines denote linear regression lines Note that for the interval within (~1155 AD to ~1199 AD) and below (~803 AD to ~1199 AD) the gradational contact linear regression lines intersect the y-axis. The value of the y-intercept indicates the average amount of inorganic nitrogen for this interval (Talbot, 2001) Dotted lines denote the 95% confidence intervals for above and below the visible contact

Geochemical Results and Interpretation

Assessment of the geochemical results has identified five stratigraphic zones in the GSL1 sediment record including the gradational contact (Figure 22). The transition from Zone 1 to the gradational contact is based on changes in all variables. The gradational contact is characterized by sharp trends in all parameters. Similarly, Zone 2 was based on changes in trend observed in all parameters. The base of Zone 3 is characterized by shifts in $\delta^{13}C_{org}$, $\delta^{15}N$ and C/N values and Zone 4 was based on changes in trends for $\delta^{13}C_{org}$, percent organic carbon and percent organic nitrogen. The four zones and gradational contact interval are described and interpreted below.

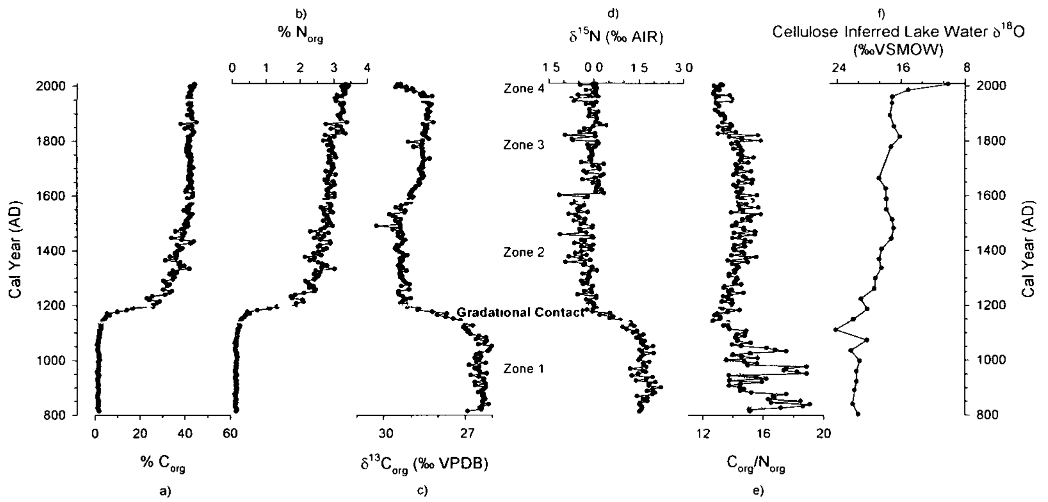

Figure 22 Geochemical records for GSL1 showing a) percent organic carbon, b) percent organic nitrogen (dark grey line denotes uncorrected values), c) $\delta^{13}C_{org}$, d) $\delta^{15}N$, e) C/N (dark grey line denotes values before N correction), f) cellulose-inferred lake water $\delta^{18}O$ Dashed lines distinguish different stratigraphic zones GSL1 KB-1 and RC-1 values are overlapped from 20 cm to 27 cm Plotted values through this interval are an average of KB-1 and RC-1 values

Zone 1 (~803 AD to ~1142 AD)

In Zone 1, organic carbon and nitrogen contents narrowly ranged from 1.5% to 1.9% and 0.05% to 0.19%, respectively. Values were the lowest in the record for both parameters. $\delta^{13}C_{org}$ and $\delta^{15}N$ values in Zone 1 ranged from -27.0‰ to -26.0‰ and 1.2‰ to 2.2‰, respectively, with little variability and were the highest in the record. Both proxies remained relatively constant throughout the zone. C/N ratios ranged from 13.6 to 19.1 and were highly variable. Values weakly increased towards the top of the zone and were the highest in the record. $\delta^{18}O_{lw}$ values are the lowest in the record ranging between -24.1‰ to -20.2‰ and remain relatively constant throughout the zone.

High C/N ratios (>15) in Zone 1 are higher than those typically produced by aquatic plants (<10), suggesting that the dominant source of organic material deposited is allochthonous (Meyers and Teranes, 2001) $\delta^{13}C_{org}$ values in Zone 1 were the highest in the GSL1 record. However, the $\delta^{13}C_{org}$ signature in Zone 1 is most likely reflecting the $\delta^{13}C_{org}$ signature of the allochthonous source of organic material deposited in GSL1 and not aquatic productivity. Similarly, low percent organic carbon and nitrogen values may also reflect the allochthonous source of organic material. However, similar to SD34, raw $\delta^{18}O$ values in Zone 1 (ranging from 3.2‰ to 7.2‰; Appendix E) are considerably lower than those typically produced by terrestrial plants (>20‰) (e.g., Saurer et al., 1997) suggesting that these values were not compromised by terrestrial organic material and that they do reflect the $\delta^{18}O_{lw}$ signature of GSL1. Low $\delta^{18}O_{lw}$ values likely reflect lake water that has undergone minimal evaporative isotopic enrichment.

Gradational Contact (~1142 AD to ~1199 AD)

Across the gradational contact, organic carbon and nitrogen contents increased substantially from 3.5% to 25.8% and 0.3% to 1.9%, respectively. $\delta^{13}C_{org}$ and $\delta^{15}N$ values decreased from -29.1‰ to -27.2‰ and -0.2‰ to 1.2‰, respectively. C/N ratios ranged from 12.7 to 14.4 with less variability than Zone 1. Values shifted to lower ratios at the onset of the gradational contact and remained relatively constant. $\delta^{18}O_{lw}$ values within the gradational contact increased from -21.9‰ to -20.2‰.

The gradational contact represents an interval of rapid change within the GSL1 sediment profile. The shift to lower C/N ratios is towards values representative of organic material that is aquatic in origin (4-10), indicating a possible change in the dominant source of organic material deposited in the basin from allochthonous to autochthonous (Meyers and Teranes, 2001). However, C/N ratios in the gradational contact are still relatively high compared to values typically observed for organic material that is aquatic in origin. The higher values are most likely the result of nitrogen-limiting conditions, which has been shown to elevate C/N ratios (Meyers and Teranes, 2001). Nitrogen-limiting conditions throughout the gradational contact are supported by $\delta^{15}N$ values that decrease towards 0‰. $\delta^{15}N$ values close to 0‰ may be associated with high abundances of nitrogen-fixing algae. Increases in percent organic carbon and nitrogen throughout the gradational contact, suggest an increase in aquatic productivity, which is consistent with a high abundance of nitrogen-fixing algae. An autochthonous source of organic material and increased aquatic productivity is consistent with the transition from silty clay to organic sediment observed in the sediment core. As well, increasing $\delta^{18}O_{lw}$ values may suggest increased evaporative loss of water from GSL1 characteristic of a lake transitioning into an isolated basin. However, conventional interpretation of $\delta^{13}C_{org}$ values through this interval suggests a decline in productivity, contradicting all other interpretations.

Zone 2 (~1199 AD to ~1577 AD)

In Zone 2, organic carbon and nitrogen content were more variable than Zone 1 and gradually increased from 25.8% to 43.2% (%C_{org}) and 1.8% to 2.8% (%N) towards the top of the zone. $\delta^{13}C_{org}$ values ranged from -30.2‰ to -29.0‰ with little variability. $\delta^{15}N$ values in Zone 2 ranged from -1.1‰ to 0.1‰ and were more variable than Zone 1. C/N ratios increased slightly from 13.3 to 16.0 and were slightly more variable than Zone 2. $\delta^{18}O_{lw}$ values gradually increased from -21.0‰ to -16.9‰ to the top of the zone.

Despite a slight increase in C/N ratios throughout Zone 2, values were consistently lower than Zone 1. This would suggest that the dominant source of organic material remained unchanged from the gradational contact and was most likely autochthonous. Similar to the gradational contact, C/N ratios were likely elevated due to nitrogen-limiting conditions. $\delta^{15}N$ values in Zone 2 were close to 0‰, indicating that nitrogen-fixing algae may have been an abundant source of organic matter Consistently high values of percent organic carbon and nitrogen indicate high levels of organic matter deposition and aquatic productivity in Zone 2. High aquatic productivity in GSL1 throughout Zone 2 is consistent with organic sediment observed above the gradational contact in GSL1 RC-1. $\delta^{18}O_{lw}$ values that increase throughout the zone may indicate continued evaporative enrichment within GSL1 that began at the gradational contact. Once again, conventional interpretation of $\delta^{13}C_{org}$ values proved inappropriate as low $\delta^{13}C_{org}$ values in Zone 2 would suggest low productivity through this interval, contradicting interpretations from all other parameters.

Zone 3 (~1577 AD to ~1957 AD)

In Zone 3, percent organic carbon ranged from 38.4% to 45.2% and was less variable than Zone 2. Values remained relatively constant throughout Zone 3. Percent nitrogen increased gradually from 2.6% to 3.2% with variability remaining similar to Zone 2. $\delta^{13}C_{org}$ values ranged from -29.1‰ to -28.1‰ and were less variable than values from Zone 2. $\delta^{13}C_{org}$ values abruptly increased through the transition of Zone 2 and 3 (from -29.3‰ to -28.9‰), and gradually increased throughout the remainder of the zone (from -28.9‰ to -28.2‰). $\delta^{15}N$ values ranged from -1.1‰ to 0.4‰ with variability similar to Zone 2. Values rapidly shifted at the base of Zone 3, increasing from -0.7‰ to 0.4‰ in ~31 years. After the shift, $\delta^{15}N$ values decreased gradually throughout the remainder of the zone from 0.4‰ to -0.3‰. C/N ratios gradually decreased from 16.8 to 13.7 and maintained variability similar to Zone 2. $\delta^{18}O_{lw}$ values are relatively constant ranging from -18.7‰ to -17.0‰.

C/N ratios throughout Zone 3 had a similar range (13.7 to 16.8) as Zone 2 (13.3 to 16.0). This similar range of values indicates that the source of organic material deposited in GSL1 had not likely changed from Zone 2 to 3 and that it remained autochthonous despite relatively high C/N ratios. As well, throughout most of Zone 3, $\delta^{15}N$ values ranged close to 0‰, indicating nitrogen-limiting conditions. Similar to Zone 2, nitrogen-limitation was likely the cause of elevated C/N ratios in Zone 3. Additionally, consistently high percent organic carbon values and increasing percent nitrogen values suggest that high aquatic productivity and organic matter deposition continued from Zone 2 to 3. High aquatic productivity and autochthonous deposition of organic material is consistent with visibly organic sediment observed through this interval of the GSL1 sediment profile. Additionally, the positive shift in $\delta^{15}N$ values at the onset of Zone 3 may indicate a brief change in nitrogen cycling within GSL1. Elevated $\delta^{15}N$ signatures at the bottom of Zone 3 may reflect a brief influx of nitrogen from outside the basin. $\delta^{18}O_{lw}$ values are higher in Zone 3 than Zone 2, suggesting an increase in evaporative enrichment within GSL1. Similar to $\delta^{15}N$, $\delta^{13}C_{org}$ values abruptly increased at the onset of Zone 3, a shift that is conventionally associated with increased aquatic productivity. However, there is a lack of evidence in any other parameter to support an abrupt increase in aquatic productivity, therefore it is unlikely that a conventional interpretation of $\delta^{13}C_{org}$ is appropriate for this zone

Zone 4 (~1957 AD to ~2007 AD)

In Zone 4, percent organic carbon and nitrogen values gradually increased from 41.4% to 44.4% and 2.9% to 3.3%, respectively. $\delta^{13}C_{org}$ values decreased from -29.5‰ to -28.2‰. $\delta^{15}N$ values ranged from -0.5‰ to 0.1‰ with a similar variability to Zone 3 and remained constant. C/N ratios ranged from 13.4 to 14.6 and were among the lowest in the record. Variability remained the same as Zone 3 and values were relatively constant throughout the zone. $\delta^{18}O_{lw}$ values in Zone 4 increased markedly from -17.1‰ to -10.1‰ and were the highest in the record.

C/N ratios in Zone 4 (13.4 to 14.6) were among the lowest in the GSL1 record. These ratios were the closest in the record to ratios typically reported as aquatic in origin suggesting that the supply of organic material in Zone 4 was from an autochthonous source. As well, in Zone 4, $\delta^{15}N$ values of around 0‰ suggest that nitrogen was limited. Nitrogen-limiting conditions are then likely the reason C/N ratios in Zone 4 are slightly higher than those expected from autochthonous organic material. Zone 4 also represents the highest percent organic carbon and nitrogen values in the GSL1 record. These values indicate high aquatic productivity and deposition of organic material similar to Zone 3. Percent organic carbon and nitrogen values in Zone 4 that are slightly higher than Zone 3 are likely the result of recently deposited sediment that has not yet undergone diagenesis. An autochthonous source of organic material and high aquatic productivity is consistent with visibly organic sediment at the top of the GSL1 sediment record. $\delta^{18}O_{lw}$ values that increase to the highest in the record may suggest that the highest degree of evaporative enrichment occurred in Zone 4. As well, the $\delta^{18}O_{lw}$ value of -10.1‰ at the top of Zone 4 is typical of values found in the evaporation-dominated lakes of SRD (Brock et al., 2007). Declining $\delta^{13}C_{org}$ values are conventionally associated with declining aquatic productivity (Schelske and Hodell, 1991; Hodell and Schelske, 1998; Meyers and Teranes, 2001). Such an interpretation would contradict all other parameters, suggesting that conventional interpretation is not appropriate for Zone 4. As well, diagenesis can cause an increase in $\delta^{13}C_{org}$ values (Herczeg, 1988). Therefore, the sharp decrease in $\delta^{13}C_{org}$ values near the top of Zone 4 may be the result of uppermost sediments not having undergone diagenesis.

Chapter 5 - *Discussion*

Constructing a millennial-scale hydrologic history for the Slave River system requires a systematic examination of data obtained from the stratigraphic records of SR1, SD34 and GSL1. A change in depositional environment interpreted from a change in almost all parameters at the visible contact in each of the stratigraphic records will initially be discussed. This will help to determine the timing, and potential drivers of change at each study site. In addition, a variety of factors that have caused conventional interpretation of C/N ratios to be contradictory to other measured parameters at each study site will be discussed. An open-drainage diatom indicator record for GSL1 is then explored to aid in the paleohydrological reconstruction and is compared to parameters measured for GSL1 within this study. A second interval of hydrologic change not widely identified in the geochemical record of GSL1 is evident in the diatom record. This change appears to be captured in only the $\delta^{18}O_{lw}$ and $\delta^{13}C_{org}$ records, highlighting the sensitivity of these two records to hydrologic change that occurred at GSL1. Complications with conventional interpretation of $\delta^{13}C_{org}$ in GSL1 and SD34 are then addressed in order to establish a $\delta^{13}C_{org}$ interpretation consistent with all other parameters. Lastly, interpretations of key parameters from each study lake are used in conjunction with published reconstructed climate and hydrologic records to detail a ~1200-year record of hydrologic variability within the Slave River system.

5.1. A Change in Depositional Environment at the Sediment Contacts of SR1, SD34 and GSL1

A prominent stratigraphic change occurs at the inorganic-organic sediment contact common to all study sites. At each site, the inorganic sediment occurred at the base of the record and more organic-rich sediment extended from the contact to the top of the record. Interpretation of the organic material source above and below the contacts within each study lake was complicated by factors affecting the C/N ratio that differed among these lakes. The interpretation of C/N ratios at SR1 was conventional. At SR1, ratios below the contact were higher than values typically produced by aquatic sources (<10) (Figure 23), clearly suggesting that organic material below the contact was from an allochthonous source. C/N values above the contact approach the range typically produced by aquatic sources (Figure 23) more so than the values below the contact, suggesting that organic material above the contact in SR1 was autochthonous.

In contrast to SR1, C/N ratios below the contact in SD34 were among the lowest in the record (Figure 23). An abrupt change in all parameters (Figure 17) was interpreted to suggest that diagenesis had affected the geochemical parameters below ~1980 AD, indicating that elevated ratios above the contact were likely attributed to nitrogen loss as a result of diagenesis. An increase in aquatic productivity indicated by percent organic matter content, percent organic carbon and percent organic nitrogen values indicated that organic material above the contact was likely from an autochthonous source, similar to SR1. Additionally, low percent organic matter content, percent organic carbon and percent organic nitrogen values coupled with mineral-rich sediment (Figure 17), suggested an allochthonous source of organic material below the contact despite comparatively low C/N ratios.

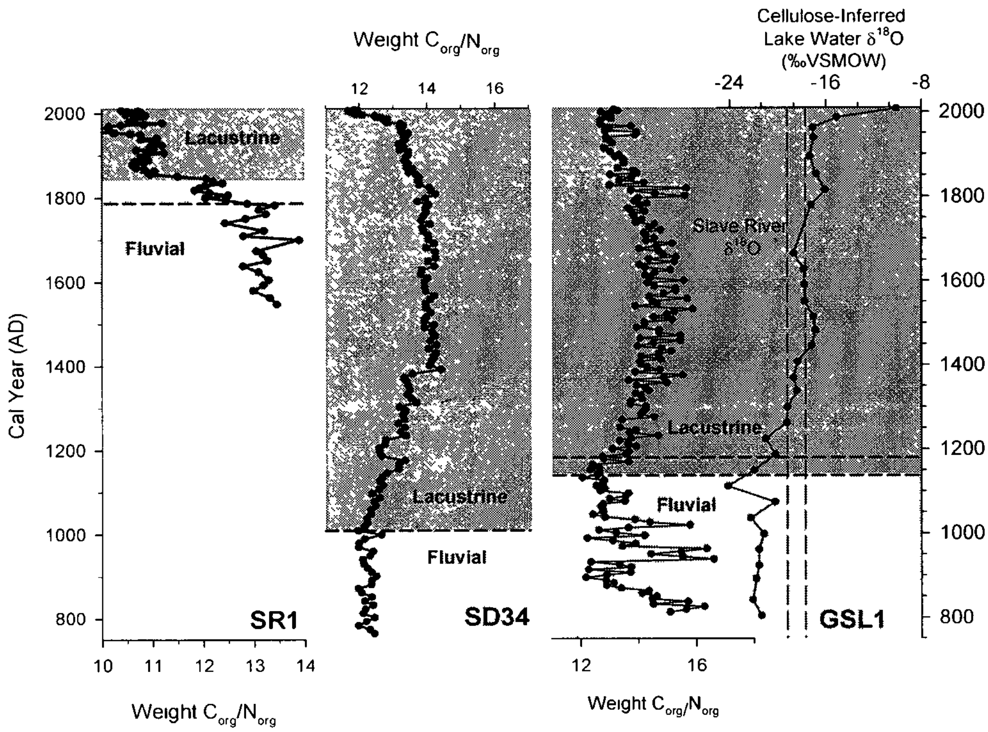

Figure 23 C/N ratios for study lakes, SR1, SD34 and GSL1 Visible sediment contacts are marked by horizontal dashed lines (bottom and top of GSL1 gradational contact are marked with dashed lines) Cellulose-inferred lake water $\delta^{18}O$ is also included for GSL1 with the range of Slave River $\delta^{18}O$ as reported by Brock et al (2008) identified as a vertical dashed lines

In the GSL1 record, C/N ratios below the contact were higher than those typically derived from aquatic sources (Figure 23), suggesting that organic material in this interval was allochthonous. Similar to SD34, C/N ratios above the contact in GSL1 remained high. However, $\delta^{15}N$ values close to zero above the contact (Figure 22) suggested nitrogen-limiting conditions that have been shown to elevate C/N ratios (Meyers and Teranes, 2001). Therefore, elevated C/N ratios due to nitrogen-limiting conditions coupled with high percent organic carbon and percent organic nitrogen values suggested autochthonous organic mater deposition above the contact in GSL1, similar to SD34 and SR1. The shift in organic material source observed at the contact of each study lake was accompanied by a change in sediment composition, likely indicating a change in depositional environment.

Allochthonous organic material below the visible contact corresponds with low percent organic carbon and percent organic nitrogen values in each study lake and because the source of organic material is from outside the study basins, these values reflect the allochthonous source of organic material Therefore, low percent organic carbon and organic nitrogen values below the visible contacts of each study lake indicate that any supply of in-lake, aquatic organic material to each study basin is diluted by the high inorganic content of the allochthonous source.

Geochemical analysis of freshly deposited Slave River flood sediment collected in 2005 reveals that Slave River sediment has low organic carbon and organic nitrogen contents and high C/N ratios, not unlike the values observed below the visible contacts of SR1, SD34 and GSL1 (Table 4). As well, laminations observed at the base of the GSL1 sediment profile likely represent sporadic pulses of sediment to the basin suggesting riverine influence below the contact. Laminations in the sediment of GSL1, geochemical and isotopic characteristics similar to Slave River sediment and close proximity to relict Slave River distributary channels (Figure 24) suggest that the Slave River is a likely source of allochthonous organic material deposition in the lower strata of SR1, SD34 and GSL1. Additionally, $\delta^{18}O_{lw}$ values measured from the Slave River and below the contact in GSL1 (Brock et al, 2008) are both low (Figure 23), likely reflecting water that has undergone minimal evaporative isotopic enrichment. However, $\delta^{18}O_{lw}$ values below the contact of GSL1 (-24.1‰ to -20.2‰) are noticeably lower than contemporary Slave River values (-17.7‰ to -19 2‰) and may represent a Slave River $\delta^{18}O$ signature that is more depleted than the present, possibly due to increased snowmelt runoff from headwater regions.

Table 4 Comparison of percent organic carbon, percent nitrogen and C/N ratios measured from recently deposited Slave River flood sediment (Brock et al, 2010) to values measured below the sediment contacts of SR1, SD34 and GSL1

Sample	%C_{org}	%N (*SR1, SD34, GSL1 values corrected for inorganic nitrogen*)	C/N (*SR1, SD34, GSL1 values corrected for inorganic nitrogen*)
Slave River	1 0	0 06	15 9
SR1	2 6 – 10 2	0.22 – 0.81	11 4 – 13 9
SD34	3 0 – 9 6	0 30 – 1 30	12 0 – 12 6
GSL1	1 5 – 1 9	0 06 – 0 19	13 6 – 19 1

GSL water proximal to the SRD is turbid due to sediment supplied by the Slave River (Rawson, 1950). As a result, suspended sediment in GSL would have a similar geochemical signature to that of the Slave River. Therefore, GSL is also a potential source of allochthonous organic material to SD34 and GSL1 as both lakes are similarly elevated from the present-day shore of the lake (Figure 7). Reconstructions of the delta front using radiocarbon ages of wood samples by Vanderburgh and Smith (1988) have indicated that at ~1180 years BP, the delta front was located northwest of both SD34 and GSL1 (Figure 24). This would suggest that the position of the delta front likely did not cause the current positions of SD34 and GSL1 to be inundated by GSL within the last ~1200 years.

Time intervals for sediment deposited below the contact (SD34: ~762 AD to ~998 AD, GSL1: ~803 AD to ~1142 AD) for both SD34 and GSL1 correspond to extremely low lake levels reconstructed for Lake Athabasca upstream (Wolfe et al., 2008a). Lake Athabasca and GSL are both large natural reservoirs in the same river system that have been shown to respond similarly during wet and dry years in the observational record (Bennett, 1970), making it unlikely that GSL water levels were high enough ~1000 years ago to inundate the two study lakes. Relatively low lake levels in GSL coupled with a documented SRD front that was lakeward of the current positions of SD34 and GSL1 would suggest that GSL is likely not the source of inorganic sediment below the contacts.

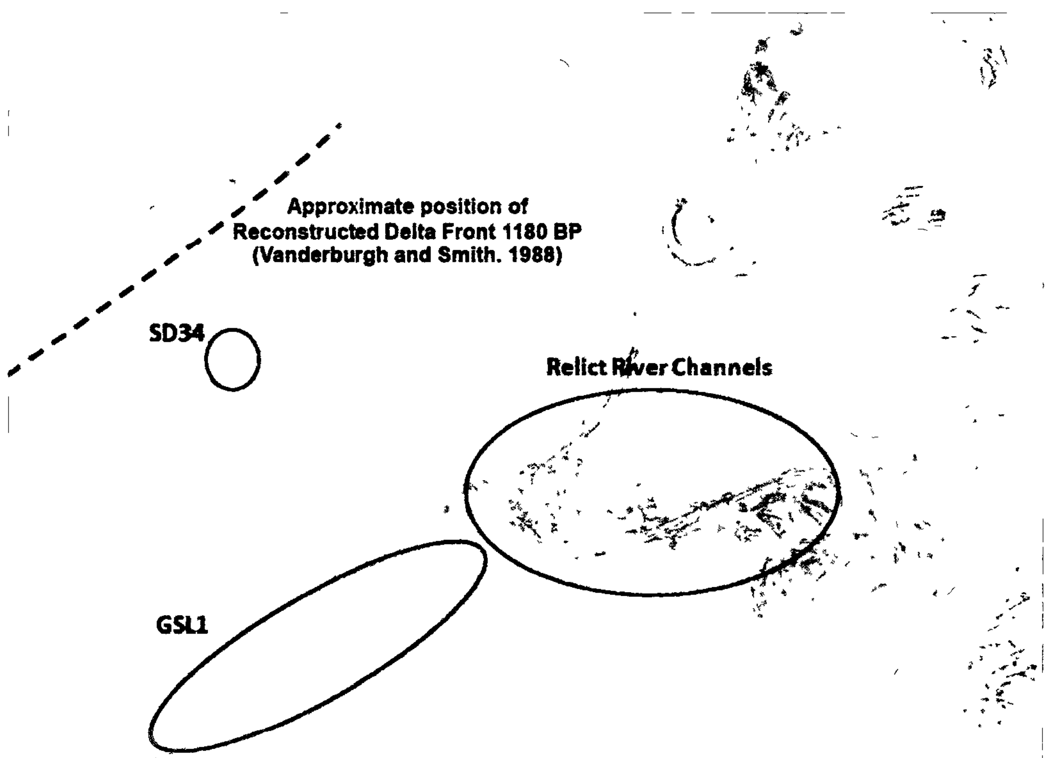

Figure 24. Soil map of Slave River Delta and surrounding area (Canada Department of Agriculture, 1971). Study Sites GSL1 and SD34 are highlighted as well as relict river channels located to the north of GSL1. Approximate position of SRD front at ~1180 years BP is drawn as a dashed line (Vanderburgh and Smith, 1988).

The change in the source of organic matter above the contacts of SR1, SD34 and GSL1 from allochthonous to autochthonous marks a change in the depositional environment of each study lake Autochthonous deposition of organic material and high aquatic productivity (as indicated by percent organic carbon, percent organic nitrogen, $\delta^{13}C_{org}$ and $\delta^{15}N$) indicate depositional conditions within SR1, SD34 and GSL1 that are lacustrine above the visible contact. As well, ^{210}Pb background is reached at similar depths for all three study sites (SR1: 15.25 cm, SD34: 15.25 cm, GSL1: 12.25 cm) indicating that sedimentation rates in the uppermost sediments are relatively consistent among study sites. These sedimentation rates (SR1: 0.082 cm/year; SD34: 0.061 cm/year; GSL1: 0.083 cm/year) are similar to rates from lacustrine environments upstream in the PAD (0.069, 0.056, 0.069 cm/year for PAD 5, 9, Bustard Island North Pond, respectively; Wolfe et al., 2008a).

A change in depositional environment from fluvial to lacustrine occurs at the contact within each study lake. However, this transition does not appear to occur simultaneously at SR1, SD34 and GSL1. In the shorter record of SR1, the sediment contact occurs at ~1786 AD and geochemical parameters shift at ~1818 AD. At SD34, the sediment contact is coupled with a change in geochemical parameters at ~1000 AD, indicating a shift to lacustrine conditions at the onset of the last millennium, much earlier than SR1. The sediment record of GSL1 is similar in length to SD34, however, the timing of the sediment contact and geochemical changes appears to occur ~144 years later than SD34. The significance of the temporal offset of the contact between SD34 and GSL1 is difficult to evaluate as dates for both sediment records have been extrapolated based solely on the ^{210}Pb stratigraphy and may be associated with uncertainties associated with modeling.

5.2 Diatom Record at GSL1

A diatom record was established for GSL1 to supplement the geochemical stratigraphy. Diatom counts were conducted on GSL1 RC1 by Michelle Tai from the University of Waterloo Environmental Change Laboratory. Diatom algae are sensitive to changes in physical, chemical and biological conditions and microhabitat availability and have been shown to be useful biomonitors of hydrologic change (Hall et al. 2004). Upstream in the PAD, small benthic and epipsammic diatom *Fragılarıa* taxa have been shown to dominate in turbid open-drainage lakes and under flood conditions (Hall et al., 2004), making these taxa a likely indicator of past open-drainage intervals at GSL1.

High percent abundance of *Fragılarıa construens v venter* below the gradational contact in GSL1 suggest open-draınage conditions consistent with the fluvıal deposıtional environment interpreted from physical and geochemical data (Figure 25). As well, the shift to a lacustrine depositional environment above the contact is associated with low abundance of *Fragılarıa construens v venter* However, at ~1550 AD there is a re-emergence of these open-drainage diatom indicators. The re-emergence of *Fragılarıa construens v venter* suggests a change in hydrological conditions at GSL1. Hydrological change at ~1550 AD is not evident in the sediment composition of GSL1 and a second interval of open-drainage conditions appears to be captured by only two geochemical parameters ($\delta^{13}C_{org}$ and $\delta^{18}O_{lw}$) (Figure 25). Changes in the GSL1 $\delta^{18}O_{lw}$ and $\delta^{13}C_{org}$ records coincide with those in the diatom record (Figure 25). However, conventional interpretation of increased $\delta^{13}C_{org}$ corresponding to increased aquatic productivıty within GSL1 has been contradictory to other geochemical parameters thus far. Therefore, because the $\delta^{13}C_{org}$ record appears to be one of two sensitive geochemical parameters that capture a second interval of open-drainage conditions was suggested by the GSL1 diatom record, further investigation is required to evaluate the factors that influence the carbon isotope signature of organic material in these sediments.

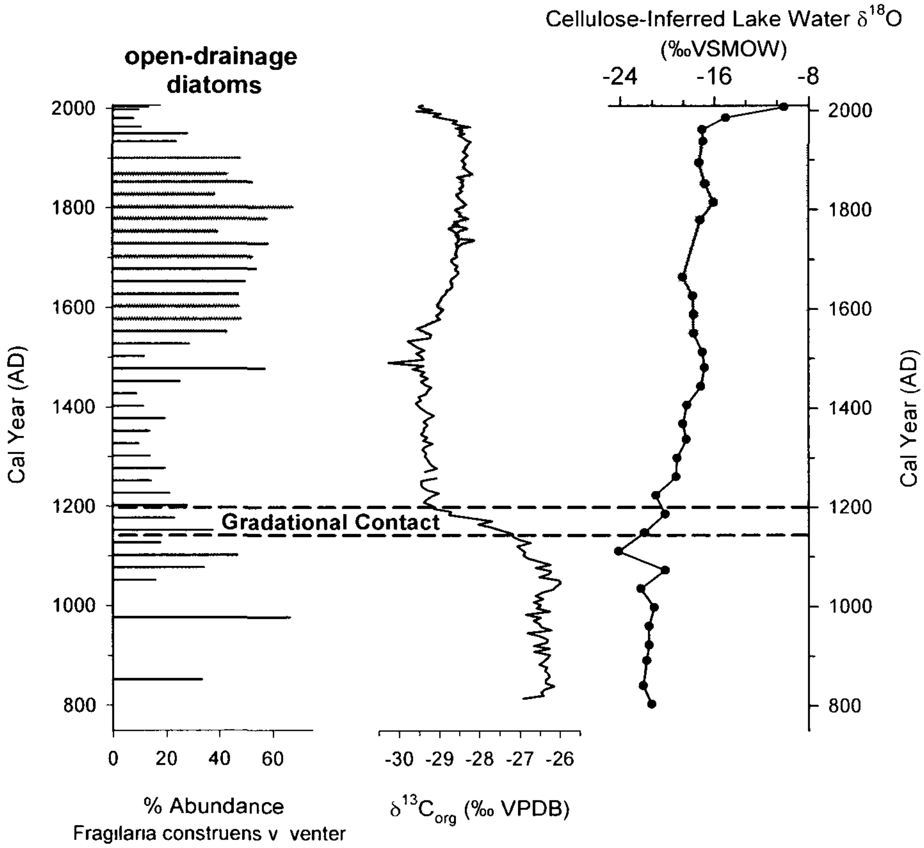

Figure 25 GSL1 open-drainage diatom indicator record, GSL1 $\delta^{13}C_{org}$ record and GSL1 cellulose-inferred lake water $\delta^{18}O$ record Shaded interval indicates interval of open-drainage conditions above the gradational contact at GSL1 captured by the three parameters

5.3 Establishing an Alternative Interpretation of $\delta^{13}C_{org}$ at GSL1 and SD34

Correspondence of the diatom and $\delta^{13}C_{org}$ records from GSL1 suggests that $\delta^{13}C_{org}$ is a sensitive indicator of hydrologic change. However, conventional interpretation of lake sediment $\delta^{13}C_{org}$ proved to be contradictory to all other measured parameters in the GSL1 record. Therefore, an alternative interpretation of $\delta^{13}C_{org}$ is required. In order to develop an alternative interpretation for $\delta^{13}C_{org}$, factors influencing the carbon isotope signature of organic material in the sediment record from GSL1 were evaluated.

$\delta^{13}C_{org}$ in lake sediment is primarily determined by the $\delta^{13}C$ of the dissolved inorganic carbon source ($\delta^{13}C_{DIC}$). Processes controlling the $\delta^{13}C_{DIC}$ include the source and supply of inorganic carbon (e.g., from catchment runoff), ^{13}C-enrichment from preferential uptake of ^{12}C by phytoplankton during photosynthesis, isotopic exchange with atmospheric CO_2, recycling of ^{13}C-depleted CO_2 from respiration/decay of water column and bottom sediment organic matter, and uptake of bicarbonate ($HCO_3^-{}_{(aq)}$) at elevated pH (Wolfe et al., 2000).

Recent studies in the upstream PAD by Light (2010) and Lyons (2010) provide a basis for interpretation of $\delta^{13}C_{org}$ in lake sediment core records. Investigation of water chemistry in PAD lakes of varying hydrologic classifications (open-drainage, closed-drainage and restricted-drainage) by Lyons (2010) revealed that at the beginning of the open-water season (May), closed-drainage basins had much higher dissolved inorganic carbon (DIC) concentration than open- and restricted-drainage basins (Figure 26). Early season productivity, as indicated by chlorophyll *a* values, was also greatest in the closed-drainage basins early in the open-water season (Figure 25). Lyons (2010) observed that in early spring, $\delta^{13}C_{phytoplankton}$ of closed-drainage basins was lower than the open-drainage basins (Figure 26). This is opposite what might be anticipated, as higher productivity would be expected to cause an increase in the $\delta^{13}C_{phytoplankton}$ of closed-drainage basins within the PAD which are more productive than open-drainage basins (Hall et al., 2004). The lower $\delta^{13}C_{phytoplankton}$ values in closed-basins was attributed to high DIC concentrations allowing for high carbon isotope fractionation between the DIC and phytoplankton (Figure 26), as is typically observed when carbon is not limiting (Keeley and Sandquist 1992). The low $\delta^{13}C_{phytoplankton}$ values of closed-drainage lakes observed in the early spring may translate to lower $\delta^{13}C_{org}$ values in the sediment record of these lakes in comparison to sediments deposited in open-drainage lakes.

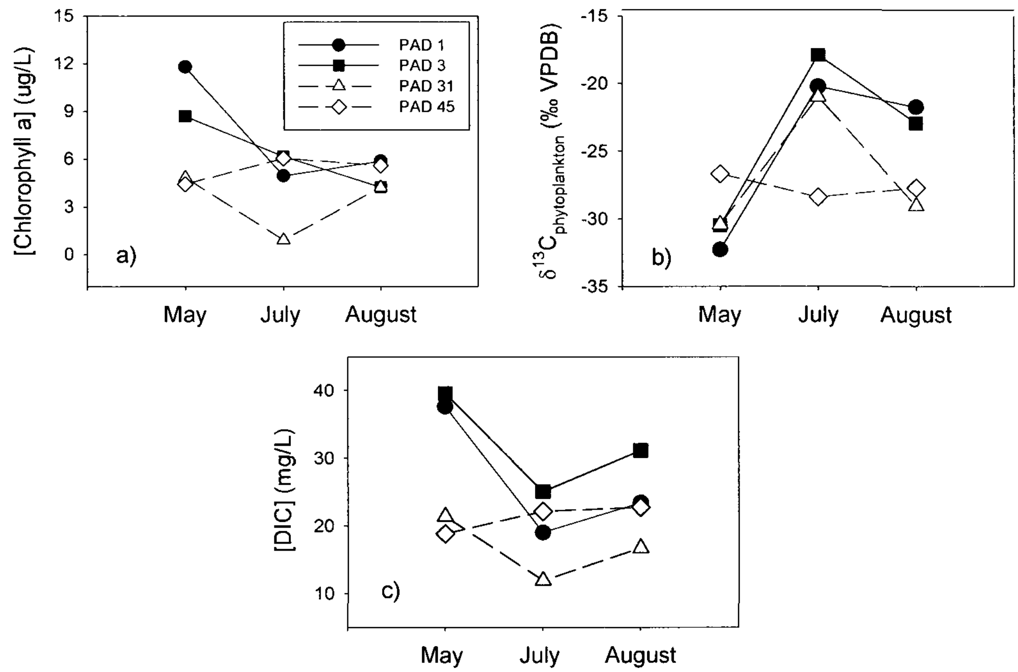

Figure 26 Spatial and temporal variability of a) concentration of chlorophyll a, b) carbon isotope composition of phytoplankton and c) concentration of DIC from four PAD lakes based on samples from the 2007 open-water season and the spring of 2008 The May values represent an average of the 2007 and 2008 data Drainage type is indicated by symbol type closed-drainage basins are solid, restricted-drainage basin is shaded, and open- drainage basin is an open symbol (from Lyons, 2010)

Insight into the controlling factors influencing carbon isotope dynamics in PAD lakes by Lyons (2010) has been used by Light (2010) to interpret a lake sediment $\delta^{13}C_{org}$ record from PAD1, a closed-drainage lake. Multi-proxy paleolimnological analysis has revealed westward expansion of Lake Athabasca into the low lying interior of the PAD during the Little Ice Age (LIA), a period of increased summer discharge in the Peace-Athabasca system (Wolfe et al., 2008a; Sinnatamby et al., 2010; Johnston et al., 2010). Light (2010) developed a ~600-year $\delta^{13}C_{org}$ record for PAD 1 (Figure 27) which was situated at the margin of Lake Athabasca water levels during the LIA. $\delta^{13}C_{org}$ values at the top and bottom of the PAD1 record were lower than those during the LIA (~1600 AD to ~1900 AD) (Figure 27). High $\delta^{13}C_{org}$ values during the LIA correspond to a variety of parameters that suggest open-drainage conditions at PAD1 as a result of Lake Athabasca inundation (Johnston et al., 2010). This suggests that the early season $\delta^{13}C_{phytoplankton}$ signature is captured in the lake sediment of PAD1 and that $\delta^{13}C_{org}$ signatures during highly productive closed-drainage conditions within the PAD can be significantly lower than intervals of open-drainage conditions.

PAD1 and GSL1 are both closed-drainage basins and are hydrologically isolated from lake or river influence. These basins have noticeable similarities in their $\delta^{13}C_{org}$ stratigraphic records. Both profiles are characterized by low $\delta^{13}C_{org}$ values at the top of the record and high values during the LIA (Figure 27). The low values at the top of the GSL1 record correspond to closed-drainage conditions, similar to PAD1. Therefore, it appears that the early season $\delta^{13}C_{phytoplankton}$ signature captured in the lake sediment of PAD1 is also captured in the sediment of GSL1. Interpreting high GSL1 $\delta^{13}C_{org}$ values to correspond with open-drainage conditions, is consistent with interpretation of fluvial, open-drainage conditions below the sediment contact and is also consistent with diatom and $\delta^{18}O_{lw}$ records that suggest GSL1 has experienced three hydrologic shifts in the past ~1200 years (Figure 27).

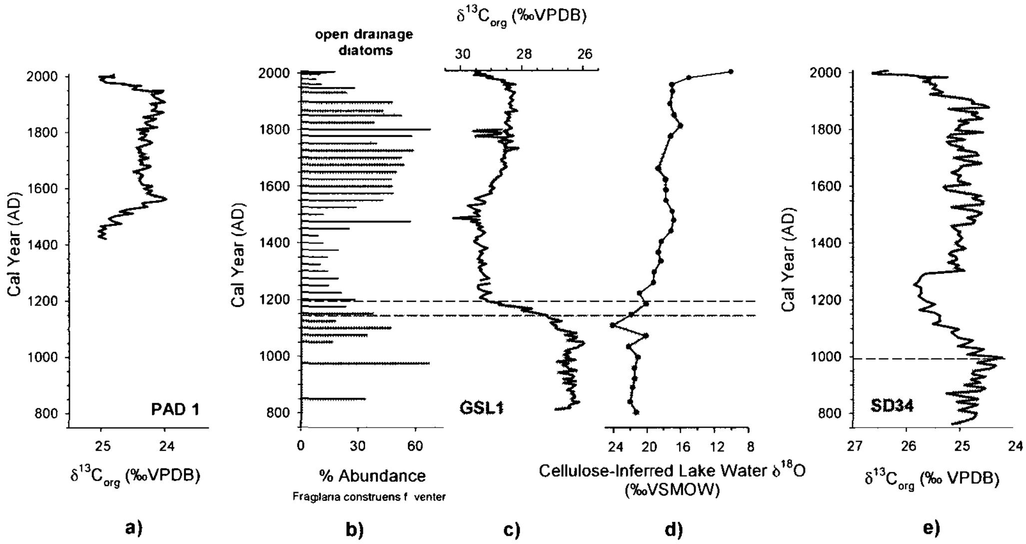

Figure 27 Comparison of $\delta^{13}C_{org}$ records from three closed-drainage basins a) PAD1 $\delta^{13}C_{org}$ record (from Light, 2010), b) GSL1 open-drainage diatom indicator record, c) GSL1 $\delta^{13}C_{org}$ record, d) GSL1 cellulose-inferred lake water $\delta^{18}O$ record and e) SD34 $\delta^{13}C_{org}$ record Shaded intervals indicate open-drainage conditions Dashed black lines indicate sediment contacts for GSL1 (gradational contact) and SD34 (abrupt contact)

SD34 is classified as a closed-drainage basin and is currently hydrologically similar to both GSL1 and PAD1. The SD34 $\delta^{13}C_{org}$ profile shows some similarities to the $\delta^{13}C_{org}$ profile profiles from GSL1 and PAD1 (Figure 27). Low $\delta^{13}C_{org}$ values at the top of the SD34 record that correspond to closed-drainage conditions suggest that, similar to GSL1 and PAD 1, the early season $\delta^{13}C_{phytoplankton}$ signature is captured in the lake sediment. It is then likely that low $\delta^{13}C_{org}$ values in the SD34 record correspond to closed-drainage conditions and high values correspond to open-drainage conditions. The interpretation of high $\delta^{13}C_{org}$ values below the contact of SD34 is consistent with other geochemical parameters that suggest fluvial, open-drainage conditions. However, the $\delta^{13}C_{org}$ record of SD34 suggests a second interval of change above the contact. New interpretation of the

SD34 $\delta^{13}C_{org}$ record suggests a re-emergence of open-drainage conditions at ~1300 AD that is not captured by any other geochemical parameter in the SD34 record.

5.4 Paleohydrology of the Slave River and Great Slave Lake over the Past Millennium

New understanding of GSL1 and SD34 $\delta^{13}C_{org}$ records contribute to developing a ~1200-year paleohydrologic reconstruction of the Slave River and GSL. The paleohydrology of the PAD, an upstream delta similar to the SRD that has been extensively studied will be used to compare with paleohydrologic interpretation downstream. Discussion of the paleohydrologic record of the Slave River and GSL is separated into five time intervals based on interpreted hydrologic change at the study basins and are discussed in chronological order: Early Medieval Period, Medieval Period, Late Medieval Period, Little Ice Age and Post Little Ice Age.

5.4.1 Early Medieval Period (~750 AD to ~1150 AD)

At the beginning of the last millennium, the climate at the headwaters of the Peace-Athabasca river system was characterized by warm winter temperatures and high growth season relative humidity of the MP (Edwards et al., 2008). The warm climate was coupled with a spring melt of annual snowpack that was too rapid to adequately sustain streamflow, which caused low summer discharge through the Peace-Athabasca river system (Edwards et al., 2008; Wolfe et al., 2008a). The rapid melt of the annual snowpack in the headwaters of the Peace-Athabasca river system caused a very large, but "flashy" spring freshet (Wolfe et al., 2008a). Because the Peace and Athabasca rivers are major tributaries of the Slave River, it is likely that a flashy freshet occurred downstream as well. Additionally, research by Jarvis (2008) has identified the MP as a time of high ice-jam flood frequency in the PAD. Years of increased ice-jam flood frequency in the PAD have been shown to correspond to similar conditions downstream in the SRD (Mongeon, 2008; Brock et al., 2010). Therefore, it is likely that during the Early MP, ice-jam flood frequency at the SRD was also high. Frequent ice-jam flood events coupled with a large flashy spring freshet early in the last millennium could deliver river water, heavily laden with inorganic sediment to SRD lakes and could account for fluvial depositional environments below the contacts of SD34 and GSL1. $\delta^{13}C_{org}$ values below the contact in SD34 (-25.9‰ to -24.2‰) are similar to those measured from Slave River flood sediment (-24.6‰) by Brock et al. (2010), suggesting frequent Slave River flooding at SD34 Frequent Slave River flooding at GSL1 at the beginning of the last millennium is supported by laminations in the basal sediment as well as high abundances of open-drainage indicator diatoms. Additionally, $\delta^{18}O_{lw}$ values below the contact are low (-24.0‰ to -20.2‰) (Figure 28), likely reflecting water that has undergone minimal evaporative isotopic enrichment characteristic of an open-drainage basin. However, $\delta^{18}O_{lw}$ values below the contact of GSL1 (-24.1‰ to -20.2‰) that are noticeably lower than contemporary Slave River values (-17.7‰ to -19.2‰) may represent a Slave River $\delta^{18}O$ signature that is more depleted than the present, possibly due to increased snowmelt runoff from headwater regions.

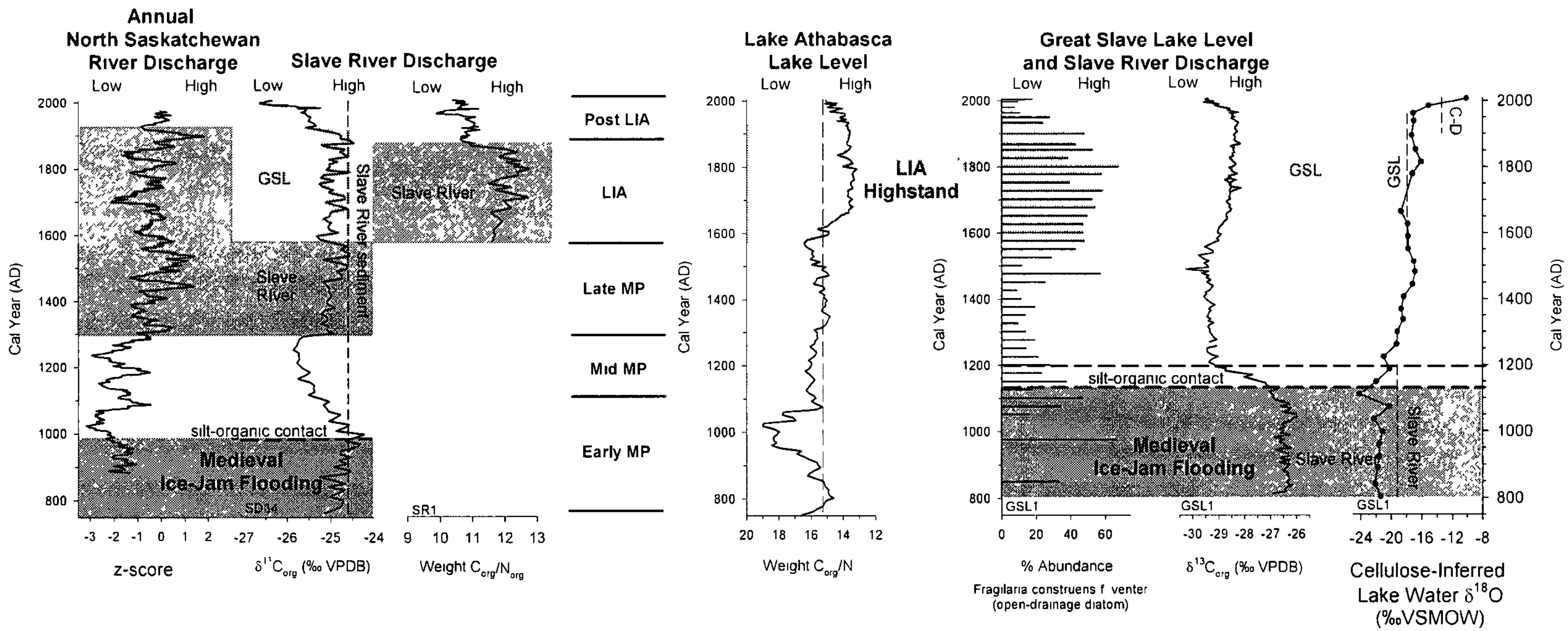

Figure 28 Records of Slave River discharge (SD34 and SR1) compared to modeled North Saskatchewan River discharge (Model 1)(Case and MacDonald, 2003) and Great Slave Lake level record compared to Lake Athabasca lake level record (Bustard Island North Pond C/N ratios) (Wolfe et al , 2008a) SD34 Slave River discharge developed using $\delta^{13}C_{org}$ values (vertical dashed line indicates the $\delta^{13}C_{org}$ (-24 6‰) of 2005 Slave River flood sediment (Brock et al , 2010)), SR1 Slave River discharge record developed using C/N ratios and GSL1 Great Slave Lake level record developed using $\delta^{18}O_{lw}$, $\delta^{13}C_{org}$ values and open drainage diatom indicators Vertical dashed lines within $\delta^{18}O_{lw}$ record indicate $\delta^{18}O$ values of the Slave River (-19 2‰), GSL (-17 9‰) and an average value for closed-drainage lakes in the SRD (-13 4‰) (Brock et al , 2007) Dark grey shaded intervals denote open-drainage conditions because of direct inundation of SD34 and GSL1 by the Slave River Light grey shaded intervalsfor SD34and GSL1 denote open-drainage conditions caused by high GSL water levels during the LIA

5.4.2 Middle Medieval Period (~1150 AD to ~1300 AD)

Slave River influence on the hydrology of GSL1 and SD34, indicated by fluvial conditions depositing inorganic sediment, appears to end at the mineral-organic contact common to both sites. Isolation from Slave River flooding is characterized by a change in sediment composition from mineral-rich to organic-rich, accompanied by shifts in all geochemical parameters above the contacts of SD34 (~1000 AD) and GSL 1 (~1150 AD to ~1200 AD) and likely represents a shift to a lacustrine depositional environment.

$\delta^{13}C_{org}$ in SD34 declines to values lower than Slave River sediment after ~1000 AD and GSL1 open-drainage diatom indicators decline after ~1150 AD suggesting a reduced influence of Slave River flooding on the two study sites above their respective contacts (Figure 28). Increased $\delta^{18}O_{lw}$ values at GSL1 above the contact indicate increased evaporation, further supporting a reduction in Slave River flood waters entering GSL1 above the contact. However, ice-jam flooding upstream in the PAD remains high until the end of the MP (Jarvis, 2008; Wolfe et al., 2008a), ~400 years later than reduced SRD ice-jam flood frequency suggested by the hydrologic isolation of SD34 and GSL1.

Chronological uncertainties within the SD34 and GSL1 sediment records could account for a temporal offset in the establishment of closed-drainage conditions between the SRD sites and the PAD. However, uncertainties in chronological modeling of GSL1 and SD34 are likely not large enough to account for a ~400 year offset. Geomorphologic setting of SD34 and GSL1 could account for the ~400 year offset, as the SRD sites may have had higher sill elevations than the PAD sites, making them less susceptible to river flooding. Additionally, shifts in distributary channel routing within the SRD may have contributed to the isolation of the basins during the Middle MP.

Reduced hydrological influence of the Slave River at the contacts of SD34 (~1000 AD) and GSL 1 (~1150 AD to ~1200 AD), however, does occur during an interval (~1000 AD to ~1300 AD) of low reconstructed North Saskatchewan River discharge inferred from tree-ring records (Case and MacDonald, 2003) (Figure 28). The North Saskatchewan River shares headwaters with the Peace-Athabasca-Slave river system, in the Columbia Icefields in the eastern Rocky Mountains. The Athabasca Glacier at the head of the Athabasca River is only ~6 km from the Saskatchewan Glacier, a key headwater source for the North Saskatchewan River. Therefore, the discharge histories of these two river systems are likely to be similar.

Middle MP closed-drainage conditions at SD34 (~1000 AD to ~1300 AD) parallels low North Saskatchewan River discharge as well as an interval of Rocky Mountain glacier expansion during the MP (~1100 AD to ~1380 AD) outlined by Edwards et al. (2008) and the "Medieval Megadrought" (~900 AD to ~1300 AD), a period of widespread hydrologic drought throughout western North America (Cook et al., 2004; Meko et al., 2007). Glacier expansion may have reduced inflow to glacier-sourced rivers such as the North Saskatchewan, Peace, Athabasca and Slave. Therefore, glacier expansion coupled with drought conditions within the Slave River basin, likely reduced Slave River discharge similar to the North Saskatchewan River and may have contributed to the establishment of closed-drainage conditions at SD34 and GSL1.

The emergence of closed-drainage conditions at SD34 (~1000 AD) precedes similar closed-drainage conditions at GSL1 by ~140 years (Figure 28). The apparent delay in the isolation of GSL1 could be the result of uncertainties within the extrapolation of both SD34 and GSL1 chronologies. However, the ~140-year offset may alternatively represent a delay in GSL1 isolation from Slave River influence, possibly due to the hydrologic setting of GSL1 in the landscape. GSL1 is a relict river channel and may have been connected to the main drainage network of the Slave River during the early MP by a small channel active during high water periods. Evidence of other relict river channels that lead back to the Slave River can be observed a short distance north of GSL1 (Figure 24). Therefore, GSL1 may have been temporarily connected to these channels during frequent ice-jam flooding below the gradational sediment contact (~800 AD to ~1150 AD), as is suggested by laminations and the $\delta^{13}C_{org}$, $\delta^{18}O_{lw}$ and open-drainage diatom indicator records. A channel connecting GSL1 to the main drainage network of the Slave River may account for the ~140 year delay in isolation of GSL1 compared to SD34, indicating that early MP ice-jam flooding was prolonged at GSL1 because its hydrogeomorphological setting was more susceptible to flooding than SD34. Additionally, the gradational contact of GSL1 (~1150 AD and ~1200 AD) may also suggest that isolation of the basin occurred more gradually than at SD34, which had a much more abrupt sediment contact suggesting a sudden change in hydrological conditions.

5.4.3 Late Medieval Period (~1300 AD to ~1550 AD)

Closed-drainage conditions during the Middle MP at SD34 appear to end at ~1300 AD as $\delta^{13}C_{org}$ values shift back to values similar to Slave River flood sediment (Figure 28). High $\delta^{13}C_{org}$ values in the SD34 record indicate that a second period of open-drainage conditions occurred between ~1300 AD ~1918 AD. The change in the hydrology of SD34 at ~1300 AD suggested by the $\delta^{13}C_{org}$ record corresponds to increasing North Saskatchewan River discharge as indicated by the Case and MacDonald (2003) record (Figure 28) North Saskatchewan River discharge increased to some of the highest levels observed in the last millennium at the end of the 11^{th} century and remained high from the late MP-LIA transition to the end of the Little Ice Age (LIA) (~1300 AD to ~1900 AD) (Figure 28). The increase in discharge at this horizon is likely in response to cooler climatic conditions during the transition from the Late MP to LIA, resulting in a more prolonged melt of the annual snowpack in the eastern Rocky Mountains (Case and MacDonald, 2003; Edwards et al., 2008). High North Saskatchewan River discharge coupled with the re-emergence of open-drainage conditions at SD34 suggests that Slave River discharge was high throughout the Late MP.

5.4.4 Little Ice Age (~1550 AD to ~1860 AD)

The SD34 $\delta^{13}C_{org}$ record suggests that Slave River discharge becomes high during the Late MP and the sediment record of SR1 that spans ~480 years indicates that it remained high throughout the LIA. High C/N values suggest allochthonous deposition of organic material at SR1 between ~1550 AD and ~1860 AD, indicating a fluvial depositional environment (Figure 28). Since SR1 is located on an island in the Slave River upstream of the SRD and has no apparent inlets or outlets, it is expected that the basin would only receive Slave River flood water during a period of anomalously high discharge. Therefore, a fluvial depositional environment at SR1 between ~1550 AD and ~1860 AD suggests that during the LIA, Slave River discharge was considerably higher than present.

The onset of a second interval of open-drainage conditions at GSL1 during the LIA occurs ~250 years later than a similar re-emergence of open-drainage conditions at SD34. The shift to open-drainage conditions in GSL1 is indicated by high $\delta^{13}C_{org}$ values between ~1550 AD and ~1960 AD that correspond to increased open-drainage diatom abundance and $\delta^{18}O_{lw}$ values (-17.8‰ to -17.0‰) similar to that of GSL (-17.9‰) (Brock et al., 2007) (Figure 28). $\delta^{18}O_{lw}$ values similar to GSL and open-drainage conditions indicated by $\delta^{13}C_{org}$ and increased abundance of open-drainage diatoms appear to parallel increased Lake Athabasca water levels during the LIA (Wolfe at al., 2008a; Sinnatamby et al., 2010; Johnston et al., 2010) (Figure 28). Because Lake Athabasca and GSL are both large reservoirs within the same river system, it is likely that high LIA Lake Athabasca water levels would correspond to high LIA GSL water levels. Therefore, the re-emergence of open-drainage conditions during the LIA at GSL1 appears to represent inundation of GSL1 by GSL levels that are considerably higher than the present. This is the first evidence that GSL experienced a high-stand during the LIA, similar to that of Lake Athabasca and that the high-stand may have occupied the strandline visible in the landscape to the south of the SRD (Figure 3).

The approximate elevation range of GSL1 (between 161 masl and 163 masl) is between ~3.6 m and ~5.6 m above the highest gauged GSL water level (~157.4 masl) (Gibson et al., 2006a) (Figure 7), indicating that GSL water levels during the LIA would have to be at least ~3.6 m higher than the present to inundate GSL1. GSL water levels ~3.6 m greater than the present would be slightly larger than the average lake level change estimated for Lake Athabasca (2.3 m) during the LIA (Johnston et al., 2010). An increase in GSL water levels by at least 3.6 m would not only have inundated GSL1, but would have also inundated SD34 because the approximate elevation of SD34 (~159 masl) is lower than GSL1 (Figure 7). This would suggest that during the LIA, SD34 was inundated by GSL. It is likely that open-drainage conditions in SD34 at the transition from late MP to LIA were initially the result of high Slave River water levels inundating the lake and that during the LIA (~1550 AD to ~1960 AD), elevated GSL lake levels began to inundate SD34. Additionally, the strandline observed in the landscape to the south of the SRD intersects GSL1 across its western end (Figure 3), suggesting that at present, it may have a similar elevation as GSL1. Therefore, the high-stand of GSL that inundated both GSL1 and SD34 during the LIA would likely have occupied the strandline as well.

The C/N record of SR1 indicates high water levels in the Slave River during the LIA. Because the water level of GSL is strongly influenced by riverine input and output (Gibson, 2006a), prolonged high Slave River discharge would expectedly raise lake levels. However, the large outlet at the mouth of the Mackenzie River results in water residence times that are relatively short for a lake the size of GSL (Gibson et al., 2006). These short residence times likely act to slow lake level rise in response to increased Slave River discharge. For GSL to inundate GSL1, Slave River input to the lake would likely have been high well before the onset of open-drainage conditions in GSL1 at ~1550 AD. The $\delta^{13}C_{org}$ record of SD34 suggests that Slave River discharge increased at ~1300 AD and remained high throughout the Late MP. Therefore, because GSL water level is closely linked to Slave River input it is likely that GSL water level began to rise at ~1300 AD and that ~250 years of high Slave River discharge elevated GSL water levels enough to inundate GSL1 throughout the LIA. In order to inundate GSL1, GSL water levels would have to increase ~3.6 m in ~250 years, at an average annual rate of ~0.01 m/year. An increase of GSL water levels by ~0.01 m/year is considerably less than typical GSL annual water level fluctuations (0.4 m) (Gibson et al., 2006), suggesting that the estimated rate of lake level rise is plausible.

5.4.5 Post Little Ice Age (~1860 AD to ~2007 AD)

Interpretation of SR1, SD34 and GSL1 sediment records characterize the LIA as an interval of high discharge within the Slave River-GSL system. Alternatively, the sediment records of all three sites suggest that the transition from the LIA to the 20th century is characterized by declining water levels. C/N ratios similar to those expected from an autochthonous source suggest a shift in depositional environment at SR1 from fluvial to lacustrine at the onset of the 20th century (Figure 28). A lacustrine depositional environment at SR1 indicates isolation of the basin due to declining Slave River discharge. As well, declining $\delta^{13}C_{org}$ values after ~1918 AD in SD34 suggest closed-drainage conditions as a result of reduced Slave River discharge and GSL water level (Figure 28). In the GSL1 record, declining $\delta^{13}C_{org}$ values and open-drainage diatom indicator abundance (Figure 28) also suggest closed-drainage conditions early in the 20th century, likely the result of lower GSL water levels. 20th century GSL lake levels that are lower than the LIA are also indicated by GSL1 $\delta^{18}O_{lw}$ values (-15.1‰ to -10.1‰) that diverge from values similar to GSL and become similar to present-day measurements from closed-drainage basins in the SRD (Figure 28) (-16.2‰ to -10.6‰; Brock et al., 2007).

Declining Slave River discharge as indicated by multi-parameter paleolimnological analysis corresponds to similar declines in discharge reconstructed for the North Saskatchewan (Case and MacDonald, 2003), Peace and Athabasca rivers (Schindler and Donahue, 2006; Wolfe at al., 2008a) at the onset of the 20th century. Reduced summer discharge through these river systems is thought to be the result of warmer 20th century climate causing a flashy spring freshet that is significantly lower in magnitude than that observed during the MP (Wolfe et al., 2008a). A low-magnitude, flashy spring freshet coupled with low summer discharge in the Slave River at the onset of the 20th century appears to have caused SR1 to become isolated from riverine influence. The $\delta^{13}C_{org}$, $\delta^{18}O_{lw}$ and open-drainage diatom records of GSL1 coupled with the $\delta^{13}C_{org}$ record of SD34 indicate closed-basin conditions in the 20th century (Figure 28). This indicates that GSL water levels have declined since the end of the LIA in response to reduced Slave River discharge, resulting in the hydrological isolation of GSL1 and SD34. Declining GSL levels throughout the 20th century is consistent with declines in riverine input from the Slave River suggested by SR1 as well as declining Lake Athabasca water levels throughout the 20th century as indicated by Wolfe et al. (2008a), Sinnatamby et al. (2010) and Johnston et al. (2010).

Analysis of lake sediment from SD34, GSL1 and SR1 suggests that water levels in the Slave River system have varied considerably over the past ~1200 years. Water levels declined throughout the 20th century from millennial high levels reconstructed for the LIA. Low water levels throughout the 20th century and the beginning of the 21st century have resulted in closed-drainage conditions at the three study sites. In the past ~1200 years, closed-drainage conditions appear to occur only twice at SD34 and GSL1: from the

20th century to the present and during the MP. This suggests that currently, hydrological conditions within the Slave River system may have become similar to that of the Middle MP. However, high $\delta^{18}O_{lw}$ values throughout the 20th century at GSL1 that are unique within the record may suggest that hydrological conditions at this site are unprecedented over last ~1200 years.

Chapter 6 - *Conclusions*

6.1 Summary

Multi-proxy analysis of lake sediment cores collected from SD34, GSL1 and SR1 provided a ~1200-year record of water level variation within the Slave River and Great Slave Lake. Sediment composition and elemental and stable isotope geochemistry proved to be sensitive indicators of hydrologic change for the three study basins. This study was also able to highlight complexities inherit in the interpretation of lake sediment records of C/N ratios and $\delta^{13}C_{org}$ values.

Interpretation of lake sediment C/N ratios and $\delta^{13}C_{org}$ values from SD34, GSL1 and SR1 revealed that conventional, straightforward interpretation of these commonly applied paleolimnological measurements is not always appropriate. Conventional interpretation suggests that high C/N ratios (>10) correspond to an allochthonous source of organic material. However, interpretation of the high ratios above the contacts of SD34 and GSL1 using a conventional approach contradicted all other measured parameters. Interpretations from other geochemical parameters measured at the two study sites revealed that C/N ratios of autochthonous organic matter were elevated due to nitrogen limitation at GSL1 and diagenesis at SD34. Conventional interpretation of $\delta^{13}C_{org}$ suggests that high values correspond to high productivity (Schelske and Hodell, 1991; Hodell and Schelske, 1998; Meyers and Teranes, 2001). Interpreting the SR1 $\delta^{13}C_{org}$ record in this way appeared appropriate, however similar interpretation of the SD34 and GSL1 $\delta^{13}C_{org}$ records contradicted interpretations of all other measured parameters. $\delta^{13}C_{org}$ records from SD34 and GSL1 were both deemed sensitive records of hydrologic change only after new understanding of sediment $\delta^{13}C_{org}$ from upstream in the PAD provided a basis for non-conventional interpretation.

Interpretation of geochemical parameters such as C/N ratios, $\delta^{18}O_{lw}$ and $\delta^{13}C_{org}$ in conjunction with sediment composition indicated riverine inundation of SD34 (~760 AD to ~1000 AD) and GSL1 (~800 AD ~1200 AD) during the Early MP. River inundation of SD34 and GSL1 before the last millennium was attributed to Slave River discharge dominated by a large flashy spring freshet and high ice-jam flood frequency that delivered riverine sediment to the two study lakes. These hydrologic conditions are similar to that reconstructed for the upstream PAD and were likely caused by warm MP climate resulting in early, rapid melt of snowpack in headwater regions (Wolfe et al., 2008a; Jarvis, 2008).

A shift from a fluvial to lacustrine depositional environment at the contacts of SD34 (~1000 AD) and GSL1 (~1150 AD to ~1200 AD) appeared to mark a shift to closed-drainage conditions early in the last millennium. Closed-drainage conditions at SD34 coincided with the "Medieval Megadrought" (~900 AD to ~1300 AD), a period of widespread hydrologic drought throughout western North America (Cook et al., 2004; Meko et al., 2007) and corresponded to an interval of extremely low North Saskatchewan River discharge reconstructed by Case and MacDonald (2003). Drought conditions in western North America coupled with low North Saskatchewan River discharge likely correspond to low annual Slave River discharge from ~1000 AD to ~1300 AD. Low Slave River discharge may have contributed to the onset of closed-drainage conditions by reducing the impact of ice-jam flood events at SD34 and GSL1. However, reduced ice-jam flood frequency indicated by closed-drainage conditions at SD34 and GSL1 precede similar conditions in the PAD by ~400 years. Different geomorphic settings between SRD and PAD sites, shifts in the distributary channel network of the SRD and low Slave River discharge likely combined to account for the ~400 year offset and explain why SD34 and GSL1 became isolated during the MP when ice-jam flood frequency was high (Jarvis, 2008)

Low Slave River discharge appeared to end at ~1300 AD with a re-emergence of open-drainage conditions indicated by the SD34 $\delta^{13}C_{org}$ record. Open-drainage conditions were attributed to high Slave River discharge inundating SD34 throughout the Late MP. High Slave River discharge appeared to continue throughout the LIA as the SR1 sediment record identified high discharge from ~1550 AD to ~1863 AD. These records indicate that Slave River discharge increased through the transition from Late MP to LIA and that discharge remained high throughout the LIA (Figure 29). Increased discharge was attributed to a delay in snowmelt generated runoff that sustained higher annual river discharge as a result of a shift to cooler climate conditions characteristic of the LIA (Wolfe et al., 2008a)

Cooler LIA climate and increased Slave River discharge appeared to cause high water levels in GSL during the LIA, similar to that observed upstream in Lake Athabasca (Sinnatamby et al., 2010, Johnston et al., 2010). Open-drainage diatom indicator abundance and $\delta^{13}C_{org}$ records of GSL1 indicated open-drainage conditions in GSL1 throughout the LIA and $\delta^{18}O_{lw}$ values that were similar to GSL suggested that the open-drainage conditions were the result of GSL inundation. GSL inundation of GSL1 during the LIA further indicated that the GSL strandline visible to the landscape south of the SRD was likely been occupied during the LIA. Therefore, the SD34, SR1 and GSL1 sediment records indicated that GSL water levels began to rise at ~1300 AD as a result of elevated Slave River discharge at the transition from MP to LIA, reaching maximum levels during the LIA.

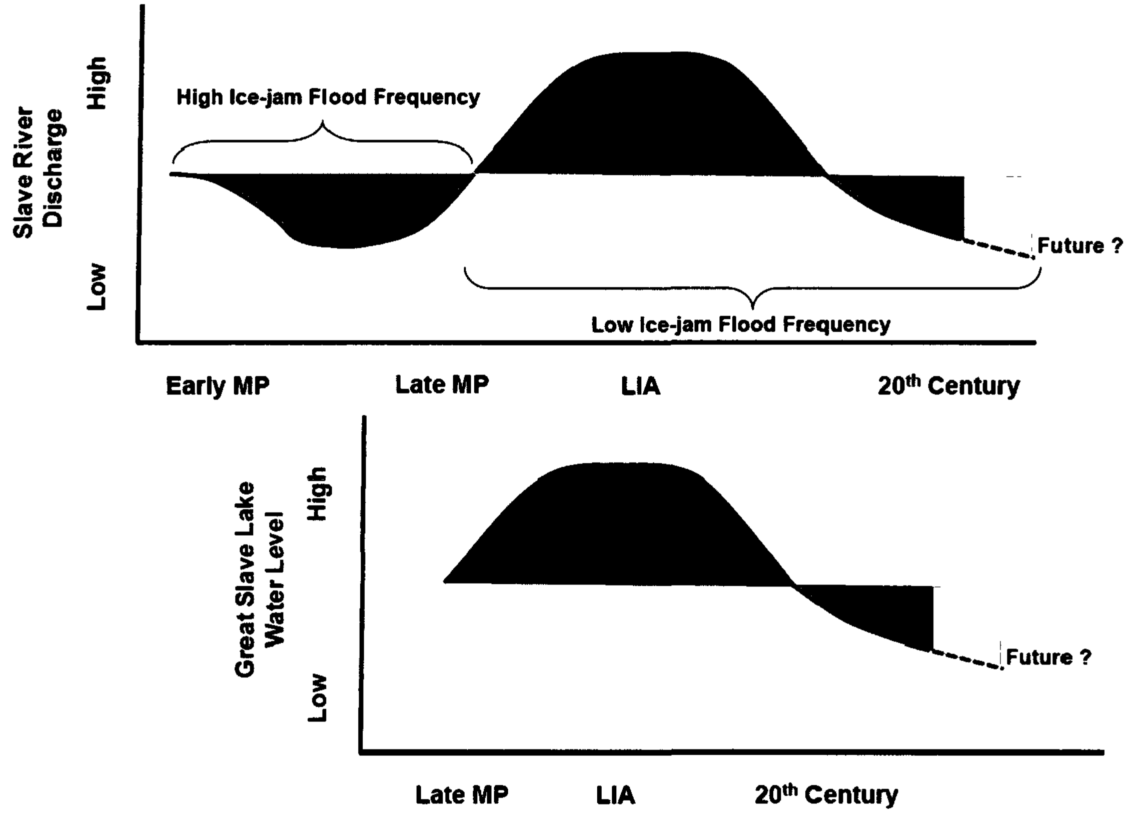

Figure 29. ~1200 year variation of Slave River discharge and multi-centennial change in Great Slave Lake water level. Schematic discharge profile is based on paleohydrologic records from SRD study sites GSL1, SD34 and SR1. Future discharge (dashed line) is based on expected discharge trends for upstream Peace and Athabasca rivers (Barnett et al, 2005; Wolfe et al., 2008a) Schematic water level profile is based on interpretation of GSL1 sediment record.

Millennial high water levels within the Slave River system during the LIA declined at the beginning of the 20th century (Figure 29). A decline in Slave River discharge at the onset of the 20th century appears to be captured in the SR1 and SD34 sediment records as a re-establishment of closed-drainage conditions. A decline in discharge through the Slave River system at the end of the LIA is further supported by $\delta^{18}O_{lw}$ and $\delta^{13}C_{org}$

records of GSL1 that suggest isolation of the basin from GSL likely due to 20^{th} century declines in GSL lake level (Figure 29).

20^{th} century decline in discharge parallels a shift to a warmer climate regime that has been shown to cause an earlier, more rapid melt of the spring snowpack in the headwaters of the Peace and Athabasca rivers (Wolfe et al., 2008a). The sediment records of the three study lakes indicated that water levels within the Slave River system have declined from the high levels that characterized the LIA, falling to levels potentially similar to the Middle MP. However, high $\delta^{18}O_{lw}$ values throughout the 20^{th} century at GSL1 that are unique within the ~1200 record may suggest that hydrological conditions at this site are unprecedented in the last ~1200 years.

These findings are able to establish a link between hydrologic conditions within the Slave River system and those upstream in the PAD and Lake Athabasca. Sediment records from SD34, GSL1 and SR1 demonstrated that in response to shifting climate regimes, the hydrology of the Slave River system responded broadly similar to the PAD. This indicates that hydrologic change upstream in the headwaters of the Slave River has historically translated downstream to the SRD and GSL. River discharge in the Peace-Athabasca river system is expected to continue to decline throughout the 21^{st} century as a result of reduced glacier extent and snow pack depth in its headwater regions (Wolfe et al., 2008a). Therefore, Slave River discharge and GSL water levels that have declined over the last ~200 years are also likely to continue declining throughout the next century, possibly reaching levels unprecedented in the last ~1200 years, if such levels have not already been reached.

6.2 Management Implications

This study has established a ~1200-year paleohydrologic record for the Slave River and GSL. It has shown the interconnectedness in the hydrology of the SRD and PAD and has been able to demonstrate how the Slave River system responds to changes in climate. Although climate and water levels in the Slave River system appear to have returned to those similar to the Middle MP (increasing winter temperatures, growth season relative humidity, flashy spring freshet and lower discharge), it is likely that the flashy freshet will be considerably smaller than earlier in the millennium (Wolfe et al., 2008a). Snowpack depth and alpine glaciers in Peace-Athabasca-Slave river headwater regions that have historically contributed to annual flow have been shown to be in decline (Barnett et al., 2005; Lapp et al., 2005; Rood et al., 2005). A decline in source water entering the Peace-Athabasca-Slave system that is expected to continue would suggest that water levels may be heading toward unprecedented low levels in the context of the last millennium.

Declining streamflow will likely amplify current challenges in the management of water within Peace-Athabasca-Slave system as various stakeholders depend on this water resource. As the water available for stakeholder use declines, balancing the natural environment, water supply for hydroelectric facilities and consumptive use by humans will be a major challenge for future management of this river system. Of principle concern is the Athabasca Tar Sands development, which continues to expand, removing water from the Athabasca River for use in oil extraction. If declining streamflow in the Peace-Athabasca-Slave system is not managed carefully in the future, it may lead to unprecedented water shortages throughout the basin.

6.3 Future Recommendations

The ~1200-year hydrologic record for the Slave River system could be strengthened in a variety of ways. Interpretation of C/N ratios from GSL1 attributed elevated ratios to nitrogen limitation and pigment analysis of GSL1 sediment could be used to test this hypothesis. Additionally, establishing a diatom record for SD34 would supplement geochemical parameters and may possibly strengthen SD34 $\delta^{13}C_{org}$ interpretation.

Because GSL1 appears to lie at the margin of the LIA GSL high-stand, the GSL1 water level record only represents maximum GSL levels. Sampling several other lakes south of GSL1 that are closer to the GSL shoreline would provide insight into the timing, rate and extent of GSL expansion during the LIA. As well, locating a study site on GSL similar to the Bustard Island North Pond on Lake Athabasca (Wolfe et al., 2008a; Johnston et al., 2010) would most likely provide a more detailed long-term record of GSL water level change. The record of GSL water level established in this thesis is based on high-water intervals, thus a record that captures low-water intervals (such as the Bustard Island North Pond record) would improve understanding of long-term GSL hydrology.

References

Appleby, P.G., 2001. Chronostratigraphic Techniques in Recent Sediments. In Tracking Environmental Change Using Lake Sediments: Volume 1: Basin Analysis, Coring, and Chronological Techniques, Developments in Paleoenvironmental Research. W.M. Last and J.P. Smol (Eds). Kluwer Academic Publishers, Dordrecht, pp 171-203.

Atlas of Canada, 6th Edition, 2006. 85H4.

Barnett, T.P., Adam, J.C., Lettenmaier, D.P., 2008. Human-induced changes in the hydrology of the western United States, Science, 319: 1080–1083.

Bennett, R.M., 1970. Lake Athabasca Water Levels 1930-1970. Water Survey of Canada.

Bernasconi, S.M., Barbieri, A., Simona, M., 1997. Carbon and nitrogen isotope variations in sedimenting organic matter in Lake Lugano. Limnology and Oceanography, 42: 1755-1765.

Birks, S.J., Edwards, T.W.D., Gibson, J.J., Drimmie, R.J., Michel, F.A., 2004. Canadian Network for Isotopes in Precipitation http://www.science.uwaterloo.ca/~twdedwar/cnip/cniphome.html.

Björk, S., Wohlfarth, B., 2001. ^{14}C Chronostratigraphic Techniques in Paleolimnology. In Tracking Environmental Change Using Lake Sediments: Volume 1: Basin Analysis, Coring, and Chronological Techniques, Developments in Paleoenvironmental Research. W.M. Last and J.P. Smol (Eds). Kluwer Academic Publishers, Dordrecht, pp 205-245.

Brenner, M., Whitmore, T.J., Curtis, J.A., Hodell, D.A., Schelske, C.L., 1999. Stable isotope ($\delta^{13}C$ and $\delta^{15}N$) signatures of sedimented organic matter as indicators of historic lake trophic state. Journal of Paleolimnology, 22: 205-221.

Brock, B.E., Wolfe, B.B., Edwards, T.W.D, 2007. Characterizing the hydrology of shallow floodplain lakes in the Slave River Delta, NWT, Canada, using water isotope tracers Arctic, Antarctic and Alpine Research, 39: 388–401.

Brock, B.E , Wolfe, B.B., Edwards, T.W.D, 2008. Spatial and temporal perspectives on ice-jam flooding in the Slave River Delta, NWT. Hydrological Processes, 22: 4058-4072.

Brock, B.E., Martin, M.E., Mongeon, C.L., Sokal, M.A., Wesche, S.D., Armitage, D., Wolfe, B.B., Hall, R.I., Edwards, T.W.D., 2010. Flood frequency variability during the past 80 years in the Slave River Delta, NWT, as determined from multi-proxy paleolimnological analysis. Canadian Water Resources Journal, 35: 281-300.

Campbell, D., Spitzer, A., 2007. High and Dry. Up Here, Accessed April 5, 2008: http://www.uphere.ca/node/141.

Case, R.A., MacDonald, G.M., 2003. Tree ring reconstruction of streamflow for three Canadian prairie rivers Journal of American Water Resources Association, 39: 7 03-716.

Cook, E.R., Woodhouse, C.A., Eakin, C.M., Meko, D.M., Stahle, D.W., 2004. Long-term aridity changes in the western United States, Science, 306: 1015-1018.

Dean, W.E., 1974. Determination of carbonate and organic matter in calcareous sediments and sedimentary rocks by loss on ignition: comparison with other methods. Journal of Sedimentary Petrology, 44: 242- 248.

Canada Department of Agriculture, Cartography Section, Soil Research Institute, Research Branch, 1971. Soil Map: Slave River Lowland, Northwest Territories, Sheet 1. Surveys and Mapping Branch, Department of Energy, Mines and Resources.

Dery, S.J., Wood, E.F., 2005. Decreasing river discharge in northern Canada. Geophysical Research Letters, 32: doi:10.1029/2005GL022845.

Dery, S.J., Hernandez-Henrıquez, M.A., Burford, J.E., Wood, E.F., 2009. Observational evidence of an intensifying hydrological cycle in northern Canada. Geophysical Research Letters, 36: doi:10.1029/2009GL038852.

Edwards. T.W.D., McAndrews, J.H., 1989. Paleohydrology of a Canadian Shield lake inferred from ^{18}O in sediment cellulose. Canadian Journal of Earth Sciences, 26: 1850-1859.

Edwards, T.W.D., 1993. Interpreting past climate from stable isotopes in continental organic matter. In Climate Change in Continental Isotopic Records. Swart, P. K., Lohmann, K. C., McKenzie, J., and Savin, S. (Eds). Geophysical Monograph 78, American Geophysical Union, Washington, pp 333-341.

Edwards, T.W.D., Birks, S.J., Luckman, B.H, MacDonald, G.M., 2008. Climatic and hydrologic variability during the past millennium in the eastern Rocky Mountains and northern Great Plains of western Canada. Quaternary Research, 70: 188-197.

English, M.C. 1984. Implications of upstream impoundment on the natural ecology and environment of the Slave River Delta, Northwest Territories. In Northern Ecology and Resource Management. Olsen, R.,Geddes, F. and Hastings, R. (Eds).The University of Alberta Press, Edmonton, Alberta, pp 311-336.

English, M.C., Hill, R.B., Stone, M.A., Ormson, R., 1997. Geomorphological and botanical change on the outer Slave River Delta, NWT, before and after impoundment of the Peace River. Hydrological Processes, 11: 1707–1724.

Environment Canada, 2002 Canadian Climate Normals 1971–2000. Environment Canada.

Evans, M.S , 2000. The large lake ecosystems of northern Canada. Aquatic Ecosystem Health and Management, 3: 65-79.

Fogel, M L., Cifuentes, L A., 1993. Isotope fractionation during primary production. In Organic Geochemistry: Principles and Applications. Engel, M.H. and Mako, S.A. (Eds). Plenum Press, New York, pp 73-98.

Foster, I , Mighall, T., Proffitt, H., Walling, D., Owens, P., 2006. Postdepositional ^{137}Cs mobility in the sediments of three shallow coastal lagoons, southwest England.Journal of Paleolimnology 35: 881-895.

Gardner, J.T., English, M.C., Prowse, T.D., 2006. Wind forced seiche events on Great Slave Lake: hydrologic implications for the Slave River Delta, NWT, Canada. Hydrological Processes, 20· 4051–4072.

Gibson, J.J., Prowse, T.D., Peters, D.L., 2006a. Partitioning impacts of climate and regulation on water level variability in Great Slave Lake. Journal of Hydrology, 329: 196–206.

Gibson, J.J., Prowse, T D., Peters, D.L., 2006b. Hydroclimate controls on water balance and water level variability in Great Slave Lake. Hydrological Processes, 20: 4155-4172.

Glew, J.R., 1989. A miniature gravity corer for recovering short sediment cores. Journal of Paleolimnology, 5: 285-287.

Glew, J.R., Smol, J.P., Last, W.M., 2001. Sediment core collection and extrusion.In Tracking Environmental Change Using Lake Sediments: Volume 1: Basin Analysis, Coring, and Chronological Techniques, Developments in Paleoenvironmental Research. W.M. Last and J.P. Smol (Eds). Kluwer Academic Publishers, Dordrecht, pp 88-89.

Hall, R.I., Wolfe, B.B., Edwards, T.W.D., Karst-Riddoch, T.L., Vardy, S.R., McGowan, S., Sjunneskog, C., Paterson, A., Last, W.M., English, M.C., Sylvestre, F., Leavitt, P.R., Warner, B.G , Boots, B., Palmini, R., Clogg-Wright, K., Sokal, M., Falcone, M.D., van Driel, P., Asada, T., 2004. A Multi-Century Flood, Climatic, and Ecological History of the Peace-Athabasca Delta, Northern Alberta, Canada. Final Report to B.C. Hydro, 163

Hannaford, N., 2008. If cutting CO_2 is the key, there's much more to be said for hydro. Calgary Herald, Tuesday March 25, 2008.

Heiri, O., Lotter, A. F., Lemcke, G., 2001 Loss on ignition as a method for estimating organic and carbonate content in sediments: reproducibility and comparability of results. Journal of Paleolimnology, 25: 101-110.

Herczeg, A.L., Fairbanks, R.G., 1987 Anomalous carbon isotope fractionation between atmospheric CO2 and dissolved inorganic carbon induced by intense photosynthesis. Geochimica et Cosmochimica Acta, 51: 895-899.

Herczeg. A.L., 1988. Early diagenesis or organic matter in lake sediments: A stable c arbon isotope study of pore waters. Chemical Geology, 72: 199-209.

Hodell, D.A., Schelske, C.L., 1998. Production, sedimentation, and isotopic composition of organic matter in Lake Ontario. Limnology and Oceanography, 43: 200-214.

Hollander, D.A., MacKenzie, J.A., 1991. CO_2 control on carbon isotope fractionation during aqueous photosynthesis: A paleo barometer. Geology, 19: 929-932.

Hollander, D.A., MacKenzie, J A., ten Haven, H.L., 1992. A 200 year sedimentary record of progressive eutrophication in Lake Greifen (Switzerland): Implications for the origin of organic carbon rich sediments. Geology, 20: 825-828.

Jarvis, S., 2008. Reconstruction of Peace River flood frequency and magnitude for the past ~600 years from oxbow lake sediments, Peace-Athabasca Delta, Canada. MSc Thesis, Wilfrid Laurier University, Waterloo, Ontario, Canada.

Johnston, J.W., Köster, D., Wolfe, B.B., Hall, R.I., Edwards, T.W.D., Endres, A.L., Martin, M.E., Wiklund, J.A., Light, C., 2010. Quantifying Lake Athabasca (Canada) water level during the Little Ice Age highstand from paleolimnological and geophysical analyses of a transgressive barrier-beach complex. The Holocene, 20: 801-811.

Keeley, J.E., Sandquist, D.R., 1992. Carbon: freshwater plants. Plant, Cell and Environment, 15: 1021-1035.

Lapp, S., Byrne, J., Townshend, I., Kienzle, S., 2005. Climate warming impacts on snowpack accumulation in an alpine watershed, International Journal of Climatology, 25: 521–536.

Light, C., 2010. Identifying potential carbon flux responses to shifting hydroecological and climatic regimes in the Peace-Athabasca Delta. MSc Thesis, Wilfrid Laurier University, Waterloo, Ontario, Canada.

Laws, E.A., Popp, B.N., Bidigare, R.R., Kennicutt, M.C., Macko, S.A., 1995. Dependence of phytoplankton isotopic composition on growth rate and $[CO_2]aq$: Theoretical considerations and experimental results. Geochimica et Cosmochimica Acta, 59: 1131-1138.

Longmore, M.E., 1982. The cesium dating technique and associated applications in Australia.In: Ambrose, W., and Duerden, P., (Eds). Archaeometry: An Australian Perspective. ANU Press, Canberra, pp 310-321.

Lyons, S., 2010. Evaluating the influence of flooding on aquatic food-webs in basins of the Peace-Athabasca Delta using isotopic tracers. MSc Thesis, University of Waterloo, Waterloo, Ontario, Canada

McKenzie, J.A., 1985. Carbon isotopes and productivity in the lacustrine and marine environment. In: Stumm,W. (Eds). Chemical Processes in Lakes, Wiley, Toronto, pp 99–118.

Meko, D.M., Woodhouse, C.A., Basian, C.A., knight, T., Lukas, J.J., Hughes, M.K., Salzer, M.W., 2007. Medieval drought in the upper Colorado Rover basin, Geophysical Research Letters, 34, L10705, doi:10.1029/2007GL029988.

Meyers, P.A., 1997. Organic geochemical proxies of paleooceanographic, paleolimnologic, and paleoclimatic processes. Organic Geochemistry, 27: 213-250.

Meyers, P.A., Lallier-Verges, E., 1999. Lacustrine sedimentary organic matter records of Late Quaternary paleoclimates. Journal of Paleolimnology, 21: 345-372.

Meyers, P.A., Teranes, J.L., 2001. Sediment organic matter. In Tracking Environmental Change Using Lake Sediments: Volume 2: Basin Analysis, Coring, and Chronological techniques, Developments in Paleoenvironmental Research. W.M. Last and J.P. Smol (Eds). Kluwer Academic Publishers, Dordrecht, pp 239-270.

Milburn, D., MacDonald, D.D., Prowse, T.D., Culp, J.M., 1999. Ecosystem maintenance indicators for the Slave River Delta, N.W.T., Canada. In Environmental Indices Systems Analysis Approach. Pykh, Y.A., Hyatt, D.E., and Lenz, R J.M. (Eds). EOLSS Publishers Co LTD, Oxford, UK, pp 329-348.

Mongeon, C., 2008. Paleohydrologic reconstruction of three shallow basins, Slave River Delta, NWT, using stable isotope methods. MES Thesis, Wilfrid Laurier University, Waterloo, Ontario, Canada.

Prowse, T.D., Conly, F M., Church, M., English, M. C , 2002. A review of hydroecological results of the Northern River Basins Study, Canada. Part 1. Peace and Slave River. River Research and Applications, 18: 429–446.

Rawson, D.S., 1950. The Physical Limnology of Great Slave Lake. Journal of Fisheries Research Board of Canada, 8: 3-66.

Reimer P.J., M.G.L., Baillie, E., Bard, A., Bayliss, J.W., Beck, C.J.H., Bertrand et al., 2004. IntCal04 terrestrial radiocarbon age calibration, 26–0 ka BP. Radiocarbon, 46: 1029–1058.

Rood, S.B., Samuelson, G.M., Weber, J.K. , Wywrot, K.A., 2005 Twentieth-century decline in streamflows from the hydrographic apex of North America, Journal of Hydrology, 306: 215–233.

Rouse, W.R., Bello, R.L., Lafleur, P.M., 1997: The low arctic and subarctic. In The Surface Climates of Canada. W.G. Baily, T. Oke, and W.R. Rouse (Eds). Montreal, Canada: McGill-Queens University Press, pp 198-221.

Rouse, W.R., Oswald, C.M., Dinyamin, J., Dianken, P.D , Schertzer, W.M., Spence, C., 2003. Interannual and seasonal variability of the surface energy balance and temperature of central Great Slave Lake. Journal of Hydrometeorology, 4: 720-730.

Sarazin, G.G., Michard, G., Al Gharib, I., Bernat, M., 1992. Sedimentation rate and early diagenesis of particulate organic nitrogen and carbon in Aydat Lake (Puy de Dome, France). Chemical Geology, 98: 307-316.

Saurer, M., Aellen, K., Siegwolf, R., 1997. Correlating $\delta^{13}C$ and $\delta^{18}O$ in cellulose of trees. Plant, Cell and Environment, 20: 1543-1550.

Schelske, C.L., Hodell, D.A., 1991. Recent changes in productivity and climate of Lake Ontario detected by isotopic analysis of sediments. Limnology and Oceanography, 36: 961-975.

Schelske, C.L., Hodell, D.A., 1995. Using carbon isotopes of bulk sedimentary organic matter to reconstruct the history of nutrient loading and eutrophication in Lake Erie. Limnology and Oceanography, 40: 918–929.

Schindler, D.W., Donahue W.F., 2006. An impending water crisis in Canada's western prairie provinces. Proceedings of the National Academy of Sciences, 103: 7210-7216.

Sear, D.A. and Arnell, N.W., 2006. The application of paleohydrology in river management. Catena, 66: 169-183.

Sinnatamby, R.N., Yi, Y., Sokal, M., Clogg-Wright, K., Vardy, S., Karst-Riddoch, T., Last, W., Johnston, J., Hall, R., Wolfe, B.B., Edwards, T.W.D., 2010. Historical and paleolimnological evidence for expansion of Lake Athabasca (Canada) during the Little Ice Age. Journal of Paleolimnology, 43:705-717.

Sokal, M. A., Hall, R.I., Wolfe, B.B., 2008. Relationships between hydrological and limnological conditions in lakes of the Slave River Delta (NWT, Canada) and quantification of their roles on sedimentary diatom assemblages. Journal of Paleolimnology, 39: 533-550.

Stuiver M., P.J., Reimer, 1993. Extended ^{14}C database and revised CALIB radiocarbon calibration program. Radiocarbon, 35: 215–230.

Teranes, J.L., Bernasconi, S.M., 2000. The record of nitrate utilization and productivity limitation provided by $\delta^{15}N$ values in lake organic matter-A study of sediment trap and core sediments from Baldeggersee, Switzerland. Limnology and Oceanography, 45: 801-813.

Talbot, M.R., Laerdal, T., 2000. The Late Pleistocene-Holocene paleolimnology of Lake Victoria, East Africa, based upon elemental and isotopic analyses of sedimentary organic matter. Journal of Paleolimnology, 23: 141-164.

Talbot, M.R., 2001. Nitrogen isotopes in Paleolimnology. In Tracking Environmental Change Using Lake Sediments: Volume 2: Basin Analysis, Coring, and Chronological Techniques, Developments in Paleoenvironmental Research. W.M. Last and J.P. Smol (Eds). Kluwer Academic Publishers, Dordrecht, pp 401-439.

Townsend, G.H., 1984: Wildlife Resources of the Slave River and Peace-Athabasca Delta. Journal of the National and Provincial Parks Association of Canada, 20: 5-7.

Vanderburgh, S., Smith, D., 1988. Slave River Delta: geomorphology, sedimentology, and Holocene reconstruction. Canadian Journal of Earth Sciences, 25: 1990–2004.

Wolfe, B.B., Edwards, T.W.D., Aravena, R., 1999. Changes in carbon and nitrogen cycling during tree-line retreat recorded in the isotopic content of lacustrine organic matter, western Taimyr Peninsula, Russia. The Holocene, 9: 215–222.

Wolfe, B.B., Edwards, T.W.D., Duthie, H.C., 2000. A 6000-year record of interaction between Hamilton Harbour and Lake Ontario: quantitative assessment of recent hydrologic disturbance using ^{13}C in lake sediment cellulose. Aquatic Ecosystem Health and Management, 3: 47–54.

Wolfe, B.B., Edwards, T.W.D., Elgood, R.J., Beuning, K.R.M., 2001. Carbon and oxygen isotope analysis of lake sediment cellulose: methods and applications. In Tracking Environmental Change Using Lake Sediments: Volume 2: Physical and Geochemical Methods. Last, W.M., and Smol, J.P. (Eds). Kluwer Academic Publishers, Dordrecht, pp 373-400.

Wolfe, B.B., Karst-Riddoch, T.L., Vardy, S.R., Falcone, M.D., Hall, R.I., Edwards, T.W.D, 2005. Impacts of climate and river flooding on the hydro-ecology of a floodplain basin, Peace-Athabasca Delta, Canada since A.D. 1700. Quaternary Research, 64: 147-162.

Wolfe, B.B., Hall, R.I., Last, W.M., Edwards, T.W.D., English, M.C., Karst-Riddoch, T.L., Paterson, A., Palmini, R., 2006. Reconstruction of multi-century flood histories from oxbow lake sediments, Peace-Athabasca Delta, Canada. Hydrological Processes, 20: 4131-4153.

Wolfe, B.B., Karst-Riddoch, T.L., Hall, R.I., Edwards, T.W.D., English, M C., Palmini, R., 1 McGowan, S., Leavitt, P.R., Vardy, S.R., 2007a. Classification of hydrological regimes of northern floodplain basins (Peace–Athabasca Delta, Canada) from analysis of stable isotopes ($\delta^{18}O$, $\delta^{2}H$) and water chemistry. Hydrological Processes, 21: 151-168.

Wolfe, B.B., Falcone, M.D., Clogg-Wright, K.P., Mongeon, C.L., Yi Y, Brock, B.E., St. Amour, N.A., Mark, W.A., Edwards, T.W.D., 2007b. Progress in isotope paleohydrology using lake sediment cellulose. Journal of Paleolimnology, 37: 221-231.

Wolfe, B.B., Hall, R.I., Edwards, T.W.D., Jarvis, S.R., Sinnatamby, R.N., Yi, Y., Johnston, J.W., 2008a. Climate-driven shifts in quantity and seasonality of river discharge over the past 1000 years from the hydrographic apex of North America. Geophysical Letters, 35: L24402, doi:10.1029/2008GL036125.

Wolfe, B.B, Hall, R.I., Edwards, T.W.D., Vardy, S.R., Falcone, M.D., Sjunneskog, C., Sylvestre, F., McGowan, S., Leavitt, P.R., van Driel, P., 2008b. Hydroecological responses of the Athabasca Delta, Canada, to changes in river flow and climate during the 20th century. Ecohydrology, 1: 131-148.

Appendix A: ^{210}Pb and ^{137}Cs results

SR1
KB-2
Coring Date 24-Mar-07
Total Activity - Corrected to coring date

Depth Interval (cm)		Midpoint Depth (cm)	Measured ^{210}Pb (dpm/g)	Measured ^{137}Cs (dpm/g)	Interpolated ^{210}Pb (dpm/g)	Interpolated ^{137}Cs (dpm/g)
0 0	0 5	0 25	6 065	0 587	6 065	0 587
0 5	1 0	0 75			6 556	0 698
1 0	1 5	1 25	7 048	0 809	7 048	0 809
1 5	2 0	1 75			7 198	0 834
2 0	2 5	2 25	7 349	0 859	7 349	0 859
2 5	3 0	2 75			7 682	0 861
3 0	3 5	3 25	8 016	0 864	8 016	0 864
4 0	4 5	4 25			6 933	0 933
4 5	5 0	4 75	5 849	1 003	5 849	1 003
5 0	5 5	5 25			5 060	1 112
5 5	6 0	5 75	4 271	1 221	4 271	1 221
6 0	6 5	6 25			4 420	1 176
6 5	7 0	6 75	4 570	1 130	4 570	1 130
7 0	7 5	7 25			4 194	1 114
7 5	8 0	7 75	3 818	1 097	3 818	1 097
8 0	8 5	8 25			3 851	1 257
8 5	9 0	8 75	3 884	1 417	3 884	1 417
9 0	9 5	9 25			4 212	1 967
9 5	10 0	9 75	4 539	2 518	4 539	2 518
10 0	10 5	10 25			3 865	1 773
10 5	11 0	10 75	3 191	1 029	3 191	1 029
11 0	11 5	11 25			3 031	0 769
11 5	12 0	11 75	2 872	0 510	2 872	0 510
12 0	13 0	12 50			2 882	0 326
13 0	13 5	13 25	2 892	0 143	2 892	0 143
13 5	14 0	13 75			3 938	0 107
14 0	14 5	14 25	4 984	0 072	4 984	0 072
14 5	15 0	14 75			3 711	0 066
15 0	15 5	15 25	2 439	0 061	2 439	0 061
15 5	16 0	15 75			2 454	-0 006
16 0	16 5	16 25	2 469	-0 072	2 469	-0 072
16 5	17 0	16 75			2 474	-0 108
17 0	17 5	17 25	2 480	-0 143	2 480	-0 143
17 5	18 0	17 75			2 580	-0 129
18 0	18 5	18 25	2 681	-0 115	2 681	-0 115
18 5	19 0	18 75			2 418	-0 070
19 0	19 5	19 25	2 155	-0 025	2 155	-0 025
19 5	20 0	19 75			2 873	-0 081
20 0	20 5	20 25	3 592	-0 136	3 592	-0 136
20 5	21 0	20 75			2 800	-0 132
21 0	21 5	21 25	2 008	-0 127	2 008	-0 127
21 5	22 0	21 75			2 102	-0 103
22 0	22 5	22 25	2 196	-0 079	2 196	-0 079
22 5	23 0	22 75			2 444	-0 069
23 0	23 5	23 25	2 692	-0 058	2 692	-0 058
23 5	24 0	23 75			2 698	-0 055
24 0	24 5	24 25	2 705	-0 051	2 705	-0 051
24 5	25 0	24 75			2 526	-0 036
25 0	25 5	25 25	2 348	-0 021	2 348	-0 021
25 5	26 0	25 75			2 414	-0 042
26 0	26 5	26 25	2 480	-0 062	2 480	-0 062

26 5	27 0	26 75			2 050	-0 033
27 0	27 5	27 25	1 620	-0 004	1 620	-0 004
27 5	28 0	27 75			1 770	-0 034
28 0	28 5	28 25	1 920	-0 063	1 920	-0 063
28 5	29 0	28 75			2 138	-0 048
29 0	29 5	29 25	2 356	-0 033	2 356	-0 033
29 5	30 0	29 75			2 237	-0 044
30 0	30 5	30 25	2 117	-0 056	2 117	-0 056
30 5	31 0	30 75			2 195	-0 050
31 0	31 5	31 25	2 273	-0 044	2 273	-0 044
31 5	32 0	31 75			2 123	-0 057
32 0	32 5	32 25	1 972	-0 070	1 972	-0 070
32 5	33 0	32 75			2 221	-0 044
33 0	33 5	33 25	2 470	-0 017	2 470	-0 017
33 5	34 0	33 75			2 515	-0 036
34 0	34 5	34 25	2 560	-0 055	2 560	-0 055
34 5	35 0	34 75			2 324	-0 054
35 0	35 5	35 25	2 088	-0 054	2 088	-0 054
35 5	36 0	35 75			2 294	-0 057
36 0	36 5	36 25	2 499	-0 059	2 499	-0 059
36 5	37 0	36 75			2 281	-0 031
37 0	37 5	37 25	2 063	-0 003	2 063	-0 003
37 5	38 0	37 75			2 470	-0 021
38 0	38 5	38 25	2 878	-0 039	2 878	-0 039
38 5	39 0	38 75			2 679	-0 036
39 0	39 5	39 25	2 480	-0 034	2 480	-0 034

SD34 KB-2
Date
Cored: 24-Mar-07
Total Activity - Corrected to coring date

			Measured		Interpolated	
Depth Interval (cm)		*Midpoint Depth (cm)*	^{210}Pb *(dpm/g)*	^{137}Cs *(dpm/g)*	^{210}Pb *(dpm/g)*	^{137}Cs *(dpm/g)*
0 0	0 5	0 25	19 522	18 563	19 522	1 750
0 5	1 0	0 75			18 881	1 824
1 0	1 5	1 25	18 241	17 281	18 241	1 898
1 5	2 0	1 75			19 307	1 980
2 0	2 5	2 25	20 373	19.413	20 373	2 063
2 5	3 0	2 75			19 320	2 371
3 0	3 5	3 25	18 267	17 308	18 267	2 679
3 5	4 0	3 75			16 353	3 203
4 0	4 5	4 25	14 439	13 480	14 439	3 727
4 5	5 0	4 75			12 209	4 288
5 0	5 5	5 25	9 979	9 020	9 979	4 849
5 5	6 0	5 75			9 549	4 920
6 0	6 5	6 25	9 120	8 160	9 120	4 991
6 5	7 0	6 75			8 822	5 528
7 0	7 5	7 25	8 525	7 566	8 525	6 066
7 5	8 0	7 75			8 589	5 797
8 0	8 5	8 25	8 654	7.695	8 654	5 528
8 5	9 0	8 75			8 497	5 217
9 0	9 5	9 25	8 340	7 381	8 340	4 906
9 5	10 0	9 75			7 431	4 560
10 0	10 5	10 25	6 521	5 562	6 521	4 215
10 5	11 0	10 75			6 720	4 081
11 0	11 5	11 25	6 919	5 960	6 919	3 947
11 5	12 0	11 75			5 383	3 828
12 0	12 5	12 25	3 848	2 888	3 848	3 709
12 5	13 0	12 75			4 136	3 046
13 0	13 5	13 25	4 425	3 466	4 425	2.383
13 5	14 0	13 75			3 636	1 789
14 0	14 5	14 25	2 847	1 887	2 847	1 195
14 5	15 0	14 75			2 805	1 010
15 0	15 5	15 25	2 764	1 804	2 764	0 824
15 5	16 0	15 75			2 063	0 641
16 0	16 5	16 25	1 362	0 403	1 362	0 457
16 5	17 0	16 75			1 549	0 322
17 0	17 5	17 25	1 735	0 776	1 735	0 188
17 5	18 0	17 75			1 817	0 234
18 0	18 5	18 25	1 899	0 940	1 899	0 280
18 5	19 0	18 75			1 903	0 196
19 0	19 5	19 25	1 907	0 948	1 907	0 112
19 5	20.0	19 75			1 883	0 209
20 0	20 5	20 25	1.858	0 899	1 858	0 306

20 5	21 0	20 75			1 924	0 155
21 0	21 5	21 25	1 990	1 031	1 990	0 005
21 5	22 0	21 75			2 032	0 019
22 0	22 5	22 25	2 074	1 115	2 074	0 033
22 5	23 0	22 75			2 354	0 024
23 0	23 5	23 25	2 633	1 674	2 633	0 015
23 5	24 0	23 75			2 587	0 034
24 0	24 5	24 25	2 541	1 582	2 541	0 054
24 5	25 0	24 75			2 155	-0 007
25 0	25 5	25 25	1 768	0 809	1 768	-0 069
25 5	26 0	25 75			1 911	-0 037
26 0	26 5	26 25	2 054	1 095	2 054	-0 006
26 5	27 0	26 75			1 666	-0 073
27 0	27 5	27 25	1 278	0 318	1 278	-0 141
27 5	28 0	27 75			1 967	-0 075
28 0	28 5	28 25	2 656	1 697	2 656	-0 008
28 5	29 0	28 75			2 320	-0 023
29 0	29 5	29 25	1 985	1 026	1 985	-0 037
29 5	30 0	29 75			1 441	-0 017
30 0	30 5	30 25	0 898	-0 062	0 898	0 004
30 5	31 0	30 75			1 238	0 004
31 0	31 5	31 25	1 578	0 618	1 578	0 004
31 5	32 0	31 75			1 788	-0 008
32 0	32 5	32 25	1 998	1 039	1 998	-0 021
32 5	33 0	32 75			1 759	-0 047
33 0	33 5	33 25	1 519	0 560	1 519	-0 074
33 5	34 0	33 75			1 793	-0 013
34 0	34 5	34 25	2 066	1 107	2 066	0 048
34 5	35 0	34 75			1 824	0 033
35 0	35 5	35 25	1 581	0 622	1 581	0 019
35 5	36 0	35 75			1 981	0 003
36 0	36 5	36 25	2 380	1 421	2 380	-0 014
36 5	37 0	36 75			2 157	-0 006
37 0	37 5	37 25	1 933	0 974	1 933	0 002
37 5	38 0	37 75				

GSL1 KB-1

Date Cored: 25-Mar-07

Total Activity - Corrected to coring date

			Measured		Interpolated	
Depth Interval (cm)		*Midpoint Depth (cm)*	^{210}Pb *(dpm/g)*	^{137}Cs *(dpm/g)*	^{210}Pb *(dpm/g)*	^{137}Cs *(dpm/g)*
0 5	1 0	0 25	14 912	14 552	14 912	3 527
1 0	1 5	0 75	15 571	15 211	15 571	4 111
1 5	2 0	1 25			15 333	4 090
2 0	2 5	1 75	15 096	14 736	15 096	4 069
2 5	3 0	2 25			14 440	4 158
3 0	3 5	2 75	13 784	13 425	13 784	4 246
3 5	4 0	3 25			11 452	4 027
4 0	4 5	3 75	9 120	8 761	9 120	3 809
4 5	5 0	4 25			7 996	3 722
5 0	5 5	4 75	6 871	6 512	6 871	3 634
5 5	6 0	5 25			4 948	2 978
6 0	6 5	5 75	3 025	2 665	3 025	2 322
6 5	7 0	6 25			3 319	2 320
7 0	7 5	6 75	3 613	3 254	3 613	2 317
7 5	8 0	7 25			3 048	1 811
8 0	8 5	7 75	2 483	2 123	2 483	1 305
8 5	9 0	8 25			2 519	1 172
9 0	9 5	8 75	2 555	2 195	2 555	1 038
9 5	10 0	9 25			2 193	0 970
10 0	10 5	9 75	1 832	1 473	1 832	0 902
10 5	11 0	10 25			2 487	0 887
11 0	11 5	10 75	3 141	2 781	3 141	0 872
11 5	12 0	11 25			2 708	0 781
12 0	12 5	11 75	2 275	1 915	2 275	0 690
12 5	13 0	12 25			1 692	0 497
13 0	13 5	12 75	1 109	0 749	1 109	0 305
13 5	14 0	13 25			0 913	0 251
14 0	14 5	13 75	0 718	0 358	0 718	0 198
14 5	15 0	14 5			0 892	0 138
15 0	15 5	15 25	1 066	0 707	1 066	0 078
15 5	16 0	15 75			0 982	0 135
16 0	16 5	16 25	0 897	0 537	0 897	0 192
16 5	17 0	16 75			0 955	0 184
17 0	17 5	17 25			1 013	0 177
17 5	18 0	17 75			1 070	0 169
18 0	18 5	18 25	1 128	0 769	1 128	0 162
18 5	19 0	18 75			0 923	0 140
19 0	19 5	19 25			0 718	0 119
19 5	20 0	19 75			0 512	0 097
20 0	20 5	20 25	0 307	-0 053	0 307	0 076
20 5	21 0	20 75			0 735	0 092
21 0	21 5	21 25	1 164	0 804	1 164	0 109

21 5	22 0	21 75			0 746	0 065
22 0	22 5	22 25			0 892	0 061
22 5	23 0	22 75			1 039	0 058
23 0	23 5	23 25	1 185	0 826	1 185	0 054
23 5	24 0	23 75			1 235	0 057
24 0	24 5	24 25			1 285	0 061
24 5	25 0	24 75			1 335	0 064
25 0	25 5	25 25	1 386	1 026	1 386	0 067
25 5	26 0	25 75			1 193	0 067
26 0	26 5	26 25			1 000	0 067

Appendix B: Study Site Chronologies

SR1-KB2 Chronology

Background 210Pb @15 25 cm (Average value 15 25-39.25cm) **2.439 dpm/g**

Unsupported Pb-210 (CRS Model): ***Extrapolating Entire Core***

Mid-point Depth (cm)	Cum Dry Mass (g/cm^2)	Interpolated Pb-210 (dpm/g)	Unsupported **Pb-210** (Interpolated - background) (dpm/g)	Unsupported **Pb-210** per interval (dpm/cm2)	Unsupported **Pb-210** cumulative mass (dpm/cm2)	$t=\frac{1}{\lambda}\ln\left(\frac{A(0)}{A}\right)$ CRS Date (Year AD)	*Extrap below 13 75 cm mid pt depth
0 25	0 0424	6 065	3 683	0 16	4 34	**2007.0**	*2007 0*
0 75	0 0827	6 556	4 175	0 17	4 19	**2005.8**	*2005 8*
1 25	0 1305	7 048	4 666	0 22	4 02	**2004.5**	*2004 5*
1 75	0 1828	7 198	4 817	0 25	3 80	**2002.7**	*2002 7*
2 25	0 2356	7 349	4 967	0 26	3 54	**2000.5**	*2000 5*
2 75	0 2835	7 682	5 301	0 25	3 28	**1998.0**	*1998.0*
3 25	0 3382	8 016	5 634	0 31	3 03	**1995.4**	*1995 4*
4 25	0 3880	6 933	4.551	0.23	2 72	**1992.0**	*1992 0*
4 75	0 4450	5 849	3 468	0 20	2 49	**1989.2**	*1989 2*
5 25	0 5086	5 060	2 679	0 17	2 29	**1986.5**	*1986 5*
5 75	0 5726	4 271	1 889	0 12	2 12	**1984.0**	*1984 0*
6 25	0 6451	4 420	2 039	0 15	2 00	**1982.2**	*1982 2*
6 75	0.7064	4 570	2.188	0 13	1 86	**1979.7**	*1979 7*

* dates are extrapolated below 13 75-cm depth using linear regression of cumulative dry mass and CRS dates (extrap date = cum dry mass -b/ m)

Cum. Dry mass Regression Line:

Slope	**-0.02601**
y-inter	**52.23721**

7 25	0 7845	4 194	1 812	0 14	1 72	**1977.3**	*1977.3*
7.75	0 8537	3.818	1 437	0 10	1 58	**1974.5**	*1974 5*
8 25	0.9339	3 851	1 470	0 12	1 48	**1972.4**	*1972.4*
8 75	1 0149	3 884	1 502	0 12	1 36	**1969.8**	*1969.8*
9 25	1.0815	4 212	1.830	0.12	1 24	**1966.8**	*1966 8*
9 75	1 1569	4.539	2.157	0.16	1 12	**1963.4**	*1963.4*
10 25	1.2406	3.865	1 483	0.12	0 96	**1958.4**	*1958 4*
10.75	1 3069	3.191	0.809	0 05	0.83	**1953.9**	*1953.9*
11 25	1 3900	3 031	0 650	0 05	0 78	**1951.8**	*1951.8*
11.75	1.4728	2 872	0 491	0 04	0 72	**1949.5**	*1949.5*
12 5	1 7016	2 882	0.500	0.11	0 68	**1947.6**	*1947 6*
13.25	1.7832	2 892	0 510	0.04	0 57	**1941.7**	*1941 7*
13.75	1 8737	3.938	1 556	0 14	0 53	**1939.3**	*1939.3*
14 25	1 9712	4 984	2 602	0 25	0 39	**1929 3*	1932 2
14 75	2 0672	3.711	1 330	0 13	0 13	**1895.1*	1928 5
15 25	2 1628	2 439	0 057	0 01	0 01	**1792 7*	1924 8
15.75	2 2462	2 454	0 072	0 01			1921 6
16.25	2 3449	2 469	0 087	0 01		*not used	1917 8
16.75	2 4386	2 474	0 093	0 01		in	1914 2
17 25	2 5468	2 480	0 098	0 01		chronology	1910 1
17 75	2 6379	2 580	0 199	0 02			1906.6
18 25	2.7207	2 681	0 299	0 02			1903 4
18 75	2 8972	2 418	0 036	0 01			1896 6
19 25	2 9668	2 155	0 010	0 00			1893 9
19 75	3 0628	2 873	0 492	0 05			1890 2
20 25	3 1636	3 592	1.211	0 12			1886 4
20 75	3 2455	2 800	0 418	0 03			1883 2

21 25	3 3440	2 008	-0 374	-0 04			1879 4
21 75	3 4482	2 102	-0 280	-0 03			1875 4
22 25	3 5496	2.196	-0 186	-0 02			1871 5
22 75	3 6574	2 444	0 062	0 01			1867.4
23 25	3 7595	2 692	0.310	0 03			1863 5
23 75	3 8666	2 698	0.317	0 03			1859.3
24.25	3 963246	2 705	0.323	0 03			1855.6
24 75	4.079397	2.526	0 145	0.02			1851 2
25 25	4 213455	2 348	-0 034	0 00			1846.0
25 75	4.360471	2 414	0 032	0 00			1840 4
26.25	4.508909	2.480	0 099	0 01			1834 6
26 75	4 655532	2 050	-0 331	-0 05			1829 0
27 25	4 784355	1 620	-0 762	-0 10			1824 1
27 75	4.937649	1 770	-0 612	-0 09			1818.2
28 25	5 073119	1.920	-0.462	-0 06			1813 0
28 75	5 237426	2 138	-0 244	-0 04			1806.6
29.25	5 402184	2 356	-0 025	0 00			1800 3
29.75	5 553589	2 237	-0 145	-0.02			1794 5
30 25	5 751164	2 117	-0 265	-0 05			1786 9
30 75	5.863134	2 195	-0 187	-0 02			1782 6
31 25	6.126097	2 273	-0 108	-0 03			1772 5
31 75	6 389748	2 123	-0.259	-0 07			1762 3
32.25	6 683234	1.972	-0 409	-0 12			1751 1
32 75	6 948176	2 221	-0 160	-0 04			1740 9
33 25	7 426934	2 470	0 089	0 04			1722 5
33.75	7 751756	2 515	0 133	0 04			1710 0
34 25	7 99587	2.560	0 178	0 04			1700 6

34.75	8 671802	2 324	-0.058	-0 04			1674 6
35 25	8.935582	2 088	-0 293	-0.08			1664 5
35 75	9 288564	2 294	-0 088	-0 03			1650.9
36 25	9 607569	2 499	0 118	0 04			1638.7
36 75	9 973961	2 281	-0.100	-0 04			1624 6
37.25	10.4579	2 063	-0.319	-0 15			1606 0
37 75	10 76425	2 470	0 089	0 03			1594 2
38 25	11 12714	2.878	0.496	0.18			1580.2
38.75	11 58337	2 679	0 297	0 14			1562 7
39 25	11 99617	2 480	0 098	0 04			1546.8

SD34
Chronology

Background 210Pb @15 25 cm
(Average value 15 25-37 25cm): **1.895 dpm/g**
Cum. Dry mass Regression Line:

Slope	**-0.019**
y-inter	**38.272**

*dates are extrapolated below 13 75-cm depth using linear reg of cumulative dry mass and CRS dates (extrap date=cum dry mass-b/m)
**dates are extrapolated below 37 25-cm depth using linear reg of depth and CRS dates from 0-37 25 cm

Unsupported Pb-210 (CRS Model): ***Extrap. KB Core*** ***Extrap. RC Core***

Mid-Point Depth (cm)	Cum Dry Mass (g/cm^2)	Inter-polated Pb-210 (dpm/g)	Unsupported **Pb-210** (Interpolated - background) (dpm/g)	Unsupported **Pb-210** per interval (dpm/cm2)	Unsupported **Pb-210** cumulative mass (dpm/cm2)	$t=\frac{1}{\lambda}\ln\left(\frac{A(0)}{A}\right)$ CRS Date (Year AD)	*Extrap below 12 75 cm mid pt depth	SD34 RC-2 Depth	**Extrap below 37 25 cm mid pt depth
0 25	0 0164	19 522	17.627	0 29	12.52	**2007.2**	*2007.2*	37 75	**1489.1**
0 75	0 0491	18 881	16.986	0 55	12 23	**2006.4**	*2006.4*	38 25	**1479.3**
1.25	0 1192	18.241	16.345	1.15	11 67	**2005.0**	*2005.0*	38 75	**1469.5**
1.75	0 1465	19 307	17 411	0 48	10 53	**2001.6**	*2001.6*	39.25	**1459.7**
2.25	0 1712	20 373	18 477	0 46	10.05	**2000.2**	*2000.2*	39.75	**1449.9**
2 75	0 2033	19.320	17.425	0 56	9.59	**1998.7**	*1998 7*	40 25	**1440.0**
3 25	0 2328	18 267	16 372	0 48	9 03	**1996.7**	*1996 7*	40 75	**1430.2**
3.75	0 2637	16 353	14.458	0 45	8.55	**1995.0**	*1995.0*	41 25	**1420.4**

4 25	0 3008	14 439	12 544	0 47	8 11	**1993.2**	*1993.2*	41 75	**1410.6**
4.75	0 3453	12 209	10.314	0 46	7 64	**1991.3**	*1991 3*	42.25	**1400.8**
5 25	0 4007	9 979	8.084	0 45	7 18	**1989.4**	*1989.4*	42.75	**1391.0**
5 75	0 4621	9.549	7.654	0.47	6 73	**1987.3**	*1987.3*	43 25	**1381.1**
6 25	0 5347	9 120	7.224	0 52	6 26	**1985.0**	*1985 0*	43 75	**1371.3**
6.75	0 5886	8.822	6 927	0 37	5 74	**1982.2**	*1982.2*	44 25	**1361.5**
7 25	0.6492	8.525	6.630	0.40	5 37	**1980.0**	*1980.0*	44 75	**1351.7**
7.75	0.7192	8 589	6.694	0.47	4.96	**1977.5**	*1977.5*	45.25	**1341.9**
8.25	0.7942	8 654	6.759	0 51	4 50	**1974.3**	*1974.3*	45.75	**1332.1**
8.75	0 8581	8.497	6.602	0 42	3 99	**1970.5**	*1970 5*	46.25	**1322.2**
9.25	0 9459	8.340	6 445	0 57	3.57	**1966.9**	*1966.9*	46 75	**1312.4**
9.75	1 0228	7 431	5.536	0 43	3 00	**1961.3**	*1961.3*	47 25	**1302.6**
10 25	1.0988	6.521	4.626	0.35	2 57	**1956.4**	*1956.4*	47.75	**1292.8**
10 75	1 1783	6 720	4.825	0.38	2 22	**1951.7**	*1951.7*	48 25	**1283.0**
11 25	1 2546	6 919	5 024	0 38	1 84	**1945.6**	*1945.6*	48 75	**1273.2**
11 75	1 3424	5 383	3 488	0.31	1 46	**1938.1**	*1938 1*	49 25	**1263.4**
12.25	1 4247	3.848	1 952	0 16	1 15	**1930.5**	*1930 5*	49 75	**1253.5**
12 75	1 5280	4 136	2 241	0 23	0 99	**1925.7**	*1925 7*	50 25	**1243.7**
13 25	1 6216	4 425	2 530	0 24	0 76	*1917 1*	**1918.7**	50.75	**1233.9**
13.75	1 7365	3 636	1 741	0.20	0.52	*1905 1*	**1912.1**	51 25	**1224.1**
14 25	1.8297	2.847	0 951	0.09	0 32	*1889 6*	**1906.8**	51 75	**1214.3**
14 75	1 9593	2 805	0 910	0 12	0.23	1879 2	**1899.4**	52.25	**1204.5**
15.25	2 0697	2 764	0.869	0.10	0 11	1856 5	**1893.1**	52 75	**1194.6**
15 75	2 1809	2.063	0 168	0.02	0 02		**1886.7**	53.25	**1184.8**
16 25	2 3317	1 362	-0 533	-0 08			**1878.1**	53.75	**1175.0**
16 75	2 4262	1.549	-0 347	-0 03			**1872.7**	54 25	**1165.2**
17 25	2 5326	1.735	-0 160	-0.02			**1866.6**	54.75	**1155.4**

17.75	2 6650	1 817	-0 078	-0 01			**1859.1**	55.25	**1145.6**
18 25	2 7743	1 899	0.004	0 00			**1852.8**	55 75	**1135.7**
18 75	2 8940	1 903	0 008	0 00			**1846.0**	56.25	**1125.9**
19 25	3 0337	1 907	0 012	0 00			**1838.0**	56.75	**1116.1**
19.75	3 1808	1 883	-0.013	0 00			**1829.6**	57 25	**1106.3**
20.25	3 2997	1.858	-0 037	0 00			**1822.8**	57.75	**1096.5**
20.75	3 4422	1 924	0 029	0 00			**1814.7**	58.25	**1086.7**
21.25	3.5747	1.990	0 095	0 01			**1807.1**	58.75	**1076.8**
21.75	3 7411	2.032	0 137	0 02			**1797.6**	59 25	**1067.0**
22.25	3 8787	2.074	0.179	0.02			**1789.7**	59 75	**1057.2**
22.75	4 0211	2.354	0 459	0 07			**1781.6**	60 25	**1047.4**
23.25	4 1542	2 633	0 738	0.10			**1774.0**	60.75	**1037.6**
23.75	4 3217	2.587	0 692	0.12			**1764.4**	61 25	**1027.8**
24.25	4 4642	2.541	0 646	0.09			**1756.3**	61.75	**1017.9**
24.75	4.6439	2 155	0.259	0 05			**1746.0**	62 25	**1008.1**
25 25	4.8157	1.768	-0 127	-0 02			**1736.2**	62 75	**998.3**
25.75	4 9470	1 911	0 016	0.00			**1728.7**	63 25	**988.5**
26 25	5 1186	2.054	0 159	0 03			**1718.9**	63.75	**978.7**
26 75	5 2860	1 666	-0 229	-0 04			**1709.3**	64 25	**968.9**
27 25	5 4568	1 278	-0 617	-0 11			**1699.5**	64 75	**959.0**
27 75	5 6160	1 967	0 072	0 01			**1690.4**	65.25	**949.2**
28 25	5 7945	2.656	0 761	0 14			**1680.2**	65 75	**939.4**
28.75	5 9675	2.320	0 425	0 07			**1670.4**	66.25	**929.6**
29 25	6.2261	1.985	0 090	0.02			**1655.6**	66 75	**919.8**
29 75	6 3545	1.441	-0 454	-0.06			**1648.2**	67 25	**910.0**
30.25	6.5659	0 898	-0.998	-0 21			**1636.2**	67 75	**900.2**
30.75	6 7176	1 238	-0.658	-0.10			**1627.5**	68 25	**890.3**

31.25	6 8937	1.578	-0 318	-0.06			**1617.4**	68 75	**880.5**
31.75	7 0623	1 788	-0.107	-0 02			**1607.8**	69.25	**870.7**
32 25	7 2292	1 998	0 103	0 02			**1598.3**	69 75	**860.9**
32 75	7 4242	1.759	-0 136	-0 03			**1587.1**	70 25	**851.1**
33 25	7 6050	1 519	-0 376	-0 07			**1576.8**	70 75	**841.3**
33 75	7 7880	1 793	-0.103	-0.02			**1566.3**	71 25	**831.4**
34 25	7 9394	2 066	0 171	0 03			**1557.7**	71 75	**821.6**
34 75	8.1344	1 824	-0.072	-0 01			**1546.5**	72.25	**811.8**
35.25	8.3011	1.581	-0.314	-0.05			**1537.0**	72 75	**802.0**
35 75	8 4929	1 981	0 086	0 02			**1526.0**	73 25	**792.2**
36.25	8 6827	2 380	0 485	0 09			**1515.2**	73 75	**782.4**
36.75	8 8408	2.157	0.261	0 04			**1506.2**	74 25	**772.5**
37.25	9 0118	1.933	0 038	0.01			**1496.4**	74 75	**762.7**

GSL1 Chronology

Background 210Pb @12.25 cm
(Average value 12 25-26 25cm) **1.082 dpm/g**
Cum. Dry mass Regression Line:

Slope	**-0.0146**
y-intercept	**29.2099**

*dates are extrapolated below 11 25-cm depth usıng lınear reg of cumulatıve dry mass and CRS dates (extrap date=cum dry mass-b/m)
**dates are extrapolated below 26 25-cm depth usıng lınear reg of depth and CRS dates from 0-26.25 cm

Unsupported Pb-210 (CRS Model): ***Extrap. KB Core*** ***Extrap. RC Core***

Mıdpoınt Depth (cm)	Cumulatıve Dry mass (g/cm^2)	Interpolated Pb-210 (dpm/g)	Unsupported **Pb-210** (Interpolated - background) (dpm/g)	Unsupported **Pb-210** per ınterval (dpm/cm2)	Unsupported **Pb-210** cumulatıve mass (dpm/cm2)	$t=\frac{1}{\lambda}\ln\left(\frac{A(0)}{A}\right)$ CRS Date (Year AD)	*Extrap. below 11 25 cm mıd pt depth	SD34 RC-2 Depth	**Extrap below 26 25 cm mıd pt depth
0 25	0 0124	14 912	13.830	0 17	5.38	**2007.2**	*2007.2*	26.75	**1720.8**
0 75	0 0378	15 571	14 489	0 37	5 21	**2006.2**	*2006.2*	27 25	**1714.5**
1 25	0.0603	15 333	14 252	0 32	4 84	**2003.8**	*2003.8*	27.75	**1708.2**
1.75	0 0960	15.096	14 014	0 50	4 52	**2001.6**	*2001.6*	28.25	**1702.0**
2 25	0 1183	14 440	13.358	0.30	4 02	**1997.8**	*1997.8*	28.75	**1695.7**

2 75	0 1575	13 784	12 703	0 50	3 72	**1995.4**	*1995.4*	29 25	**1689.4**
3 25	0 2013	11.452	10 371	0 46	3 22	**1990.8**	*1990.8*	29 75	**1683.1**
3 75	0 2471	9 120	8 039	0 37	2 77	**1985.9**	*1985.9*	30 25	**1676.8**
4 25	0 2946	7 996	6 914	0 33	2 40	**1981.3**	*1981 3*	30 75	**1670.5**
4 75	0 3422	6 871	5 790	0 28	2 07	**1976.6**	*1976 6*	31 25	**1664.3**
5 25	0 3924	4 948	3 867	0 19	1 80	**1972.0**	*1972 0*	31 75	**1658.0**
5 75	0 4905	3 025	1 944	0 19	1 60	**1968.3**	*1968 3*	32 25	**1651.7**
6 25	0 5313	3 319	2 238	0 09	1 41	**1964.2**	*1964.2*	32 75	**1645.4**
6 75	0 5873	3.613	2 532	0 14	1 32	**1962.1**	*1962 1*	33 25	**1639.1**
7 25	0.6574	3.048	1.966	0.14	1 18	**1958.4**	*1958.4*	33 75	**1632.8**
7 75	0.7278	2 483	1 401	0 10	1 04	**1954.4**	*1954 4*	34 25	**1626.6**
8 25	0 7989	2 519	1 437	0 10	0 94	**1951.2**	*1951.2*	34 75	**1620.3**
8 75	0.8779	2.555	1 473	0 12	0 84	**1947.5**	*1947.5*	35 25	**1614.0**
9 25	0 9591	2 193	1 112	0 09	0 72	**1942.7**	*1942 7*	35 75	**1607.7**
9 75	1 0436	1 832	0 751	0 06	0 63	**1938.5**	*1938.5*	36.25	**1601.4**
10 25	1 1179	2.487	1 405	0 10	0 57	**1935.1**	*1935 1*	36 75	**1595.1**
10 75	1 1907	3 141	2.059	0 15	0 46	**1928.6**	*1928 6*	37.25	**1588.9**
11 25	1 2826	2 708	1 626	0.15	0 31	**1916.1**	*1916.1*	37 75	**1582.6**
11 75	1 3749	2 275	1.193	0 11	0 17	*1895.4*	**1906.5**	38 25	**1576.3**
12 25	1 4653	1.692	0 610	0 06	0 06	*1860.1*	**1900.3**	38.75	**1570.0**
12 75	1 5487	1 109	0 027	0 00			**1894.6**	39 25	**1563.7**
13 25	1 6380	0 913	-0 168	-0 02			**1888.5**	39 75	**1557.4**
13 75	1 7433	0 718	-0.364	-0.04			**1881.3**	40 25	**1551.1**
14 5	1 9345	0 892	-0 190	-0 04			**1868.2**	40 75	**1544.9**
15 25	2.0213	1 066	-0 015	0 00			**1862.2**	41 25	**1538.6**
15.75	2 1112	0 982	-0 100	-0.01			**1856.1**	41 75	**1532.3**
16.25	2 1678	0 897	-0 185	-0 01			**1852.2**	42 25	**1526.0**

16 75	2 2791	0.955	-0 127	-0 01			**1844.6**	42 75	**1519.7**
17 25	2 3508	1 013	-0 069	0 00			**1839.7**	43 25	**1513.4**
17 75	2 4485	1 070	-0 011	0 00			**1833.0**	43 75	**1507.2**
18 25	2 5315	1.128	0 047	0 00			**1827.3**	44 25	**1500.9**
18 75	2 6220	0 923	-0 159	-0 01			**1821.1**	44 75	**1494.6**
19 25	2 7116	0 718	-0 364	-0 03			**1815.0**	45 25	**1488.3**
19.75	2 8211	0 512	-0 569	-0 06			**1807.5**	45 75	**1482.0**
20 25	2 9024	0 307	-0 775	-0 06			**1801.9**	46 25	**1475.7**
20 75	2 9764	0 735	-0 346	-0 03			**1796.8**	46 75	**1469.5**
21 25	3 0679	1 164	0 082	0 01			**1790.5**	47 25	**1463.2**
21.75	3 1518	0 746	-0 336	-0 03			**1784.8**	47.75	**1456.9**
22 25	3 2370	0 892	-0 189	-0 02			**1779.0**	48 25	**1450.6**
22 75	3 3312	1.039	-0 043	0 00			**1772.5**	48 75	**1444.3**
23 25	3 4282	1 185	0 104	0 01			**1765.9**	49.25	**1438.0**
23 75	3 51594991	1 235	0 154	0 01			**1759.9**	49 75	**1431.7**
24.25	3.61627848	1 285	0 204	0 02			**1753.0**	50 25	**1425.5**
24.75	3 71058632	1 335	0 254	0 02			**1746.5**	50 75	**1419.2**
25 25	3.81525064	1 386	0 304	0 03			**1739.4**	51 25	**1412.9**
25.75	3 87085222	1 193	0.111	0 01			**1735.6**	51 75	**1406.6**
26 25	3 9762659	1 000	-0 082	-0 01			**1728.3**	52.25	**1400.3**
								52.75	**1394.0**
								53.25	**1387.8**
								53 75	**1381.5**
								54 25	**1375.2**
								54 75	**1368.9**
								55.25	**1362.6**
								55 75	**1356.3**

								56 25	**1350.1**
								56 75	**1343.8**
								57 25	**1337.5**
								57 75	**1331.2**
								58 25	**1324.9**
								58 75	**1318.6**
								59 25	**1312.4**
								59 75	**1306.1**
								60 25	**1299.8**
								60 75	**1293.5**
								61 25	**1287.2**
								61 75	**1280.9**
								62.25	**1274.6**
								62 75	**1268.4**
								63.25	**1262.1**
								63.75	**1255.8**
								64 25	**1249.5**
								64 75	**1243.2**
								65 25	**1236.9**
								65 75	**1230.7**
								66 25	**1224.4**
								66 75	**1218.1**
								67 25	**1211.8**
								67 75	**1205.5**
								68 25	**1199.2**
								68 75	**1193.0**
								69 25	**1186.7**

								69 75	**1180.4**
								70 25	**1174.1**
								70 75	**1167.8**
								71.25	**1161.5**
								71 75	**1155.3**
								72 25	**1149.0**
								72 75	**1142.7**
								73 25	**1136.4**
								73 75	**1130.1**
								74 25	**1123.8**
								74 75	**1117.5**
								75 25	**1111.3**
								75 75	**1105.0**
								76 25	**1098.7**
								76 75	**1092.4**
								77 25	**1086.1**
								77 75	**1079.8**
								78.25	**1073.6**
								78.75	**1067.3**
								79 25	**1061.0**
								79 75	**1054.7**
								80 25	**1048.4**
								80 75	**1042.1**
								81 25	**1035.9**
								81 75	**1029.6**
								82 25	**1023.3**
								82 75	**1017.0**

								83.25	**1010.7**
								83 75	**1004.4**
								84 25	**998.2**
								84.75	**991.9**
								85 25	**985.6**
								85.75	**979.3**
								86 25	**973.0**
								86 75	**966.7**
								87 25	**960.4**
								87.75	**954.2**
								88 25	**947.9**
								88 75	**941.6**
								89 25	**935.3**
								89 75	**929.0**
								90 25	**922.7**
								90.75	**916.5**
								91 25	**910.2**
								91.75	**903.9**
								92 25	**897.6**
								92 75	**891.3**
								93 25	**885.0**
								93 75	**878.8**
								94 25	**872.5**
								94.75	**866.2**
								95 25	**859.9**
								95 75	**853.6**
								96 25	**847.3**

								96 75	**841.0**
								97 25	**834.8**
								97 75	**828.5**
								98 25	**822.2**
								98 75	**815.9**
								99 25	**809.6**
								99 75	**803.3**

Appendix C: ^{14}C Results from Beta Analytic

LAB NUMBER: Beta - 259576 1190
SAMPLE: SD34RC21
ANALYSIS : AMS-Standard delivery
MATERIAL/PRETREATMENT : (plant material): acid/alkali/acid
RADIOCARBON AGE: +/- 40 BP
13C/12C RATIO: -13.6 ‰
CONVENTIONAL RADIOCARBON AGE: 1380 +/- 40 BP
2 SIGMA CALIBRATION : Cal AD 610 to 680 (Cal BP 1340 to 1270)

LAB NUMBER: Beta - 259577 1710
SAMPLE : SD34RC22
ANALYSIS : AMS-Standard delivery
MATERIAL/PRETREATMENT : (plant material): acid/alkali/acid
RADIOCARBON AGE: 1710 +/- 40 BP 1840 +/- 40 BP
13C/12C RATIO: -16.9 ‰
CONVENTIONAL RADIOCARBON AGE: 1840 +/- 40 BP
2 SIGMA CALIBRATION : Cal AD 80 to 250 (Cal BP 1870 to 1700)

CALIBRATION OF RADIOCARBON AGE TO CALENDAR YEARS

(Variables: C13/C12=-15.6 lab. mult=1)

Laboratory number:	**Beta-259576**
Conventional radiocarbon age:	**1380±40 BP**
2 Sigma calibrated result: (95% probability)	**Cal AD 610 to 680 (Cal BP 1340 to 1270)**

Intercept data

Intercept of radiocarbon age with calibration curve:	Cal AD 650 (Cal BP 1300)
1 Sigma calibrated result: (68% probability)	Cal AD 640 to 660 (Cal BP 1310 to 1280)

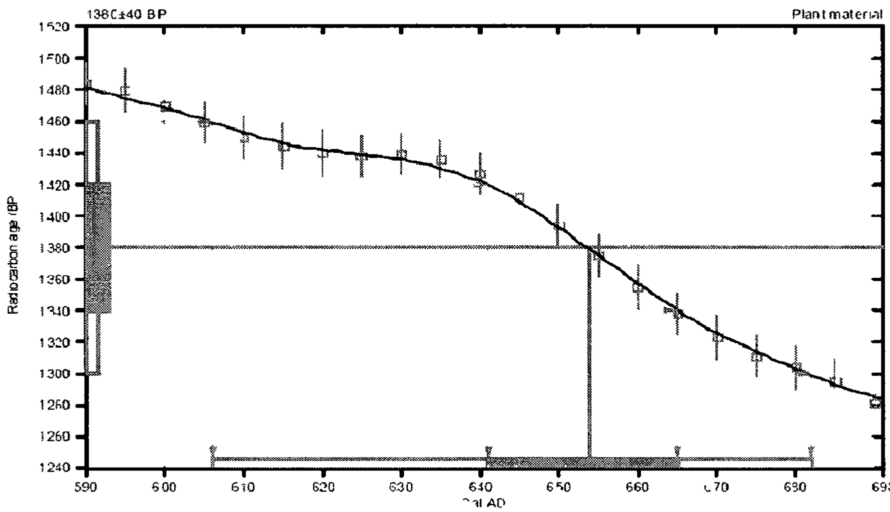

References:

Database used

INTCAL04

Calibration Database

INTCAL04 Radiocarbon Age Calibration

IntCal04: Calibration Issue of Radiocarbon (Volume 46, nr 3, 2004)

Mathematics

A Simplified Approach to Calibrating C14 Dates

Talma, A. S., Vogel, J. C., 1993, Radiocarbon 35(2), p317-322

Beta Analytic Radiocarbon Dating Laboratory

4985 S.W. 74th Court, Miami, Florida 33155 • Tel: (305)667-5167 • Fax: (305)663-0964 • E-Mail: beta@radiocarbon.com

CALIBRATION OF RADIOCARBON AGE TO CALENDAR YEARS

(Variables: C13/C12=-16.9 lab. mult=1)

Laboratory number: **Beta 259577**

Conventional radiocarbon age: **1840±40 BP**

2 Sigma calibrated result: (95% probability) **Cal AD 80 to 250 (Cal BP 1870 to 1700)**

Intercept data

Intercept of radiocarbon age with calibration curve: Cal AD 140 (Cal BP 1810)

1 Sigma calibrated result (68% probability): Cal AD 120 to 230 (Cal BP 1830 to 1720)

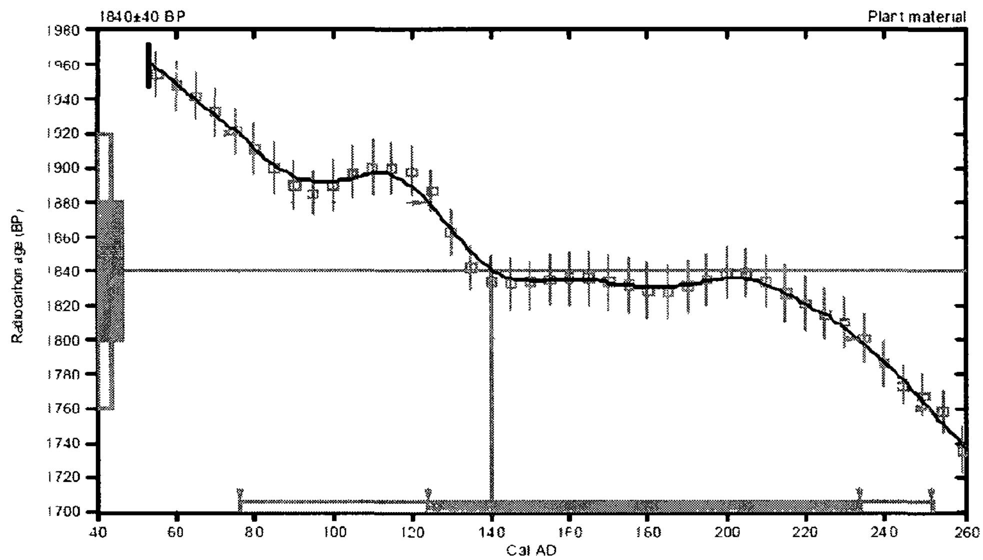

References:
Database used
INTCAL04
Calibration Database
INTCAL04 Radiocarbon Age Calibration
IntCal04: Calibration Issue of Radiocarbon (Volume 46, nr 3, 2004).
Mathematics
A Simplified Approach to Calibrating C14 Dates
Talma, A. S., Vogel, J. C., 1993, Radiocarbon 35(2), p317-322

Beta Analytic Radiocarbon Dating Laboratory

4985 S.W. 74th Court, Miami, Florida 33155 • Tel: (305)667-5167 • Fax: (305)663-0964 • E-Mail: beta@radiocarbon.com

Appendix D: LOI Results

SR1
KB-2
Coring Date: 24-Mar-07
Loss-on-Ignition Results

Sed Depth (cm)		Midpoint	%H2O	%OM	%MM	LOI 1000	%CaCO3
(Top)	(Bottom)	depth (cm)		(% dry wt)	(%dry wt)	(% dry wt)	(% dry wt)
0 0	0 5	0 25	90 23	25 37	72 07	2 56	5 82
0 5	1 0	0 75	89 01	30 15	67 28	2 57	5 85
1 0	1 5	1 25	89 05	29 58	68 24	2 18	4 95
1 5	2 0	1 75	87 70	27 35	69 74	2 91	6 62
2 0	2 5	2 25	88 21	26 73	69 91	3 36	7 64
2 5	3 0	2 75	87 64	30 51	67 33	2 16	4 90
3 0	3 5	3 25	87 06	30 30	67 42	2 27	5 17
4 0	4 5	4 25	86 72	28 63	68 05	3 32	7 54
4 5	5 0	4 75	86 32	28 26	68 79	2 95	6 71
5 0	5 5	5 25	85 91	28 35	68 06	3 60	8 18
5 5	6 0	5 75	84 81	27 93	69 37	2 70	6 14
6 0	6 5	6 25	83 96	25 07	72 13	2 80	6 36
6 5	7 0	6 75	84 57	26 47	71 04	2 50	5 67
7 0	7 5	7 25	83 91	28 69	68 74	2 56	5 83
7 5	8 0	7 75	83 51	29 74	67 04	3 22	7 32
8 0	8 5	8 25	83 19	26 10	70 75	3 15	7 16
8 5	9 0	8 75	83 37	28 50	67 87	3 62	8 23
9 0	9 5	9 25	84 60	26 66	70 27	3 07	6 98
9 5	10 0	9 75	84 79	26 09	71 29	2 62	5 96
10 0	10 5	10 25	83 62	25 94	71 31	2 74	6 23
10 5	11 0	10 75	83 70	27 24	70 11	2 64	6 01
11 0	11 5	11 25	82 46	24 94	71 99	3 07	6 98
11 5	12 0	11 75	80 95	23 94	73 49	2 57	5 84
12 0	13 0	12 50	79 97	26 51	70 88	2 61	5 93
13 0	13 5	13 25	78 59	22 46	75 17	2 36	5 37
13 5	14 0	13 75	80 92	23 91	73 85	2 24	5 09
14 0	14 5	14 25	79 88	24 16	73 23	2 61	5 94
14 5	15 0	14 75	81 18	23 38	73 77	2 85	6 47
15 0	15 5	15 25	80 62	26 68	70 92	2 39	5 44
15 5	16 0	15 75	80 96	24 03	73 23	2 73	6 21
16 0	16 5	16 25	79 20	22 38	74 79	2 83	6 44
16 5	17 0	16 75	79 73	22 43	74 38	3 19	7 25
17 0	17 5	17 25	79 84	22 89	74 27	2 84	6 45
17 5	18 0	17 75	80 16	22 95	74 55	2 50	5 67
18 0	18 5	18 25	81 09	24 24	73 03	2 73	6 20
18 5	19 0	18 75	80 09	23 10	73 29	3 61	8 20
19 0	19 5	19 25	82 04	24 20	72 91	2 88	6 55
19 5	20 0	19 75	79 02	23 17	74 51	2 32	5 27
20 0	20 5	20 25	78 99	21 35	76 54	2 12	4 81
20 5	21 0	20 75	78 74	23 56	74 74	1 70	3 87
21 0	21 5	21 25	80 02	22 73	74 81	2 46	5 60

21 5	22 0	21 75	79 18	22 98	74 77	2 25	5 12
22 0	22 5	22 25	79 88	23 29	73 98	2 73	6 20
22 5	23 0	22 75	78 75	23 12	74 98	1 90	4 33
23	23 5	23 25	78 61	21 24	76 15	2 61	5 93
23 5	24 0	23 75	77 34	21 59	75 93	2 48	5 64
24	24 5	24 25	79 36	22 91	74 65	2 44	5 55
24 5	25 0	24 75	77 23	22 91	73 90	3 19	7 24
25	25 5	25 25	74 49	20 95	76 48	2 57	5 85
25 5	26 0	25 75	71 24	20 90	76 88	2 22	5 04
26	26 5	26 25	70 84	19 11	78 32	2 57	5 84
26 5	27 0	26 75	73 63	22 44	75 32	2 24	5 08
27 0	27 5	27 25	72 77	24 36	73 70	1 94	4 40
27 5	28 0	27 75	74 87	24 56	73 76	1 68	3 82
28 0	28 5	28 25	73 11	25 53	72 43	2 05	4 65
28 5	29 0	28 75	69 31	24 01	73 72	2 27	5 15
29 0	29 5	29 25	66 67	21 31	76 23	2 46	5 58
29 5	30 0	29 75	74 55	28 60	69 18	2 22	5 05
30 0	30 5	30 25	66 21	18 63	78 51	2 86	6 49
30 5	31 0	30 75	66 08	21 98	76 10	1 92	4 36
31 0	31 5	31 25	59 89	18 70	79 21	2 09	4 75
31 5	32 0	31 75	57 51	18 49	79 59	1 92	4 36
32 0	32 5	32 25	50 37	14 80	83 23	1 97	4 47
32 5	33 0	32 75	50 77	13 10	84 72	2 18	4 96
33 0	33 5	33 25	43 75	11 64	86 64	1 71	3 89
33 5	34 0	33 75	46 86	12 02	85 80	2 18	4 96
34 0	34 5	34 25	48 69	14 24	83 56	2 19	4 99
34 5	35 0	34 75	43 41	10 30	87 76	1 94	4 42
35 0	35 5	35 25	51 02	18 29	79 83	1 87	4 26
35 5	36 0	35 75	41 28	10 95	87 22	1 83	4 16
36 0	36 5	36 25	47 56	15 54	82 66	1 80	4 10
36 5	37 0	36 75	46 62	14 63	83 73	1 63	3 71
37 0	37 5	37 25	43 09	8 08	86 83	5 09	11 56
37 5	38 0	37 75	40 42	10 37	87 63	2 00	4 55
38 0	38 5	38 25	41 35	12 11	86 21	1 68	3 82
38 5	39 0	38 75	44 24	12 17	86 47	1 35	3 07
39 0	39 5	39 25	36 20	8 90	89 63	1 47	3 34
39 5	40 0	39 75	37 31	8 26	89 85	1 89	4 29

SD34 KB-2

Coring Date: 24-Mar-07

Loss-on-Ignition Results

Sed Depth (cm)		Midpoint	%H2O	%OM	%MM	LOI 1000	%CaCO3
(Top)	(Bottom)	depth (cm)		(% dry wt)	(%dry wt)	(% dry wt)	(% dry wt)
0 0	0 5	0 25	98 27	84 95	13 98	1 08	2 44
0 5	1 0	0 75	89 26	27 86	71 77	0 37	0 84
1 0	1 5	1 25	80 69	16 87	82 36	0 77	1 75
1 5	2 0	1 75	94 04	62 09	35 95	1 96	4 46
2 0	2 5	2 25	93 53	72 59	25 30	2 11	4 79
2 5	3 0	2 75	92 90	73 47	25 20	1 33	3 01
3 0	3 5	3 25	92 59	71 53	26 24	2 23	5 06
3 5	4 0	3 75	92 65	68 78	28 43	2 79	6 35
4 0	4 5	4 25	91 38	67 96	30 32	1 72	3 91
4 5	5 0	4 75	89 06	65 37	32 59	2 04	4 63
5 0	5 5	5 25	88 70	64 40	33 82	1 78	4 05
5 5	6 0	5 75	86 93	64 60	34 19	1 21	2 75
6 0	6 5	6 25	87 17	64 70	33 00	2 31	5 24
6 5	7 0	6 75	86 93	63 29	34 56	2 15	4 89
7 0	7 5	7 25	87 00	64 70	33 38	1 92	4 36
7 5	8 0	7 75	86 46	62 94	35 31	1 75	3 98
8 0	8 5	8 25	85 38	62 71	35 31	1 98	4 49
8 5	9 0	8 75	86 74	62 95	35 24	1 81	4 11
9 0	9 5	9 25	83 65	56 87	41 48	1 65	3 76
9 5	10 0	9 75	86 23	62 27	35 60	2 13	4 85
10 0	10 5	10 25	86 49	61 88	36 05	2 07	4 71
10 5	11 0	10 75	85 86	62 01	35 41	2 58	5 86
11 0	11 5	11 25	84 85	61 96	36 23	1 81	4 12
11 5	12 0	11 75	83 49	61 67	36 12	2 21	5 03
12 0	12 5	12 25	84 52	59 43	38 33	2 24	5 09
12 5	13 0	12 75	82 10	60 98	37 33	1 70	3 86
13 0	13 5	13 25	81 57	51 87	46 14	1 99	4 52
13 5	14 0	13 75	81 48	59 78	38 34	1 88	4 27
14 0	14 5	14 25	81 95	58 18	40 06	1 76	4 00
14 5	15 0	14 75	76 08	47 70	50 68	1 62	3 69
15 0	15 5	15 25	80 65	58 60	39 14	2 26	5 13
15 5	16 0	15 75	78 95	53 67	44 72	1 61	3 66
16 0	16 5	16 25	79 31	56 36	40 96	2 67	6 08
16 5	17 0	16 75	79 11	55 74	41 94	2 32	5 26
17 0	17 5	17 25	78 87	56 20	41 79	2 02	4 58
17 5	18 0	17 75	78 78	54 29	43 63	2 08	4 72
18 0	18 5	18 25	77 49	53 38	44 25	2 37	5 39
18 5	19 0	18 75	77 04	53 48	44 11	2 41	5 47
19 0	19 5	19 25	75 18	48 36	49 58	2 06	4 68
19 5	20 0	19 75	75 24	49 83	47 54	2 63	5 97
20 0	20 5	20 25	75 34	48 96	48 81	2 24	5 09
20 5	21 0	20 75	76 17	48 52	49 16	2 32	5 27

21 0	21 5	21 25	75 46	46 64	50 67	2 68	6 10
21 5	22 0	21 75	69 43	36 35	61 64	2 01	4 57
22 0	22 5	22 25	73 25	45 49	52 13	2 38	5 40
22 5	23 0	22 75	73 03	44 80	52 94	2 26	5 13
23 0	23 5	23 25	74 19	44 32	53 15	2 53	5 76
23 5	24 0	23 75	73 17	43 29	54 43	2 27	5 17
24 0	24 5	24 25	72 20	44 17	53 50	2 33	5 30
24 5	25 0	24 75	69 97	40 28	57 48	2 24	5 09
25 0	25 5	25 25	71 58	43 61	54 12	2 27	5 17
25 5	26 0	25 75	72 53	45 27	52 54	2 19	4 99
26 0	26 5	26 25	72 48	46 99	50 74	2 28	5 17
26 5	27 0	26 75	70 46	41 59	56 31	2 10	4 78
27 0	27 5	27 25	71 98	45 24	51 75	3 02	6 85
27 5	28 0	27 75	71 67	44 42	53 35	2 23	5 07
28 0	28 5	28 25	70 25	41 36	56 19	2 45	5 56
28 5	29 0	28 75	70 38	43 72	54 60	1 68	3 83
29 0	29 5	29 25	62 08	30 59	68 09	1 33	3 02
29 5	30 0	29 75	72 09	49 19	48 45	2 36	5 37
30 0	30 5	30 25	68 73	42 19	55 79	2 02	4 59
30 5	31 0	30 75	70 08	43 51	54 33	2 16	4 92
31 0	31 5	31 25	68 85	41 18	56 70	2 11	4 80
31 5	32 0	31 75	70 66	44 21	53 18	2 61	5 93
32 0	32 5	32 25	71 16	43 52	53 63	2 85	6 48
32 5	33 0	32 75	69 65	42 81	55 05	2 14	4 87
33 0	33 5	33 25	66 91	37 89	59 80	2 32	5 26
33 5	34 0	33 75	69 55	41 69	55 68	2 63	5 97
34 0	34 5	34 25	70 72	42 77	54 98	2 25	5 12
34 5	35 0	34 75	70 11	43 35	54 32	2 33	5 30
35 0	35 5	35 25	67 62	36 93	60 75	2 32	5 27
35 5	36 0	35 75	68 56	38 30	59 38	2 33	5 29
36 0	36 5	36 25	66 52	34 21	63 15	2 64	5 99
36 5	37 0	36 75	68 37	37 90	59 79	2 30	5 24
37 0	37 5	37 25	68 37	37 17	60 00	2 83	6 43
37 5	38 0	37 75	61 61	30 03	67 73	2 23	5 07

SR1
RC-2
Coring Date: 24-Mar-07
Loss-on-Ignition Results

Sed Depth (cm) (Top)	*(Bottom)*	*Midpoint depth (cm)*	*%H2O*	*%OM (% dry wt)*	*%MM (%dry wt)*	*LOI 1000 (% dry wt)*	*%CaCO3 (% dry wt)*
0 0	0 5	0 25	87 85	66 46	31 25	2 29	5 20
0 5	1 0	0 75	86 22	64 96	32 84	2 20	5 00
1 0	1 5	1 25	85 75	65 37	32 18	2 44	5 55
1 5	2 0	1 75	85 24	65 53	31 32	3 15	7 15
2 0	2 5	2 25	84 33	64 90	32 81	2 29	5 21
2 5	3 0	2 75	84 70	63 10	34 62	2 28	5 19
3 0	3 5	3 25	83 48	62 77	34 80	2 43	5 52
3 5	4 0	3 75	81 15	64 46	33 86	1 68	3 82
4 0	4 5	4 25	84 08	62 14	35 36	2 51	5 70
4 5	5 0	4 75	82 47	61 53	36 22	2 26	5 13
5 0	5 5	5 25	82 47	62 12	35 82	2 06	4 67
5 5	6 0	5 75	82 12	62 19	36 02	1 79	4 07
6 0	6 5	6 25	82 08	62 88	35 17	1 94	4 42
6 5	7 0	6 75	82 13	61 07	36 30	2 63	5 97
7 0	7 5	7 25	80 74	62 08	36 04	1 88	4 28
7 5	8 0	7 75	81 62	60 59	36 90	2 51	5 71
8 0	8 5	8 25	82 20	61 40	36 46	2 14	4 87
8 5	9 0	8 75	81 45	63 25	34 99	1 77	4 01
9 0	9 5	9 25	81 46	61 78	36 30	1 92	4 36
9 5	10 0	9 75	81 73	61 82	35 81	2 37	5 39
10 0	10 5	10 25	81 94	62 24	35 57	2 20	4 99
10 5	11 0	10 75	82 11	62 58	35 32	2 10	4 76
11 0	11 5	11 25	81 54	62 17	35 72	2 11	4 79
11 5	12 0	11 75	81 14	60 84	36 73	2 43	5 53
12 0	12 5	12 25	79 91	60 82	36 91	2 28	5 18
12 5	13 0	12 75	80 31	60 64	36 53	2 82	6 42
13 0	13 5	13 25	79 49	61 59	36 14	2 26	5 15
13 5	14 0	13 75	80 34	64 15	33 85	2 00	4 54
14 0	14 5	14 25	79 23	61 66	36 14	2 20	5 01
14 5	15 0	14 75	79 45	58 78	38 86	2 37	5 38
15 0	15 5	15 25	79 19	59 63	37 92	2 46	5 58
15 5	16 0	15 75	78 11	59 11	38 71	2 19	4 97
16 0	16 5	16 25	78 61	59 40	38 43	2 17	4 93
16 5	17 0	16 75	79 28	59 19	38 59	2 22	5 05
17 0	17 5	17 25	78 42	59 53	38 71	1 76	4 00
17 5	18 0	17 75	78 18	58 01	40 11	1 88	4 27
18 0	18 5	18 25	76 91	57 88	39 82	2 30	5 22
18 5	19 0	18 75	78 04	57 64	40 27	2 09	4 75
19 0	19 5	19 25	77 38	56 93	40 84	2 23	5 07
19 5	20 0	19 75	77 34	57 18	41 12	1 69	3 85
20 0	20 5	20 25	78 28	57 35	40 73	1 92	4 36
20 5	21 0	20 75	78 29	56 15	41 39	2 46	5 59

21 0	21 5	21 25	77 00	56 30	41 87	1 83	4 17
21 5	22 0	21 75	78 49	56 32	41 86	1 82	4 14
22 0	22 5	22 25	77 58	56 63	41 32	2 05	4 65
22 5	23 0	22 75	76 62	55 19	42 64	2 17	4 93
23 0	23 5	23 25	77 59	56 53	41 88	1 59	3 62
23 5	24 0	23 75	76 69	55 27	42 67	2 06	4 67
24 0	24 5	24 25	76 21	55 12	43 07	1 81	4 12
24 5	25 0	24 75	78 25	53 33	44 51	2 16	4 91
25 0	25 5	25 25	76 66	56 15	42 01	1 84	4 18
25 5	26 0	25 75	76 85	58 27	39 86	1 87	4 24
26 0	26 5	26 25	75 33	53 27	44 80	1 92	4 37
26 5	27 0	26 75	75 38	53 78	44 52	1 70	3 86
27 0	27 5	27 25	75 63	52 35	45 30	2 35	5 34
27 5	28 0	27 75	75 45	52 08	45 79	2 12	4 83
28 0	28 5	28 25	75 47	53 19	45 16	1 65	3 76
28 5	29 0	28 75	75 24	50 94	47 25	1 81	4 11
29 0	29 5	29 25	76 50	52 93	45 23	1 84	4 18
29 5	30 0	29 75	75 07	51 57	46 91	1 52	3 46
30 0	30 5	30 25	75 54	52 20	45 93	1 86	4 24
30 5	31 0	30 75	75 40	50 24	47 96	1 80	4 10
31 0	31 5	31 25	75 02	50 86	47 42	1 72	3 92
31 5	32 0	31 75	72 81	50 58	47 57	1 85	4 21
32 0	32 5	32 25	73 35	50 61	47 54	1 85	4 21
32 5	33 0	32 75	72 21	49 27	48 51	2 22	5 04
33 0	33 5	33 25	73 97	49 90	48 57	1 54	3 50
33 5	34 0	33 75	73 15	49 66	49 11	1 23	2 80
34 0	34 5	34 25	73 43	50 11	48 00	1 90	4 31
34 5	35 0	34 75	72 10	47 96	50 23	1 80	4 10
35 0	35 5	35 25	72 13	48 39	48 53	3 09	7 01
35 5	36 0	35 75	71 66	46 93	50 91	2 16	4 91
36 0	36 5	36 25	70 21	44 57	52 74	2 70	6 13
36 5	37 0	36 75	70 60	45 34	52 60	2 06	4 69
37 0	37 5	37 25	69 13	43 82	54 12	2 06	4 68
37 5	38 0	37 75	69 62	44 11	53 31	2 58	5 86
38 0	38 5	38 25	67 51	44 30	53 70	2 01	4 56
38 5	39 0	38 75	70 23	44 63	53 05	2 32	5 26
39 0	39 5	39 25	70 78	45 82	51 69	2 49	5 66
39 5	40 0	39 75	71 01	47 27	50 37	2 36	5 37
40 0	40 5	40 25	71 98	45 79	52 43	1 79	4 06
40 5	41 0	40 75	71 38	42 95	54 80	2 26	5 13
41 0	41 5	41 25	71 59	44 54	53 64	1 82	4 14
41 5	42 0	41 75	70 43	44 35	53 37	2 29	5 19
42 0	42 5	42 25	68 49	43 01	54 55	2 44	5 55
42 5	43 0	42 75	67 88	42 06	55 90	2 04	4 63
43 0	43 5	43 25	70 02	41 92	55 71	2 37	5 38
43 5	44 0	43 75	68 78	41 41	56 17	2 42	5 50
44 0	44 5	44 25	68 61	41 77	56 15	2 08	4 73
44 5	45 0	44 75	69 76	39 93	56 95	3 13	7 11
45 0	45 5	45 25	68 39	40 36	57 61	2 03	4 61
45 5	46 0	45 75	70 21	42 49	55 53	1 98	4 50

46 0	46 5	46 25	68 24	41 07	56 63	2 30	5 23
46 5	47 0	46 75	69 71	41 77	55 73	2 50	5 69
47 0	47 5	47 25	69 43	41 52	56 27	2 21	5 01
47 5	48 0	47 75	68 20	38 18	59 75	2 07	4 70
48 0	48 5	48 25	68 60	38 94	58 64	2 42	5 50
48 5	49 0	48 75	66 85	35 93	61.86	2 20	5 01
49 0	49 5	49 25	66 97	34 54	62 94	2 52	5 72
49 5	50 0	49 75	67 70	36 63	60 85	2 52	5 72
50 0	50 5	50 25	68 23	37 93	59 82	2 25	5 11
50 5	51 0	50 75	63 20	30 77	66 96	2 26	5 14
51 0	51 5	51 25	63 73	32 36	65 34	2 29	5 21
51 5	52 0	51 75	64 11	30 97	66 35	2 67	6 08
52 0	52 5	52 25	62 14	30 74	66 74	2 52	5 73
52 5	53 0	52 75	60 85	28 53	69 37	2 10	4 77
53 0	53 5	53 25	60 47	28 11	69 77	2 12	4 82
53 5	54 0	53 75	59 10	25 72	71 80	2 48	5 64
54 0	54 5	54 25	59 28	25 67	71 84	2 49	5 66
54 5	55 0	54 75	60 20	26 86	70 89	2 25	5 12
55 0	55 5	55 25	60 19	26 26	71 33	2 41	5 47
55 5	56 0	55 75	57 35	26 13	71 68	2 19	4 98
56 0	56 5	56 25	57 61	25 37	72 72	1 91	4 34
56 5	57 0	56 75	53 44	22 39	75 39	2 22	5 05
57 0	57 5	57 25	56 77	22 83	74 64	2 53	5 74
57 5	58 0	57 75	56 34	23 28	74 54	2 18	4 96
58 0	58 5	58 25	56 35	20 26	75 48	4 26	9 68
58 5	59 0	58 75	49 48	17 60	80 05	2 34	5 33
59 0	59 5	59 25	52 10	17 37	80 34	2 28	5 19
59 5	60 0	59 75	44 77	11 90	85 57	2 53	5 74
60 0	60 5	60 25	43 42	11 90	85 62	2 49	5 65
60 5	61 0	60 75	49 80	17 71	80 13	2 15	4 89
61 0	61 5	61 25	34 07	7 86	89 21	2 93	6 66
61 5	62 0	61 75	42 97	11 37	86 04	2 59	5 88
62 0	62 5	62 25	41 58	10 60	86 72	2 68	6 09
62 5	63 0	62 75	31 31	7 44	89 44	3 12	7 09
63 0	63 5	63 25	35 91	9 01	88 46	2 54	5 76
63 5	64 0	63 75	32 13	7 43	89 97	2 61	5 93
64 0	64 5	64 25	31 03	6 12	91 16	2 71	6 16
64 5	65 0	64 75	32 38	6 82	90 05	3 12	7 10
65 0	65 5	65 25	31 72	6 18	90 36	3 46	7 86
65 5	66 0	65 75	35 36	7 88	88 86	3 27	7 43
66 0	66 5	66 25	35 11	8 05	88 87	3 07	6 99
66 5	67 0	66 75	39 01	9 48	87 59	2 93	6 65
67 0	67 5	67 25	30 14	5 96	90 64	3 39	7 71
67 5	68 0	67 75	30 87	6 67	89 83	3 50	7 96
68 0	68 5	68 25	32 29	6 94	89 59	3 47	7 89
68 5	69 0	68 75	33 36	7 62	88 93	3 45	7 84
69 0	69 5	69 25	35 37	7 57	89 10	3 32	7 55
69 5	70 0	69 75	35 20	7 00	89 42	3 58	8 13
70 0	70 5	70 25	38 00	7 87	88 42	3 71	8 43
70 5	71 0	70 75	28 91	5 36	91 17	3 46	7 86

GSL1 KB-1

Coring Date: 25-Mar-07

Loss-on-Ignition Results

Sed Depth (cm)		*Midpoint*	*%H2O*	*%OM*	*%MM*	*LOI 1000*	*%CaCO3*
(Top)	*(Bottom)*	*depth (cm)*		*(% dry wt)*	*(%dry wt)*	*(% dry wt)*	*(% dry wt)*
0 0	0 5	0 25					
0 5	1 0	0 75	94 30	71 21	24 49	4 30	9 77
1 0	1 5	1 25	93 66	76 99	20 73	2 28	5 18
1 5	2 0	1 75	93 87	76 43	21 84	1 73	3 94
2 0	2 5	2 25	92 74	76 57	22 25	1 17	2 66
2 5	3 0	2 75	93 06	76 36	21 56	2 09	4 74
3 0	3 5	3 25	91 71	74 60	23 23	2 16	4 92
3 5	4 0	3 75	90 50	73 45	24 12	2 42	5 51
4 0	4 5	4 25	90 40	73 80	23 37	2 83	6 43
4 5	5 0	4 75	90 39	73 39	24 56	2 05	4 67
5 0	5 5	5 25	90 40	73 31	23 64	3 05	6 94
5 5	6 0	5 75	88 67	71 24	25 79	2 98	6 76
6 0	6 5	6 25	85 39	70 72	26 87	2 42	5 49
6 5	7 0	6 75	86 97	70 76	26 32	2 92	6 65
7 0	7 5	7 25	88 07	71 09	26 08	2 83	6 43
7 5	8 0	7 75	85 91	69 97	26 99	3 04	6 92
8 0	8 5	8 25	86 92	70 71	25 98	3 32	7 54
8 5	9 0	8 75	85 10	70 76	26 71	2 53	5 74
9 0	9 5	9 25	84 97	70 12	26 59	3 29	7 49
9 5	10 0	9 75	84 63	69 76	27 41	2 83	6 43
10 0	10 5	10 25	85 29	70 12	27 38	2 50	5 67
10 5	11 0	10 75	84 96	70 39	27 97	1 64	3 72
11 0	11 5	11 25	85 62	69 88	27 21	2 92	6 63
11 5	12 0	11 75	84 04	71 56	25 71	2 73	6 20
12 0	12 5	12 25	84 02	70 42	26 87	2 70	6 14
12 5	13 0	12 75	83 47	71 00	26 08	2 92	6 64
13 0	13 5	13 25	82 99	72 16	25 15	2 68	6 09
13 5	14 0	13 75	83 11	71 70	25 43	2 87	6 53
14 0	14 5	14 25	82 59	71 55	25 57	2 88	6 54
14 5	15 5	15 00	81 90	71 84	25 46	2 70	6 13
15 5	16 0	15 75	83 55	70 68	26 10	3 22	7 32
16 0	16 5	16 25	83 25	71 60	25 60	2 80	6 37
16 5	17 0	16 75	83 31	71 71	25 90	2 40	5 44
17 0	17 5	17 25	82 88	71 18	25 90	2 92	6 64
17 5	18 0	17 75	82 71	71 94	25 12	2 94	6 68
18 0	18 5	18 25	82 54	69 80	27 53	2 67	6 07
18 5	19 0	18 75	83 63	70 32	26 74	2 93	6 66
19 0	19 5	19 25	83 04	71 37	25 82	2 81	6 38
19 5	20 0	19 75	82 92	71 67	25 68	2 65	6 03
20 0	20 5	20 25	81 93	70 70	26 49	2 81	6 38
20 5	21 0	20 75	82 88	71 82	25 33	2 85	6 48
21 0	21 5	21 25	81 97	69 86	27 35	2 79	6 35
21 5	22 0	21 75	82 53	70 78	26 36	2 86	6 50
22 0	22 5	22 25	81 86	68 49	28 74	2 77	6 29
22 5	23 0	22 75	82 05	68 94	28 42	2 64	6 01

23 0	23 5	23 25	82 41	70 73	26 46	2 80	6 37
23 5	24 0	23 75	82 53	70 96	26 31	2 73	6 20
24 0	24 5	24 25	82 77	70 95	26 14	2 91	6 62
24 5	25 0	24 75	82 44	69 62	27 56	2 81	6 39
25 0	25 5	25 25	82 20	70 29	27 05	2 66	6 04
25 5	26 0	25 75	82 39	69 58	27 72	2 70	6 14
26 0	26 5	26 25	82 32	70 10	27 02	2 88	6 55
26 5	27 0	26 75	82 01	69 18	27 91	2 90	6 59

GSL1 RC-1
Coring Date: 25-Mar-07
Loss-on-Ignition Results

Sed Depth (cm)		Midpoint	%H2O	%OM	%MM	LOI 1000	%CaCO3
(Top)	(Bottom)	depth (cm)		(% dry wt)	(%dry wt)	(% dry wt)	(% dry wt)
0 00	0 50	0.25	88.47	76.63	21.13	2 23	5 08
0 50	1.00	0.75	89.62	76 61	20 47	2 92	6 65
1 00	1 50	1 25	87 76	75.16	23 53	1 31	2 97
1 50	2.00	1 75	87.82	74.62	23 04	2.34	5 31
2 00	2 50	2 25	88 63	74 26	23 83	1 91	4 35
2 50	3 00	2 75	89 51	79 96	18 54	1 50	3 40
3 00	3 50	3 25	87 66	77.43	24.88	-2 31	-5 24
3 50	4.00	3 75	87.17	73.29	25 78	0.93	2.12
4.00	4 50	4.25	88.50	73.78	24.31	1.91	4 34
4.50	5 00	4 75	88 20	74 14	22 91	2 95	6 70
5 00	5.50	5 25	86.17	72 78	25 47	1 75	3 97
5.50	6 00	5 75	86 44	73.39	24.66	1 94	4 42
6.00	6 50	6.25	85 77	74.57	23 86	1 57	3 57
6 50	7 00	6 75	87.23	73 59	25 16	1 25	2 84
7 00	7 50	7 25	86 68	72 60	25 00	2 40	5 44
7 50	8 00	7 75	84 34	71 45	26 49	2 07	4.70
8 00	8 50	8 25	85 95	73 15	25 14	1.70	3 87
8.50	9 00	8 75	87.74	73 92	24 09	1 99	4 53
9 00	9 50	9 25	85 17	71 60	25 87	2 53	5 76
9.50	10 00	9 75	84 00	72 20	25.53	2 26	5 15
10 00	10 50	10 25	84.27	71.32	26 87	1 81	4 11
10.50	11 00	10 75	82 50	71 46	26 58	1.96	4 45
11 00	11 50	11 25	83 28	72 52	25 12	2 36	5 36
11 50	12 00	11 75	82.77	69.76	27 77	2 46	5 60
12 00	12 50	12 25	82 79	68.39	27 91	3 70	8 41
12.50	13 00	12 75	82 80	69.59	28 34	2 07	4 71
13 00	13 50	13 25	83 10	70 99	27.13	1 87	4 25
13 50	14 00	13 75	82 78	70.24	27 80	1 96	4 46
14 00	14 50	14.25	86 39	76 33	22 24	1 43	3 26
14 50	15 00	14 75	87.46	73 40	25 20	1.41	3 20
15 00	15 50	15 25	84 81	69.82	28.37	1 81	4 12
15 50	16 00	15 75	84 27	71 21	27.76	1 04	2 36
16 00	16 50	16 25	88 13	72 85	25.69	1 46	3 33
16 50	17 00	16.75	83 82	70 78	27 38	1 83	4 17
17 00	17 50	17 25	88 62	77 91	20 03	2 05	4 67
17 50	18 00	17 75	88 35	73 09	25 17	1 74	3 95
18 00	18 50	18 25	94 02	83 72	15 61	0 66	1 51
18 50	19 00	18 75	80 52	72 18	722 75	-694.93	-
19.00	19.50	19 25	82 19	70 81	27 52	1 66	3 78
19 50	20.00	19 75	81 94	70 45	28 89	0 66	1 50
20.00	20 50	20 25	82 06	70 96	26 53	2 51	5 71

20 50	21 00	20 75	81 75	71 27	27.29	1 44	3 26
21 00	21 50	21 25	81.73	71 75	25.61	2 65	6 01
21 50	22 00	21 75	82 14	73 21	25 60	1.19	2 71
22 00	22 50	22.25	81 04	72.15	26 34	1 51	3 42
22 50	23 00	22.75	81 30	72.13	26.49	1 38	3.14
23 00	23 50	23 25	81 83	72.67	25 44	1 89	4 29
23 50	24 00	23.75	81 30	68 92	27 37	3.71	8 43
24 00	24 50	24.25	79.92	70.42	27.87	1.71	3 89
24 50	25.00	24 75	81.49	82.19	27.10	-9.29	-21 11
25 00	25 50	25 25	82.70	72.83	24 24	2 93	6 66
25 50	26 00	25 75	82.02	72 26	26.32	1.43	3 24
26 00	26 50	26.25	81 89	73 23	25.05	1 71	3 89
26.50	27 00	26.75	81.64	69.62	25 27	5 12	11.63
27 00	27.50	27.25	81.16	73.58	23.74	2.68	6 10
27.50	28 00	27 75	81 31	71.61	26.15	2 24	5 09
28.00	28.50	28.25	82 22	71.71	26 33	1 96	4 45
28 50	29 00	28.75	82 15	72 26	26.43	1 32	2 99
29 00	29 50	29.25	81 57	70 26	28 04	1.69	3 85
29.50	30 00	29 75	82 01	70.74	27 39	1.87	4 25
30 00	30 50	30 25	81 49	71 12	26 60	2 28	5 18
30 50	31 00	30 75	81 00	71 56	26.88	1 56	3 55
31.00	31 50	31 25	81.59	70 59	27 49	1 91	4 34
31.50	32 00	31 75	81 56	71 22	27 51	1.28	2 91
32.00	32 50	32 25	81 11	71 26	27.79	0 95	2 15
32 50	33 00	32 75	81.42	70.25	27 66	2 09	4.74
33.00	33 50	33 25	81 27	69.80	28 72	1.48	3 36
33 50	34 00	33 75	81 17	69 16	27 60	3 25	7 38
34.00	34.50	34 25	81 46	71.96	26 76	1.28	2 91
34 50	35 00	34 75	81 58	69 44	29.37	1 19	2 70
35.00	35 50	35 25	81.75	68.67	29.59	1.75	3 97
35 50	36 00	35 75	82 66	69.90	25.42	4 68	10 64
36.00	36.50	36 25	80.93	69 75	28 45	1.80	4 10
36 50	37 00	36.75	81 90	71.02	27 44	1.54	3 49
37 00	37.50	37 25	80 24	69.60	28.92	1.48	3.37
37.50	38 00	37 75	81 49	70 24	31.74	-1 98	-4 49
38.00	38 50	38 25	81 49	70.70	28.08	1.21	2 75
38 50	39.00	38 75	82.78	70.62	-737 93	767.31	1743 89
39.00	39.50	39 25	81 72	70 46	28.99	0.56	1 27
39.50	40 00	39 75	81 01	69 29	28 75	1 96	4.47
40 00	40.50	40 25	80 77	69 78	29.19	1 03	2 34
40 50	41 00	40 75	80 96	68 65	29 71	1 64	3 73
41 00	41 50	41 25	80 74	69 48	29 57	0 95	2 16
41.50	42 00	41 75	80 57	67 12	30.91	1 98	4 49
42 00	42 50	42 25	81 79	67 19	30.80	2.01	4 57
42 50	43 00	42 75	80 69	69.18	30.51	0 31	0 71

Appendix E: Organic Carbon and Nitrogen Elemental and Stable Isotope Geochemistry

SR1 KB-2

Coring Date: 24-Mar-07

Organic Carbon and Nitrogen Elemental and Stable Isotope Geochemistry

Midpoint Depth (cm)	*Year (AD)*	*C_{org} (%)*	*Rpt*	*Avg*	*N (%)*	*Rpt*	*Avg*	*Corrected N (%) (-0 0304)*	*$\delta^{13}C_{org}$ (‰)*	*Rpt*	*Avg*	*$\delta^{15}N$ (‰)*	*Rpt*	*Avg*	*C/N*
0 25	2007 00														
0 75	2005 82	13 00		13 00	1 25		1 25	1 25	-28 36		-28 36	-0 08		-0 08	10 38
1 25	2004 51	13 56		13 56	1 27		1 27	1 27	-28 13		-28 13	-0 08		-0 08	10 72
1 75	2002 67	13 38		13 38	1 27		1 27	1 27	-28 44		-28 44	0 10		0 10	10 50
2 25	2000 47	14 01		14 01	1 30		1 30	1 30	-28 57		-28 57	0 17		0 17	10 78
2 75	1998 00	14 34		14 34	1 35		1 35	1 35	-28 75		-28 75	-0 05		-0 05	10 62
3 25	1995 41	14 35		14 35	1 37		1 37	1 37	-28 87		-28 87	0 02		0 02	10 48
4 25	1991 96	14 31		14 31	1 32		1 32	1 32	-28 41		-28 41	-0 01		-0 01	10 86
4 75	1989 17	14 18		14 18	1 31		1 31	1 31	-28 26		-28 26	0 01		0 01	10 79
5 25	1986 51	12 57		12 57	1 18		1 18	1 18	-28 23		-28 23	-0 10		-0 10	10 64
5 75	1984 03	12 28	12 25	12 27	1 16	1 16	1 16	1 16	-28 31	-28 25	-28 28	-0 20	-0 18	-0 19	10 62
6 25	1982 15	11 92		11 92	1 12		1 12	1 12	-28 50		-28 50	-0 26		-0 26	10 61
6 75	1979 69	12 58		12 58	1 18		1 18	1 18	-28 17		-28 17	-0 09		-0 09	10 65
7 25	1977 28	11 30		11 30	1 07		1 07	1 07	-28 21		-28 21	-0 05		-0 05	10 54
7 75	1974 53	13 33		13 33	1 19		1 19	1 19	-27 68		-27 68	-0 07		-0 07	11 19
8 25	1972 44	12 10		12 10	1 12		1 12	1 12	-27 94		-27 94	-0 19		-0 19	10 84
8 75	1969 77	13 66		13 66	1 32		1 32	1 32	-28 16		-28 16	-0 06		-0 06	10 38
9 25	1966 77	11 77		11 77	1 16		1 16	1 16	-28 46		-28 46	-0 15		-0 15	10 14

9 75	1963 45	12 89		12 89	1 27		1 27	1 27	-28 27		-28 27	-0 16		-0 16	10 14
10 25	1958 40	11 81		11 81	1 19		1 19	1 19	-28 05		-28 05	-0 06		-0 06	9 92
10 75	1953 94	11 85	11 80	11 82	1 20	1 19	1 19	1 20	-27 65	-27 67	-27 66	-0 11	-0 41	-0 26	9 88
11 25	1951 80	10 88		10 88	1 06		1 06	1 06	-27 50		-27 50	-0 02		-0 02	10 25
11 75	1949 49	10 98		10 98	1 04		1 04	1 04	-27 47		-27 47	-0 18		-0 18	10 57
12.50	1947 63	19 57		19 57	1 82		1 82	1 82	-27 60		-27 60	-0 02		-0 02	10 77
13.25	1941 75	11 31		11 31	1 02		1 02	1 02	-27 44		-27.44	-0 25		-0 25	11 10
13 75	1939 31	11 02		11.02	1.02		1 02	1 02	-27 61		-27.61	-0 12		-0 12	10 77
14 25	1932 20	11 55		11 55	1 04		1 04	1 04	-27 19		-27 19	-0 21		-0 21	11 08
14 75	1928 50	11 32		11 32	1 03		1 03	1 03	-27 61		-27 61	-0 17		-0 17	11 01
15 25	1924 83	11 50		11 50	1 03		1 03	1 03	-27 45		-27 45	-0 20		-0 20	11 19
15 75	1921.62	10 74	10 95	10 84	0 98	1 03	1 00	0 98	-27 55	-27 58	-27 56	-0 10	0 08	-0 01	10 96
16 25	1917 83	11 14		11 14	1 01		1 01	1 01	-27 49		-27 49	0 07		0 07	11 02
16 75	1914 23	11 11		11 11	1 04		1 04	1 04	-27 39		-27 39	0 00		0 00	10 68
17 25	1910 07	11 41		11 41	1 04		1 04	1 04	-27 33		-27 33	0 00		0 00	11 01
17 75	1906.57	11 33		11 33	1 01		1 01	1 01	-27 41		-27 41	0 04		0 04	11 23
18 25	1903 38	11 57		11 57	1 06		1 06	1 06	-27 44		-27 44	-0.04		-0 04	10 88
18.75	1896 60	11.27		11 27	1 05		1 05	1 05	-27 52		-27 52	-0 28		-0 28	10 77
19.25	1893 92	11 34		11 34	1.05		1 05	1 05	-27 55		-27 55	-0 13		-0 13	10 83
19 75	1890 24	11 61		11 61	1 06		1 06	1.06	-27 33		-27 33	-0 08		-0 08	10 92
20 25	1886 36	10 97		10.97	1 03		1 03	1 03	-27 57		-27 57	-0 15		-0 15	10 64
20 75	1883 21	11 49		11 49	1.06		1 06	1 06	-27 38		-27 38	-0.03		-0.03	10 84
21 25	1879 43	10 92	10.77	10 85	1 03	1 03	1 03	1 03	-27 44	-27 55	-27 49	-0 07	0.09	0.01	10 62
21 75	1875 42	10.91		10.91	1 02		1 02	1 02	-27 40		-27 40	0 07		0 07	10 65
22 25	1871.52	10.73		10.73	1 00		1 00	1 00	-27 51		-27 51	-0 10		-0 10	10 69
22 75	1867 38	11 04		11 04	1.02		1 02	1 02	-27 35		-27 35	-0 02		-0 02	10 84
23 25	1863 45	11 14		11 14	1 01		1 01	1 01	-27 33		-27 33	-0 07		-0 07	11 04

23.75	1859.34	11.05		11 05	1 01		1 01	1 01	-27 21		-27.21	0 06		0 06	10 91
24 25	1855 62	10 06		10 06	0 92		0 92	0 92	-27 59		-27 59	0 06		0 06	10 97
24 75	1851 16	9 99		9 99	0 87		0 87	0 87	-27 74		-27 74	0 15		0 15	11 50
25.25	1846.00	9 93		9.93	0.82		0 82	0 82	-28 02		-28 02	0 28		0 28	12 06
25 75	1840 35	10 52		10 52	0 86		0 86	0 86	-28 23		-28 23	0 27		0 27	12 19
26.25	1834.65	11 16		11 16	0 90		0 90	0.90	-28 35		-28 35	0 32		0 32	12.38
26.75	1829.01	10 87	10 99	10 93	0.90	0 91	0 91	0 90	-28 18	-28 28	-28 23	0 53	0 45	0 49	12 04
27 25	1824 06	10.34		10 34	0 87		0 87	0 87	-28.20		-28.20	0 67		0 67	11 94
27 75	1818.17	10 07		10 07	0 85		0 85	0 85	-28 05		-28 05	0 94		0 94	11 83
28 25	1812 96	10 80		10 80	0 89		0 89	0 89	-27 95		-27.95	0 96		0 96	12 12
28 75	1806 64	10 17		10.17	0 81		0 81	0 81	-28 03		-28 03	0 82		0 82	12 49
29 25	1800 31	9 08		9 08	0 75		0 75	0 75	-27 77		-27 77	0.74		0 74	12 05
29.75	1794.49	8 62		8 62	0 69		0 69	0 69	-27 84		-27 84	0 64		0 64	12 45
30 25	1786 90	8 17		8 17	0 66		0 66	0 63	-27 94		-27 94	0.65		0 65	12 87
30 75	1782 59	7 97		7 97	0 62		0 62	0 59	-27 91		-27 91	0 71		0 71	13 41
31 25	1772 48	6 97		6 97	0 56		0 56	0 53	-27 87		-27 87	0 69		0 69	13 10
31.75	1762 35	6 31		6 31	0 51		0 51	0 48	-27 81		-27 81	0 49		0 49	13 23
32 25	1751 07	5 12	5 28	5 20	0 43	0 44	0 43	0 40	-27 94	-27 81	-27 88	0 76	0 65	0 70	12 66
32 75	1740.88	4 63		4.63	0 40		0 40	0 37	-27 87		-27 87	0 65		0 65	12 43
33 25	1722.48	4 77		4 77	0 39		0 39	0 36	-27.79		-27 79	0.75		0 75	13 19
33.75	1709 99	4.21		4 21	0.36		0.36	0.33	-27 78		-27 78	0 92		0 92	12 79
34.25	1700.61	4.67		4 67	0 37		0 37	0.34	-27 65		-27 65	0 53		0 53	13 89
34 75	1674.63	4 34		4 34	0 36		0 36	0 33	-27.80		-27 80	0.83		0 83	13 04
35 25	1664 49	4 36		4.36	0 36		0 36	0 33	-27 66		-27 66	0 86		0 86	13 18
35 75	1650 92	4 71		4 71	0.39		0 39	0 36	-27 71		-27 71	1 10		1 10	13 26
36.25	1638 66	3 75		3 75	0.32		0 32	0 29	-27 81		-27 81	0.85		0 85	12 79
36 75	1624 57	3 58		3 58	0 30		0 30	0 27	-27 79		-27 79	1 27		1 27	13 09

37 25	1605 97	3 56		3.56	0 30		0 30	0 27	-27.74		-27 74	0 91		0 91	13 29
37.75	1594 20	3 44		3 44	0 29		0 29	0 26	-27 62		-27 62	0 95		0 95	13 19
38.25	1580.25	3 42		3.42	0.29		0 29	0 26	-27.75		-27 75	1.13		1.13	12 99
38 75	1562 71	2 94		2 94	0.25		0 25	0 22	-27 51		-27.51	1 17		1 17	13 31
39 25	1546 84	2 57		2.57	0 22		0 22	0 19	-27.42		-27.42	1.10		1 10	13 45

SD34 KB-2

Coring Date: 24-Mar-07

Organic Carbon and Nitrogen Elemental and Stable Isotope Geochemistry

Midpoint Depth (cm)	*Year (AD)*	*C_{org} (%)*	*Rpt*	*Avg*	*N (%)*	*Rpt*	*Avg*	*$\delta^{13}C_{org}$ (‰)*	*Rpt*	*Avg*	*$\delta^{15}N$ (‰)*	*Rpt*	*Avg*	*C/N*
0.25	2007 20	41.04		41 04	3 46		3.46	-26.35		-26 35	2 50		2 50	11 85
0 75	2006 45	41.50		41 50	3.47		3 47	-26 41		-26 41	2.36		2 36	11 95
1 25	2004 96	41 19		41 19	3 53		3 53	-26 49		-26.49	2 43		2.43	11 67
1 75	2001.64	41 07		41 07	3.49		3 49	-26 49		-26 49	2 31		2 31	11 76
2 25	2000.16	40 75		40 75	3 44		3 44	-26 63		-26 63	2 22		2 22	11 83
2 75	1998 66	40.75		40 75	3 45		3 45	-26 58		-26.58	2 41		2 41	11 82
3 25	1996.73	39 85		39 85	3.35		3 35	-26 64		-26 64	2.36		2.36	11 90
3 75	1994 97	38 68		38 68	3 20		3 20	-26 47		-26 47	2.17		2.17	12 08
4 25	1993.25	38 49		38 49	3 15		3 15	-26 28		-26.28	2 03		2.03	12.22
4 75	1991 35	37 67	36 31	36 99	3.12	2 96	3 04	-26 00	-26 02	-26 01	2 11	1 96	2 03	12 17
5.25	1989 36	35 99		35 99	2 94		2 94	-25 70		-25.70	2 02		2 02	12 23
5 75	1987 29	35 32		35.32	2 86		2 86	-25 67		-25.67	1 98		1 98	12 34
6 25	1984 97	35 78		35 78	2 87		2 87	-25 43		-25.43	1 91		1 91	12 48
6.75	1982.16	35.17		35 17	2 84		2 84	-25 39		-25 39	1 90		1 90	12 39
7 25	1980 00	34 66		34 66	2 80		2 80	-25 22		-25 22	1 95		1 95	12 40
7 75	1977.50	35 20		35 20	2 84		2 84	-25 11		-25 11	1 94		1 94	12.39
8.25	1974 32	34 90		34.90	2 84		2 84	-25 02		-25 02	1 89		1 89	12 29
8 75	1970 47	36 14		36 14	2 87		2 87	-25 10		-25 10	2 06		2 06	12 60
9.25	1966 88	34 52		34 52	2 79		2 79	-24 96		-24 96	1 92		1 92	12 36
9 75	1961.34	35 12	34.64	34 88	2 85	2 81	2 83	-24 96	-24 92	-24 94	1.91	1 86	1 88	12 33
10.25	1956 42	34 62		34 62	2 81		2 81	-24 83		-24 83	1 84		1 84	12 34
10 75	1951 71	34 46		34 46	2 77		2 77	-24 85		-24 85	1 78		1 78	12 45

11 25	1945 63	34 64		34 64	2.80		2.80	-24 83		-24 83	1 83		1 83	12 38
11 75	1938 12	34 30		34.30	2 72		2 72	-24 87		-24 87	1.76		1 76	12 59
12 25	1930 54	34 32		34 32	2.74		2 74	-24 81		-24 81	1 64		1 64	12 53
12 75	1925 71	34 32		34 32	2.73		2 73	-24 65		-24 65	1.55		1.55	12 57
13 25	1918 68	33 19		33 19	2.61		2 61	-24 91		-24 91	1 81		1.81	12 70
13 75	1912 12	33 64		33.64	2 65		2.65	-24 92		-24 92	1 77		1 77	12 71
14.25	1906.79	33 25		33.25	2.55		2 55	-24 96		-24 96	1 78		1 78	13.05
14 75	1899.39	32 77	33.30	33.03	2.55	2 60	2.57	-24 97	-24.95	-24 96	1 68	1 69	1.69	12 83
15 25	1893 08	33 98		33.98	2.62		2.62	-24 92		-24.92	1.64		1.64	12.99
15 75	1886.73	33 80		33.80	2.59		2 59	-24 92		-24 92	1 66		1.66	13 06
16 25	1878.11	33 68		33 68	2.58		2 58	-25.05		-25.05	1.76		1.76	13 07
16 75	1872 71	32 80		32.80	2 54		2 54	-24 99		-24 99	1 64		1 64	12 89
17 25	1866 63	31 58		31 58	2 33		2 33	-25 30		-25 30	1 84		1.84	13.56
17 75	1859 06	30 91		30 91	2 27		2 27	-25 30		-25.30	1 79		1 79	13 62
18 25	1852 82	31 04		31 04	2.25		2 25	-25 44		-25 44	1 89		1 89	13 80
18 75	1845 98	29.95		29 95	2.21		2 21	-25 36		-25 36	1 68		1.68	13 53
19.25	1837 99	30.30		30 30	2.29		2 29	-25 23		-25.23	1 73		1 73	13 24
19 75	1829 59	28.03		28 03	2 04		2 04	-25 39		-25 39	1 56		1.56	13 74
20 25	1822 79	28.51		28 51	2.07		2.07	-25 48		-25 48	1.46		1 46	13 78
20 75	1814 65	27 73		27 73	2 03		2 03	-25 62		-25 62	1 44		1.44	13 68
21 25	1807 08	27 30		27 30	2 02		2 02	-25 54		-25 54	1.40		1 40	13 54
21.75	1797 57	26.09	26.74	26 41	1 92	1.98	1 95	-25 62	-25 67	-25 65	1 24	1.45	1.34	13.55
22.25	1789.71	26 32		26.32	1 94		1 94	-25 66		-25 66	1 35		1.35	13 56
22.75	1781 57	26 68		26 68	1.97		1.97	-25.59		-25 59	1 39		1 39	13 53
23 25	1773 96	26 08		26 08	1.95		1.95	-25 71		-25 71	1 46		1.46	13 36
23 75	1764 39	24 87		24 87	1 89		1 89	-25 72		-25 72	1.63		1 63	13 17
24 25	1756 25	26.45		26.45	2 01		2 01	-25 70		-25 70	1 78		1.78	13 17

24 75	1745 98	25.90		25 90	1 97		1 97	-25 47		-25 47	1 70		1 70	13 15
25 25	1736.17	25 94		25 94	1 96		1 96	-25 68		-25.68	1 69		1 69	13 22
25.75	1728.66	25 57		25 57	1.89		1 89	-25 72		-25 72	1 41		1 41	13 51
26 25	1718.86	26 11		26.11	1 93		1.93	-25 68		-25 68	1 35		1 35	13.56
26.75	1709.29	25 55	25.78	25 67	1 88	1 90	1 89	-25 62	-25 59	-25 61	1 46	1 30	1.38	13 59
27 25	1699.53	25 71		25 71	1.92		1 92	-25 61		-25 61	1.53		1.53	13 40
27 75	1690.43	25.87		25 87	1.90		1 90	-25 60		-25 60	1 22		1 22	13 60
28.25	1680.23	26.17		26.17	1.94		1.94	-25 54		-25.54	1.30		1.30	13 52
28 75	1670.35	25 08		25.08	1.87		1 87	-25 53		-25 53	1 39		1 39	13 43
29 25	1655 57	25 75		25 75	1.88		1.88	-25 66		-25 66	1.30		1.30	13 68
29.75	1648 23	26 71		26.71	1 97		1 97	-25 61		-25.61	1.33		1 33	13 55
30.25	1636 15	24 36		24.36	1 78		1 78	-25 63		-25.63	1 27		1 27	13 68
30 75	1627 49	25.78		25 78	1 90		1.90	-25 67		-25 67	1 41		1.41	13 57
31 25	1617 42	26 77		26.77	1 98		1 98	-25 71		-25 71	1 36		1 36	13 54
31.75	1607 79	25 52	25.41	25 47	1 89	1 88	1 89	-25 69	-25 79	-25 74	1.45	1 36	1 40	13 51
32 25	1598.25	23 70		23 70	1 77		1 77	-25 75		-25 75	1 28		1.28	13 42
32.75	1587.11	21 62		21.62	1 62		1 62	-25 64		-25.64	1.28		1.28	13 32
33 25	1576 78	22 65		22 65	1 72		1 72	-25 78		-25 78	1.32		1.32	13 15
33 75	1566 32	23 66		23.66	1 78		1 78	-25 76		-25 76	1 12		1.12	13 32
34 25	1557 67	24 29		24.29	1 81		1.81	-25 74		-25.74	1 36		1.36	13 40
34 75	1546.52	23 47		23 47	1.77		1.77	-25 77		-25 77	1.16		1 16	13 26
35 25	1537 00	22 64		22 64	1 76		1.76	-25 63		-25.63	1 23		1 23	12 84
35 75	1526.04	23 39		23.39	1.76		1 76	-25 78		-25 78	0 94		0 94	13 28
36 25	1515 19	20 92		20 92	1 62		1.62	-25 64		-25.64	1 00		1 00	12 91
36 75	1506.16	21.54	20 84	21.19	1.66	1 62	1 64	-25.62	-25.63	-25 63	1.04	0 91	0 98	12 92
37 25	1496.39	19 54		19 54	1.52		1 52	-25 64		-25 64	0.89		0 89	12 82
37.75	1489 12	20.16		20.16	1 62		1.62	-25 64		-25 64	1 17		1 17	12 48

SD34 RC-2

Coring Date: 24-Mar-07

Organic Carbon and Nitrogen Elemental and Stable Isotope Geochemistry

Midpoint Depth (cm)	*Year (AD)*	*C_{org} (%)*	*Rpt*	*Avg*	*N (%)*	*Rpt*	*Avg*	*Corrected N (%) (-0 0414)*	*$\delta^{13}C_{org}$ (‰)*	*Rpt*	*Avg*	*$\delta^{15}N$ (‰)*	*Rpt*	*Avg*	*C/N*
4 25	1993.25	36.48		36.48	2.86		2 86	2.86	-25 99		-26.0	2 1		2.1	12 8
4 75	1991.35	37 97		37.97	2 94		2 94	2.94	-26 00		-26.0	2 1		2 1	12 9
5.25	1989.36	38 23		38 23	2.95		2.95	2.95	-25.79		-25.8	2 0		2.0	12.9
5.75	1987 29	36 40		36 40	2 80		2.80	2 80	-25.80		-25.8	2 0		2.0	13 0
6 25	1984 97	36 17		36 17	2.74		2 74	2 74	-25 24		-25.2	1 9		1.9	13 2
6 75	1982 16	37 69		37.69	2 87		2.87	2 87	-25 76		-25 8	2 0		2 0	13.1
7 25	1980 00	36 81		36 81	2 79		2 79	2.79	-25 55		-25 6	2 1		2 1	13 2
7 75	1977 50	36 53		36 53	2 75		2 75	2 75	-25 57		-25.6	2.0		2 0	13 3
8.25	1974.32	35 72		35.72	2 70		2 70	2 70	-25 57		-25.6	1 9		1 9	13 2
8.75	1970 47	35 17	35.46	35 31	2.64	2 68	2.66	2 67	-25.70	-25.64	-25 7	1 9	2 0	1.9	13 2
9 25	1966.88	36 08		36.08	2.73		2 73	2 73	-25 56		-25.6	1 9		1 9	13 2
9 75	1961.34	35 76		35 76	2 70		2 70	2 70	-25.56		-25 6	1 8		1 8	13.3
10.25	1956.42	35 72		35 72	2 70		2 70	2.70	-25 45		-25 5	1.9		1 9	13 2
10 75	1951 71	35 74		35 74	2 66		2 66	2 66	-25.47		-25 5	1 9		1 9	13 4
11 25	1945 63	36 06		36 06	2.71		2 71	2 71	-25 52		-25 5	2 0		2 0	13.3
11 75	1938 12	35 84		35 84	2.68		2 68	2 68	-25.39		-25 4	1 9		1 9	13 4
12 25	1930 54	35 54		35 54	2.68		2 68	2 68	-25.33		-25 3	1 9		1 9	13 3
12.75	1925.71	35 41		35 41	2.69		2.69	2 69	-25 56		-25 6	2 0		2 0	13 2
13.25	1918 68	35.37		35 37	2.66		2 66	2.66	-25.31		-25 3	1 8		1.8	13 3
13 75	1912.12	34 45	34 96	34 71	2 61	2 63	2.62	2 63	-25 01	-24.93	-25 0	1 7	1 8	1 7	13.2
14 25	1906.79	34 82		34.82	2 59		2.59	2 59	-24 84		-24 8	1 8		1 8	13 4

14 75	1899.39	35 16		35 16	2.62		2 62	2 62	-24 75		-24 7	1 8		1 8	13 4
15 25	1893 08	35 14		35 14	2 63		2 63	2 63	-24 79		-24 8	1 7		1 7	13 4
15 75	1886 73	34 67		34 67	2 60		2 60	2 60	-24 58		-24 6	1 8		1 8	13 3
16 25	1878 11	35 11		35 11	2 61		2 61	2 61	-24 46		-24 5	1 8		1 8	13 4
16.75	1872 71	34.96		34.96	2 61		2 61	2 61	-25 22		-25.2	1 9		1 9	13 4
17.25	1866.63	35 60		35.60	2 62		2 62	2 62	-25 05		-25 0	1.8		1 8	13 6
17 75	1859 06	34 79		34 79	2.58		2 58	2 58	-24 67		-24.7	2 0		2 0	13 5
18.25	1852.82	35 33		35.33	2 58		2 58	2 58	-24 79		-24.8	1 9		1 9	13 7
18 75	1845 98	32 95	34 58	33 77	2 39	2 53	2.46	2 50	-24 70	-24 60	-24.7	1 9	2 0	1.9	13 5
19 25	1837.99	34 22		34.22	2.49		2.49	2 49	-24.59		-24 6	1 9		1 9	13 7
19.75	1829 59	33.95		33.95	2 46		2.46	2 46	-25 04		-25 0	1 9		1 9	13 8
20 25	1822.79	34 96		34.96	2.49		2.49	2.49	-24 85		-24 8	1.8		1.8	14 1
20.75	1814.65	33 72		33.72	2 39		2 39	2.39	-25 03		-25 0	1.9		1 9	14 1
21.25	1807.08	34 38		34.38	2 41		2 41	2 41	-25 01		-25 0	1 8		1 8	14 3
21 75	1797 57	32 69		32.69	2 34		2.34	2 34	-25 10		-25 1	1 7		1.7	14.0
22 25	1789.71	33 54		33 54	2 45		2 45	2 45	-24 57		-24 6	1.8		1 8	13 7
22 75	1781.57	32 76		32 76	2 33		2 33	2 33	-25 17		-25 2	1.7		1 7	14 0
23 25	1773 96	33 03		33 03	2 37		2 37	2 37	-25.23		-25.2	1 8		1.8	14 0
23 75	1764 39	33 69	33 09	33.39	2 41	2 39	2 40	2 39	-24 92	-25.28	-25 1	1.7	1 8	1 8	14 0
24 25	1756.25	33 29		33 29	2 40		2 40	2 40	-25 26		-25 3	1 8		1 8	13 9
24 75	1745.98	32 95		32 95	2 38		2 38	2 38	-25 17		-25 2	1 6		1 6	13 8
25 25	1736 17	32 30		32 30	2.29		2 29	2 29	-24 94		-24 9	1 7		1.7	14.1
25.75	1728.66	30 24		30 24	2 18		2 18	2 18	-25 04		-25 0	1 8		1 8	13 9
26 25	1718.86	31 68		31 68	2.28		2.28	2 28	-24 70		-24.7	1 7		1 7	13 9
26 75	1709.29	31.60		31.60	2 25		2.25	2.25	-24.66		-24 7	1 8		1.8	14 0
27.25	1699 53	32 41		32.41	2 31		2.31	2 31	-25.11		-25.1	1 8		1 8	14.1
27 75	1690.43	33.55		33.55	2 36		2 36	2 36	-24.88		-24 9	1 8		1.8	14.2

28 25	1680 23	31 39		31 39	2 25		2 25	2 25	-24 60		-24 6	1 7		1 7	14 0
28.75	1670.35	32 77	32 07	32.42	2 30	2 28	2 29	2 28	-24 98	-24.77	-24 9	1.6	1 5	1 6	14 2
29.25	1655 57	32 68		32.68	2.29		2 29	2 29	-25 04		-25 0	1 7		1 7	14 3
29 75	1648 23	32 03		32 03	2.28		2 28	2 28	-25 17		-25 2	1 5		1 5	14 0
30 25	1636 15	32 37		32.37	2 28		2 28	2 28	-24.99		-25 0	1.5		1 5	14.2
30 75	1627 49	29 94		29 94	2 16		2 16	2 16	-25 05		-25 0	1 5		1 5	13 8
31 25	1617 42	30.61		30.61	2 22		2 22	2 22	-25 04		-25 0	1 2		1 2	13.8
31.75	1607.79	30.37		30 37	2 17		2 17	2 17	-24 83		-24.8	1 5		1 5	14 0
32 25	1598.25	30 41		30.41	2.18		2.18	2 18	-25 31		-25.3	1 5		1.5	13 9
32 75	1587.11	30 04		30 04	2.16		2.16	2 16	-25 24		-25.2	1.5		1 5	13 9
33 25	1576 78	28 90		28 90	2 07		2 07	2 07	-24 93		-24.9	1.6		1.6	14 0
33 75	1566.32	30 38	28 86	29.62	2.14	2 08	2.11	2.09	-24.61	-24.69	-24 7	1.5	1 5	1 5	14 2
34 25	1557.67	28 69		28.69	2.04		2 04	2 04	-24 77		-24.8	1.3		1.3	14 1
34 75	1546 52	29 63		29.63	2.12		2 12	2 12	-24.57		-24.6	1.7		1.7	14.0
35 25	1537 00	29 45		29.45	2.11		2.11	2 11	-24 57		-24 6	1 4		1 4	14 0
35 75	1526 04	28.78		28.78	2.04		2 04	2 04	-25 17		-25.2	1.4		1.4	14.1
36 25	1515.19	28.44		28.44	2 03		2 03	2 03	-24.77		-24 8	1.4		1 4	14 0
36.75	1506 16	28 17		28.17	2 02		2 02	2.02	-24.60		-24 6	1 6		1.6	13 9
37 25	1496 39	28 40		28.40	2 00		2 00	2 00	-24 67		-24 7	1 5		1 5	14 2
37.75	1489 12	28 10		28.10	2.02		2 02	2 02	-24 86		-24 9	1.5		1.5	13.9
38.25	1479.31	28 41		28.41	2 01		2 01	2 01	-24.73		-24 7	1.5		1 5	14 2
38 75	1469 49	27 19	27 17	27 18	1.91	1 92	1.92	1 92	-24 76	-24.62	-24.7	1 4	1 2	1.3	14.2
39 25	1459 67	26 85		26 85	1 90		1 90	1 90	-25 16		-25 2	1 4		1 4	14 1
39 75	1449 86	26 68		26 68	1 87		1.87	1 87	-25 11		-25 1	1 1		1 1	14 3
40 25	1440.04	26 31		26.31	1 87		1.87	1 87	-25 02		-25.0	1 5		1 5	14.0
40 75	1430.23	25.88		25 88	1.82		1.82	1 82	-25 04		-25 0	1 2		1 2	14 3
41 25	1420 41	25 63		25 63	1 80		1.80	1 80	-24 98		-25 0	1 5		1.5	14 2

41 75	1410 59	26 16		26 16	1.85		1 85	1 85	-25 00		-25 0	1.4		1 4	14 1
42 25	1400 78	24 87		24 87	1 77		1 77	1 77	-25 09		-25 1	1 4		1 4	14 1
42 75	1390 96	25 12		25.12	1 74		1 74	1 74	-25 04		-25 0	1.3		1 3	14 4
43 25	1381 14	25 56		25 56	1 88		1 88	1 88	-24 90		-24 9	1 3		1 3	13 6
43 75	1371.33	26.06	25.67	25 87	1 96	1 93	1 95	1 94	-25 14	-25 14	-25 1	1.2	1 2	1.2	13.3
44 25	1361.51	24.82		24.82	1 85		1 85	1 85	-25 21		-25 2	1.3		1 3	13 4
44 75	1351 70	25 05		25.05	1 86		1 86	1 86	-25 07		-25 1	1.1		1 1	13 4
45.25	1341 88	25 14		25 14	1.86		1.86	1 86	-25 07		-25.1	1 2		1 2	13 5
45 75	1332.06	23 93		23 93	1 78		1 78	1 78	-25 22		-25 2	1.2		1.2	13 4
46.25	1322 25	24 28		24 28	1 79		1.79	1 79	-25 03		-25 0	1 2		1 2	13 5
46 75	1312 43	24 17		24.17	1.77		1.77	1 77	-25.10		-25 1	1.0		1 0	13 7
47 25	1302 62	24.45		24.45	1 85		1 85	1 85	-24 92		-24 9	1.0		1 0	13 2
47 75	1292.80	22 80		22.80	1 71		1 71	1 71	-25 65		-25 7	1 2		1 2	13 4
48 25	1282 98	23 77		23 77	1.79		1.79	1 79	-25 73		-25.7	1 1		1.1	13 3
48 75	1273 17	23 81	23.59	23 70	1.79	1 76	1 77	1 77	-25 76	-25.72	-25 7	1 1	1 0	1 1	13.4
49 25	1263.35	22 90		22 90	1.74		1 74	1 74	-25 79		-25.8	1 1		1.1	13 1
49.75	1253 53	23 12		23 12	1 73		1 73	1 73	-25 87		-25.9	1 2		1 2	13 3
50 25	1243 72	21 98		21 98	1 66		1 66	1 66	-25 73		-25 7	1.2		1.2	13.2
50.75	1233 90	22 61		22.61	1 69		1 69	1 69	-25 73		-25 7	0.9		0 9	13 4
51 25	1224.09	22 26		22 26	1.74		1.74	1.74	-25 72		-25 7	1 0		1 0	12.8
51.75	1214 27	22 35		22.35	1 75		1 75	1 75	-25 78		-25 8	1 2		1 2	12 8
52.25	1204 45	21 13		21.13	1.68		1 68	1 68	-25 71		-25 7	1 3		1 3	12 6
52 75	1194 64	20 64		20 64	1.64		1.64	1 64	-25 63		-25 6	0.9		0 9	12.6
53 25	1184 82	21 64		21 64	1.71		1.71	1 71	-25 47		-25 5	1 1		1.1	12 7
53 75	1175 01	22 29	22.81	22.55	1 67	1.73	1 70	1 72	-25 59	-25.51	-25.5	1 1	1 2	1 1	13 1
54 25	1165 19	20 41		20.41	1.55		1.55	1 55	-25.77		-25 8	1 1		1.1	13 2
54.75	1155 37	19.68		19.68	1.50		1.50	1.50	-25 48		-25 5	1 1		1.1	13.2

55 25	1145 56	17 83		17 83	1 39		1 39	1 39	-25 38		-25 4	1 1		1 1	12 8
55 75	1135 74	17 40		17 40	1 37		1 37	1 37	-25 40		-25 4	1 0		1 0	12 7
56.25	1125 92	15 98		15 98	1 27		1 27	1 27	-25 37		-25 4	1 0		1 0	12 6
56 75	1116.11	16 37		16 37	1 29		1 29	1 29	-25 52		-25 5	0 8		0 8	12 7
57 25	1106 29	15 06		15 06	1 20		1 20	1 20	-25 27		-25 3	0 8		0 8	12 6
57.75	1096 48	14 79		14 79	1 19		1 19	1 19	-25 02		-25 0	0 9		0 9	12 4
58 25	1086 66	16 28		16.28	1.29		1 29	1 29	-25 17		-25 2	0 8		0 8	12 6
58.75	1076 84	15.35	15.45	15 40	1.23	1 25	1 24	1 24	-25.10	-25 14	-25 1	0 7	1.0	0 8	12 4
59 25	1067 03	14 43		14.43	1 16		1 16	1 16	-25 05		-25 0	0 7		0 7	12 5
59 75	1057.21	13.32		13 32	1 08		1.08	1 08	-24 77		-24 8	0 8		0 8	12 3
60 25	1047 39	12 55		12 55	1 02		1 02	1 02	-24.88		-24 9	0.7		0.7	12 3
60 75	1037 58	12 58		12 58	1 03		1 03	1 03	-25 05		-25 0	0 8		0.8	12 2
61 25	1027 76	12 41		12 41	1.01		1 01	1 01	-24.56		-24 6	0.7		0 7	12 2
61 75	1017.95	11 73		11 73	0 97		0 97	0 97	-24 67		-24 7	0 7		0 7	12 2
62 25	1008.13	10 76		10 76	0 90		0 90	0 90	-24 88		-24 9	0 6		0 6	12 0
62 75	998.31	9 61		9.61	0 80		0 80	0 76	-24.22		-24 2	0.8		0.8	12 6
63.25	988.50	6 53		6 53	0 58		0 58	0 54	-24 43		-24.4	0.7		0 7	12 1
63.75	978 68	8.98	8 73	8 86	0.79	0 76	0 78	0 73	-24.67	-24.38	-24 5	0 8	0 9	0 8	12 1
64.25	968 87	8 10		8 10	0 72		0.72	0 68	-24 33		-24 3	0.7		0.7	12 0
64 75	959.05	6.33		6 33	0 55		0.55	0 51	-24.44		-24.4	0 9		0.9	12 4
65 25	949.23	4 62		4.62	0 42		0.42	0.38	-24.76		-24.8	0 7		0 7	12 3
65 75	939 42	4 62		4 62	0.42		0 42	0 38	-24.78		-24 8	0 8		0.8	12 1
66 25	929.60	4 24		4.24	0 39		0.39	0 35	-24 53		-24 5	0 7		0 7	12 1
66.75	919 78	3 87		3 87	0.36		0 36	0 32	-24 80		-24 8	0.9		0 9	12 2
67.25	909.97	3 72		3 72	0.34		0.34	0 30	-24 63		-24 6	0 8		0 8	12.4
67 75	900 15	3 27		3 27	0.30		0 30	0 26	-24 93		-24 9	1.0		1.0	12 5
68.25	890 34	3.08		3.08	0.29		0.29	0 25	-24 54		-24 5	1 3		1 3	12 3

68.75	880 52	3 23	3 35	3 29	0 30	0 32	0 31	0 27	-24 62	-24 83	-24 7	1 0	0 8	0 9	12 3
69 25	870 70	3 61		3.61	0 34		0 34	0 30	-25 25		-25 3	1 0		1 0	12 0
69 75	860 89	5 14		5.14	0.47		0 47	0 43	-24 96		-25 0	0 9		0 9	12 1
70 25	851 07	3 94		3.94	0 36		0 36	0 32	-24 67		-24 7	0 9		0 9	12 4
70.75	841 26	3 90		3.90	0 36		0.36	0 32	-25 06		-25.1	1 0		1 0	12 1
71 25	831.44	3 99		3 99	0 36		0 36	0 32	-24 68		-24.7	0 8		0 8	12 4
71 75	821 62	3 49		3.49	0 33		0.33	0 29	-24.84		-24.8	1 0		1 0	12 2
72 25	811 81	3 38		3.38	0.32		0 32	0.28	-25 03		-25 0	0 9		0 9	12 1
72.75	801 99	3 13		3.13	0 29		0 29	0.25	-24 71		-24 7	0 9		0 9	12 4
73 25	792 17	3 10		3 10	0 30		0 30	0 25	-24.73		-24 7	0 7		0 7	12 2
73 75	782 36	3.64	3 60	3 62	0 35	0 34	0 34	0 30	-24 76	-24.82	-24 8	0 6	0.8	0 7	12.0
74 25	772.54	3 20		3 20	0 30		0 30	0 26	-24 93		-24 9	1 2		1 2	12 3
74 75	762 726	3 25		3 25	0 30		0.30	0 26	-25 14		-25 1	1 1		1 1	12 4

GSL1 KB-1

Coring Date: 25-Mar-07

Organic Carbon and Nitrogen Elemental and Stable Isotope Geochemistry

Midpoint Depth (cm)	*Year (AD)*	C_{org} (%)	*Rpt*	*Avg*	*N (%)*	*Rpt*	*Avg*	$\delta^{13}C_{org}$ (‰)	*Rpt*	*Avg*	$\delta^{15}N$ (‰)	*Rpt*	*Avg*	*C/N*
0 75	2007 2	44 13		44 13	3 35		3 35	-29 37		-29 37	0 06		0 06	13 17
1 25	2006 2	44 42		44 42	3 38		3 38	-29 50		-29 50	-0 04		-0 04	13 16
1.75	2003 8	43 83		43 83	3 29		3 29	-29 51		-29 51	-0 45		-0 45	13 30
2.25	2001 6	43 79		43 79	3 44		3 44	-29 45		-29 45	-0 03		-0 03	12 72
2 75	1997 8	42 25		42 25	3 24		3 24	-29 17		-29 17	0.03		0 03	13 05
3 25	1995 4	43 80		43 80	3 40		3 40	-29.57		-29 57	0 00		0 00	12 90
3 75	1990 8	42 72		42 72	3 31		3 31	-28 95		-28 95	0 10		0 10	12 89
4.25	1985 9	42 93		42 93	3 28		3 28	-29 15		-29 15	-0 27		-0 27	13 08
4 75	1981 3	42 57		42 57	3 35		3 35	-28 89		-28 89	0.04		0 04	12 72
5.25	1976 6	42 01		42 01	3 31		3 31	-28 55		-28 55	-0 02		-0 02	12 69
5 75	1972 0	41 60	42 27	41 94	3 31	3 33	3 32	-28 73	- 28 67	-28 70	0 10	0 05	0 07	12 64
6 25	1968.3	42 52		42.52	3.09		3 09	-28 49		-28 49	-0 52		-0 52	13 76
6 75	1964 2	41 68		41 68	3 23		3 23	-28 22		-28 22	-0 16		-0 16	12 92
7 25	1962.1	41 41		41 41	3 19		3 19	-28.60		-28 60	0 14		0 14	12 99
7.75	1958 4	41 48		41 48	3 23		3 23	-28.42		-28 42	-0.10		-0 10	12 86
8.25	1954 4	41 98		41 98	3 01		3 01	-28 50		-28 50	-0.75		-0 75	13 93
8.75	1951 2	42 89		42.89	3 08		3.08	-28 37		-28 37	-0.48		-0 48	13 93
9 25	1947 5	42 92		42.92	3 09		3 09	-28.53		-28 53	-0 64		-0 64	13 90
9.75	1942 7	42 68		42 68	3 31		3 31	-28 40		-28 40	0 10		0 10	12 91
10.25	1938 5	42.72	42 35	42 54	3 31	3 29	3 30	-28 34	- 28 10	-28 22	-0 07	-0.17	-0 12	12 89
10 75	1935 1	41 70		41 70	3 21		3 21	-28 22		-28 22	-0 25		-0 25	12 99
11 25	1928.6	42 90		42 90	3.27		3 27	-28 28		-28.28	0 01		0 01	13 12

11.75	1916 1	42 18		42 18	3 29		3 29	-28 38		-28 38	-0.13		-0 13	12 83
12 25	1906 5	43 20		43 20	3 31		3.31	-28 28		-28.28	0 17		0 17	13 04
12.75	1900 3	43.16		43 16	3.23		3 23	-28 36		-28 36	-0 11		-0 11	13 34
13.25	1894 6	41.37		41.37	3.13		3 13	-28 43		-28 43	0.07		0 07	13 21
13 75	1888 5	43 11		43 11	3 20		3 20	-28.34		-28.34	-0 16		-0 16	13.49
14 25	1881.3	43 40		43 40	3 21		3 21	-28.39		-28 39	0 12		0 12	13 50
15 00	1868 2	45 24		45 24	3.40		3 40	-28 16		-28 16	0 07		0 07	13 31
15 75	1862 2	38 41	43 35	40.88	2 78	3 11	2.94	-28 54	-28 3	-28.46	0.21	0 43	0 32	13 89
16.25	1856 1	41 98		41 98	3 22		3 22	-28.44		-28.44	0 00		0 00	13 04
16 75	1852 2	40 27		40 27	2 93		2 93	-28 39		-28 39	-0 30		-0.30	13 76
17.25	1844 6	43 57		43 57	3 26		3 26	-28.48		-28.48	-0.11		-0 11	13 36
17 75	1839 7	44 18		44 18	3 11		3 11	-28 43		-28 43	-0 45		-0 45	14 21
18.25	1833 0	43 78		43 78	3 36		3 36	-28 56		-28 56	0.06		0 06	13 01
18 75	1827 3	43 19		43 19	2 76		2.76	-28.51		-28 51	-0.95		-0.95	15 67
19 25	1821 1	41.69		41.69	3 03		3 03	-28 42		-28 42	0 06		0 06	13 75
19 75	1815 0	42 02		42 02	2 88		2 88	-28 33		-28 33	-0 72		-0 72	14 59
20.25	1807 5	42 11		42 11	2 82		2 82	-28 43		-28 43	-0 84		-0.84	14 95
20 75	1801 9	41 69	42.14	41.92	3 14	3 16	3 15	-28.60	-28 6	-28 61	0 06	-0 33	-0 13	13.31
21 25	1796 8	42 74		42 74	3 26		3 26	-28 47		-28 47	-0 03		-0 03	13 12
21 75	1790 5	41.91		41.91	3.07		3 07	-28.48		-28 48	-0 58		-0 58	13 63
22.25	1784.8	41.76		41 76	3 12		3 12	-28 27		-28 27	-0 30		-0 30	13 40
22 75	1779 0	40 26		40 26	3 09		3 09	-28 61		-28 61	-0 48		-0 48	13 01
23 25	1772 5	41 58		41 58	3 13		3 13	-28 50		-28 50	-0.42		-0 42	13 27
23 75	1765 9	38 88		38 88	2 98		2 98	-28 75		-28 75	-0 21		-0 21	13 04
24 25	1759 9	41 74		41 74	3 22		3 22	-28 62		-28 62	-0 35		-0 35	12 98
24 75	1753 0	41.17		41 17	3 16		3 16	-28 51		-28 51	-0 14		-0 14	13.02
25 25	1746 5	42 47		42.47	3 15		3 15	-28.53		-28 53	-0 70		-0 70	13 49
25 75	1739 4	43.00	44.52	43 76	3 02	3.24	3 13	-28 12	-28.5	-28 33	-0 46	-0 50	-0 48	13 98
26 25	1735 6	43 85		43 85	3 25		3 25	-28 43		-28 43	-0 42		-0 42	13 50
26.75	1728.3	42.23		42 23	2 96		2 96	-28.55		-28 55	-0 50		-0 50	14 29

GSL1 RC-1
Coring Date: 25-Mar-07
Organic Carbon and Nitrogen Elemental and Stable Isotope Geochemistry

Midpoint Depth (cm)	*Year (AD)*	*C_{org} (%)*	*Rpt*	*Avg*	*N (%)*	*Rpt*	*Avg*	*Corrected N (%)*	*$\delta^{13}C_{org}$ (‰)*	*Rpt*	*Avg*	*$\delta^{15}N$ (‰)*	*Rpt*	*Avg*	*C/N*
20 25	1801 88	42 65		42 65	2 69		2 69	2.69	-28 7		-28.7	-0 51		-0.51	15 9
20 75	1796 81	41 65		41.65	2 92		2 92	2 92	-29 6		-29.6	0 18		0 18	14 3
21 25	1790 55	40 65		40 65	2 92		2 92	2 92	-28 7		-28 7	0 38		0 38	13 9
21 75	1784 80	40 62		40 62	2 82		2 82	2 82	-28 7		-28 7	0 20		0 20	14 4
22.25	1778 96	43.30		43 30	2 99		2.99	2 99	-29.5		-29 5	0.44		0 44	14 5
22 75	1772.51	41 62		41 62	2 97		2 97	2 97	-28 5		-28.5	0 18		0 18	14 0
23.25	1765 87	41 96		41 96	2.87		2 87	2 87	-28 6		-28.6	0.33		0.33	14 6
23 75	1759 86	43 21		43 21	2.97		2.97	2 97	-28 3		-28 3	0 08		0 08	14 6
24 25	1752.99	43 47		43 47	3 03		3 03	3 03	-28 5		-28 5	0.29		0 29	14 4
24 75	1746.53	41 91		41 91	2 87		2 87	2 87	-28 6		-28 6	0 06		0 06	14 6
25 25	1739 36	43 52	40 94	42 23	3 08	2 64	2 86	2 75	-28 5	-28 5	-28 5	0 44	-0 37	0 03	15 4
25 75	1735 55	42 06		42 06	2 89		2.89	2 89	-28 5		-28 5	0 25		0 25	14 6
26 25	1728 33	41 98		41 98	2 90		2.90	2 90	-28 6		-28 6	0 29		0 29	14 5
26 75	1720 82	42 85		42 85	2 85		2 85	2 85	-28 5		-28 5	-0 30		-0 30	15 0
27 25	1714 53	42 38		42 38	2 98		2 98	2 98	-28 6		-28 6	0 34		0 34	14 2
27.75	1708 25	42 21		42 21	2 96		2 96	2 96	-28 6		-28 6	-0 02		-0 02	14 3
28 25	1701 96	43.66		43 66	3 00		3 00	3 00	-28 5		-28 5	0 17		0 17	14 6
28 75	1695 68	42 22		42 22	2 96		2 96	2 96	-28 7		-28 7	0 20		0 20	14 3
29.25	1689.40	42 16		42 16	2 77		2 77	2 77	-28 6		-28 6	-0 33		-0 33	15 2

29 75	1683 11	42 52	42 77	42.64	2 91	3 03	2 97	3 00	-28 5	-28.5	-28 5	-0.23	-0 05	-0 14	14 2
30 25	1676 83	43 05		43.05	3.06		3.06	3 06	-28.6		-28.6	0 34		0 34	14 0
30 75	1670 54	41.69		41.69	2.83		2 83	2 83	-28.5		-28 5	0.24		0.24	14 7
31 25	1664 26	42 28		42 28	2 84		2 84	2 84	-28.6		-28 6	0.05		0 05	14 9
31 75	1657 98	41 87		41 87	2 73		2 73	2.73	-28 7		-28.7	-0.36		-0 36	15 3
32 25	1651 69	43 10		43 10	3 00		3 00	3 00	-28 7		-28 7	0 17		0 17	14.4
32 75	1645 41	42.89		42.89	2 81		2 81	2 81	-28 7		-28 7	-0 03		-0 03	15.3
33.25	1639.12	42.61		42 61	3 03		3 03	3 03	-28 7		-28.7	0.18		0.18	14 1
33 75	1632 84	41 64		41.64	2.93		2 93	2 93	-28 8		-28 8	0 13		0 13	14 2
34 25	1626 56	43 31	42.72	43 01	2.87	2.97	2.92	2 94	-28 8	-28.9	-28.9	0.09	0 07	0 08	14.6
34 75	1620 27	40 89		40 89	2 81		2 81	2.81	-28 9		-28 9	0.28		0 28	14 6
35 25	1613 99	40 50		40 50	2 84		2 84	2 84	-29 0		-29 0	0 09		0 09	14 3
35.75	1607.70	43 69		43.69	3 03		3 03	3 03	-29 0		-29 0	0 35		0.35	14 4
36 25	1601 42	43.75		43 75	2 81		2 81	2 81	-29 0		-29.0	-1.13		-1 13	15 6
36 75	1595.14	43 41		43 41	3 03		3 03	3 03	-28 9		-28.9	-0 19		-0 19	14 3
37.25	1588 85	41 29		41 29	2.83		2.83	2.83	-29.0		-29 0	-0 21		-0 21	14 6
37.75	1582 57	41.65		41 65	2 73		2.73	2 73	-29 1		-29 1	-0 30		-0 30	15 3
38 25	1576 28	43.23	42 68	42.96	2.83	3.04	2.93	2 99	-29 0	-28 9	-29 0	-0.65	0.28	-0 19	14.4
38.75	1570 00	43.20		43 20	2 90		2 90	2 90	-29 2		-29 2	-0 71		-0 71	14 9
39 25	1563 72	42 16		42 16	2.93		2 93	2 93	-29 3		-29 3	-0 32		-0 32	14 4
39 75	1557 43	41 21		41 21	2 63		2 63	2 63	-29 5		-29 5	-0 45		-0 45	15 7
40 25	1551 15	41 88		41 88	2 89		2 89	2 89	-29 4		-29 4	-0 53		-0 53	14 5
40 75	1544 86	39 72		39 72	2 71		2 71	2 71	-29 2		-29 2	-0 50		-0 50	14 7
41 25	1538 58	41 46		41 46	2 98		2.98	2 98	-29 2		-29 2	-0 18		-0 18	13 9
41 75	1532 29	43 30		43 30	2 73		2 73	2 73	-29 8		-29 8	-0 82		-0 82	15 9
42 25	1526.01	42 71		42 71	2 80		2 80	2 80	-29 7		-29 7	-0 59		-0 59	15 2
42 75	1519 73	42 06		42 06	2 80		2 80	2 80	-29 5		-29 5	-0 47		-0 47	15 0

43.25	1513.44	41 43	41 30	41.36	2.85	2 82	2 83	2 83	-29 4	-29 4	-29.4	-0.27	-0.34	-0 31	14.6
43 75	1507 16	40 71		40 71	2.68		2 68	2 68	-29.6		-29 6	-0.66		-0 66	15 2
44 25	1500 87	41 16		41 16	2.90		2 90	2 90	-29 4		-29.4	-0 30		-0 30	14 2
44.75	1494 59	40 01		40 01	2 81		2.81	2 81	-29 4		-29 4	-0 42		-0.42	14 2
45.25	1488 31	41 51		41 51	2 98		2 98	2 98	-30 2		-30 2	-0 02		-0 02	13 9
45.75	1482 02	40 21		40 21	2 73		2 73	2 73	-29 4		-29.4	-0 04		-0 04	14 7
46 25	1475 74	38 69		38 69	2 63		2 63	2 63	-29 7		-29 7	-0.46		-0 46	14 7
46.75	1469 45	35.83		35 83	2.32		2.32	2 32	-29 4		-29 4	-0.43		-0.43	15.5
47.25	1463 17	40 12		40 12	2 85		2.85	2 85	-29.5		-29 5	-0 24		-0 24	14 1
47 75	1456 89	39.15		39 15	2 53		2 53	2 53	-29 3		-29 3	-1 12		-1 12	15 5
48 25	1450 60	39 42	38 33	38 87	2 71	2 68	2 70	2 69	-29 4	-29 4	-29 4	-0.05	-0.37	-0 21	14 5
48 75	1444 32	33 99		33 99	2 43		2 43	2 43	-29.4		-29 4	0.00		0 00	14.0
49.25	1438 03	38 67		38.67	2 61		2 61	2 61	-29 2		-29 2	-0 39		-0 39	14 8
49 75	1431 75	43 92		43 92	2.90		2 90	2 90	-29 3		-29 3	-0 29		-0.29	15 2
50.25	1425.47	42 72		42 72	2 90		2 90	2 90	-29 3		-29.3	-0 63		-0.63	14 7
50 75	1419 18	36.59		36.59	2 59		2 59	2 59	-29 5		-29 5	-0.01		-0 01	14.1
51 25	1412 90	37 47		37 47	2 53		2 53	2 53	-29 4		-29 4	-0 40		-0 40	14 8
51 75	1406 61	39 16		39 16	2.79		2.79	2 79	-29 6		-29 6	-0.13		-0 13	14 1
52.25	1400.33	37 95		37 95	2 69		2.69	2 69	-29 5		-29 5	-0 04		-0 04	14 1
52 75	1394.05	36 51	36 25	36 38	2.55	2.47	2 51	2.49	-29 4	-29.3	-29 4	-0.39	-0 36	-0 38	14 6
53 25	1387 76	35 60		35 60	2.41		2 41	2 41	-29 3		-29 3	-0 60		-0 60	14 8
53 75	1381 48	36.63		36 63	2.64		2.64	2 64	-29 1		-29.1	-0.23		-0 23	13 9
54 25	1375 19	33.39		33 39	2 15		2 15	2 15	-29 3		-29 3	-0 82		-0 82	15 5
54 75	1368 91	36 14		36 14	2 43		2 43	2 43	-29 4		-29 4	-0 42		-0 42	14 9
55 25	1362 63	31 42		31 42	2 30		2 30	2 30	-29 3		-29 3	-0 11		-0 11	13 7
55 75	1356.34	38 10		38 10	2 54		2.54	2 54	-29 4		-29 4	-0 94		-0 94	15 0
56 25	1350 06	37 20		37 20	2 67		2 67	2 67	-29 4		-29 4	-0 29		-0 29	13 9

56.75	1343 77	39 84		39 84	2 79		2 79	2 79	-29 5		-29 5	-0 32		-0 32	14 3
57.25	1337 49	38.02		38.02	2.64		2.64	2 64	-29 3		-29.3	-0 03		-0.03	14.4
57.75	1331 21	42.06	41.30	41.68	3 03	2.89	2 96	2 92	-29 4	-29.4	-29 4	-0.06	-0.58	-0.32	14.3
58.25	1324.92	34.74		34 74	2.46		2.46	2 46	-29 2		-29.2	0.11		0 11	14 1
58 75	1318 64	36.70		36 70	2 60		2 60	2 60	-29 4		-29 4	-0 14		-0 14	14 1
59.25	1312 35	33 33		33 33	2 42		2 42	2 42	-29 4		-29 4	-0.36		-0 36	13 7
59.75	1306.07	35 08		35.08	2.55		2 55	2 55	-29 3		-29 3	-0.16		-0.16	13.7
60 25	1299 78	35 45		35 45	2.48		2 48	2 48	-29 4		-29.4	-0.12		-0.12	14.3
60 75	1293 50	34 71		34 71	2 43		2 43	2 43	-29 3		-29 3	-0.19		-0 19	14 3
61 25	1287 22	30 55		30 55	2 16		2 16	2 16	-29 2		-29 2	-0 41		-0 41	14 1
61 75	1280 93	31 38		31 38	2 23		2 23	2 23	-29 2		-29 2	-0 21		-0 21	14 1
62 25	1274 65	33 18		33 18	2 28		2 28	2 28	-29 0		-29 0	-0.34		-0 34	14 6
62 75	1268.36	32 21		32 21	2 40		2.40	2.40	-29 3		-29 3	-0.02		-0 02	13 4
64.25	1249 51	30 44		30 44	2 27		2 27	2 27	-29 1		-29.1	-0 08		-0 08	13.4
64 75	1243.23	34 27		34.27	2 46		2 46	2 46	-29 4		-29 4	-0.32		-0 32	13 9
65.25	1236 94	33 27		33 27	2 43		2.43	2 43	-29 4		-29.4	-0.06		-0 06	13 7
65 75	1230 66	31 23		31.23	2 12		2.12	2.12	-29.4		-29.4	-0.53		-0 53	14 7
66.25	1224 38	25 52		25 52	1 85		1.85	1.85	-29 3		-29.3	0 08		0.08	13.8
66.75	1218 09	23.13		23.13	1 73		1 73	1 73	-29.0		-29 0	0.08		0 08	13 4
67.25	1211 81	24.19		24 19	1.77		1.77	1.77	-29.2		-29.2	-0 25		-0.25	13.7
67 75	1205 52	28.88		28 88	2.07		2.07	2 07	-29.3		-29 3	-0 11		-0 11	13 9
68 25	1199 24	27 51	26 81	27 16	2.10	2 08	2.09	2 05	-29 4	-29.3	-29.3	-0 01	0 12	0 05	13.3
68.75	1192 96	25 80		25 80	1.89		1.89	1.85	-29 2		-29 2	-0 20		-0.20	14 0
69 25	1186.67	25 97		25 97	1 91		1 91	1 87	-29 1		-29 1	0 12		0 12	13 9
69 75	1180 39	16 87		16 87	1 32		1 32	1.28	-28 7		-28 7	0.01		0.01	13 2
70 25	1174 10	14.20		14 20	1 11		1 11	1 07	-28 8		-28 8	-0 23		-0 23	13 3
70.75	1167 82	10.11		10 11	0 74		0 74	0 70	-28 2		-28.2	-0.03		-0 03	14 4

71 25	1161.54	5 52		5 52	0 44		0 44	0 40	-27 7		-27 7	0 54		0.54	13.7
71 75	1155 25	6 67		6 67	0 53		0 53	0 51	-28 0		-28.0	0 19		0 19	13 0
72 25	1148 97	4 96		4 96	0.40		0.40	0 39	-27 7		-27 7	0.64		0.64	12.8
72.75	1142.68	4 55		4.55	0.36		0 36	0 35	-27 4		-27 4	0.53		0 53	13 2
73 25	1136 40	3 54	3.48	3.51	0 28	0.28	0 28	0 27	-27 2	-27.0	-27 1	0 88	0 99	0 94	13 2
73 75	1130 12	3 22		3 22	0.27		0 27	0 25	-27.2		-27.2	1.22		1 22	12.7
74 25	1123 83	2 75		2 75	0 22		0.22	0 20	-27 0		-27 0	1 23		1 23	13 7
74 75	1117.55	2.67		2.67	0.21		0.21	0.20	-26.7		-26.7	1.34		1 34	13 7
75 25	1111 26	2 81		2 81	0 22		0 22	0 21	-27.1		-27.1	0.96		0 96	13 4
75 75	1104 98	2 75		2.75	0 21		0.21	0 20	-27.0		-27 0	1.10		1 10	13 7
76.25	1098 70	2.17		2 17	0 17		0 17	0 16	-26 9		-26.9	1 44		1 44	13 8
76 75	1092 41	2 25		2 25	0 17		0 17	0 15	-26 9		-26 9	1 30		1 30	14 9
77.25	1086 13	2 14		2 14	0 16		0.16	0 14	-26 8		-26 8	1 65		1 65	14 8
77 75	1079 84	1 99		1 99	0 15		0 15	0 14	-26 5		-26.5	1.51		1 51	14 3
78 25	1073.56	2.04	1 99	2 01	0 15	0 15	0 15	0 14	-26.2	-26 4	-26 3	1.43	1 53	1 48	14 8
78.75	1067 27	1 77		1 77	0 14		0 14	0 13	-26 6		-26 6	1.57		1.57	14 2
79 25	1060 99	1 53		1 53	0 12		0 12	0 11	-26 2		-26 2	1.71		1 71	14 3
79 75	1054 71	1 62		1 62	0 13		0 13	0.11	-26 3		-26.3	1.58		1 58	14 3
80 25	1048 42	1.10		1 10	0.09		0 09	0 07	-26 5		-26 5	1.64		1 64	15 2
80 75	1042 14	1 54		1.54	0 12		0 12	0 11	-26 0		-26 0	1.98		1 98	13 9
81 25	1035 85	1 49		1.49	0 12		0 12	0 10	-26 0		-26.0	1 76		1 76	14 5
81 75	1029.57	1 29		1 29	0 09		0.09	0 08	-26.1		-26.1	1 52		1.52	16 2
82 25	1023 29	1.36		1 36	0.10		0.10	0.08	-26 2		-26.2	1.60		1 60	16 8
82.75	1017 00	1 73	1 64	1 69	0 11	0 11	0 11	0 10	-26.5	-26.3	-26.4	2.00	1 61	1 81	17 5
83 25	1010 72	1 89		1 89	0 14		0 14	0 13	-26 6		-26 6	1.65		1 65	15 1
83 75	1004 43	1.77		1 77	0 14		0 14	0 13	-26 4		-26 4	1 57		1 57	14 0
84 25	998 15	1.95		1 95	0 15		0.15	0.13	-26 6		-26.6	1.54		1 54	14 6

84 75	991 87	2 12		2 12	0 15		0 15	0 14	-26 5		-26 5	1.49		1 49	15 6
85 25	985 58	1 69		1.69	0 14		0.14	0 12	-26 6		-26 6	1 86		1 86	13 6
85 75	979 30	1 60		1 60	0 12		0 12	0 11	-26.2		-26 2	1 65		1 65	14 7
86 25	973.01	1.73		1 73	0 13		0 13	0 11	-26 9		-26 9	1 67		1 67	15 6
86 75	966 73	1 77		1 77	0 13		0 13	0 12	-26 5		-26 5	1.76		1 76	15 0
87 25	960.45	1 65	1 62	1 64	0.10	0 10	0.10	0 09	-26 7	-26.7	-26 7	1 21	1 48	1 34	18 9
87.75	954 16	1 77		1 77	0 12		0 12	0.10	-26 5		-26 5	1.63		1 63	17 5
88 25	947 88	1.15		1 15	0.08		0.08	0 07	-26.5		-26.5	1.73		1.73	17 4
88 75	941 59	1 41		1 41	0 09		0 09	0 08	-26 2		-26 2	1.47		1 47	18 2
89 25	935 31	1 85		1 85	0 11		0 11	0.10	-26 8		-26 8	1.27		1.27	18.9
89 75	929 03	1 67		1.67	0.14		0 14	0 12	-26 5		-26 5	1 96		1 96	13 7
90 25	922 74	1 28		1 28	0 10		0 10	0 08	-26 3		-26.3	1.74		1 74	15 5
90.75	916 46	1 21		1 21	0 09		0.09	0 07	-26.3		-26 3	1.40		1 40	16 2
91 25	910 17	1 52		1.52	0.13		0.13	0 11	-26.6		-26 6	2 06		2 06	13 8
91.75	903 89	1 52	1 55	1 54	0 11	0 11	0.11	0 10	-26 3	-26 2	-26 2	1 84	2 02	1 93	15 9
92 25	897 61	1 59		1 59	0 12		0 12	0 11	-26 6		-26 6	1 83		1 83	14 5
92 75	891 32	1.44		1 44	0.12		0 12	0 10	-26 2		-26 2	2.23		2 23	13 7
93 25	885 04	1 60		1 60	0 12		0 12	0 11	-26.3		-26.3	1.96		1 96	14.4
93 75	878 75	1 64		1.64	0 13		0 13	0 11	-26 4		-26 4	1.78		1 78	14 7
94.25	872 47	1 59		1.59	0.12		0.12	0.11	-26 5		-26.5	2.04		2 04	14 5
94 75	866 19	1 53		1.53	0.12		0 12	0 10	-26 3		-26 3	1 96		1 96	15 2
95 25	859 90	1 07		1 07	0.07		0 07	0.06	-26 4		-26 4	1 44		1 44	17 5
95 75	853 62	1 25		1.25	0.09		0 09	0 07	-26 3		-26.3	1 78		1 78	16 7
96 25	847 33	1.46	1 59	1 53	0.10	0 11	0 11	0 09	-26 3	-26 2	-26 2	1.64	1 94	1 79	16 7
96.75	841 05	1 73		1 73	0 12		0 12	0 11	-26 4		-26 4	1 78		1 78	16.3
97.25	834 76	1 41		1 41	0 09		0 09	0 08	-26 4		-26.4	1 54		1 54	18 5
97 75	828.48	1.60		1 60	0 11		0 11	0 10	-26 1		-26 1	1 51		1 51	16 5

98 25	822 20	1 49		1 49	0 09		0 09	0 08	-26 4		-26.4	1 59		1 59	19 1
98.75	815 91	1.32		1.32	0 09		0 09	0 07	-26 5		-26 5	1.60		1.60	18 6
99 25	809 63	1.69		1 69	0.11		0 11	0 10	-26.4		-26 4	1.57		1 57	17.2
99 75	803.34	1 89		1.89	0.14		0 14	0 13	-26 9		-26 9	1 52		1 52	15.0

Appendix F: Cellulose Oxygen Isotope Results

SD34 RC-2

Date Cored: 24-Mar-07

Cellulose Inferred Oxygen Isotope Analysis

Midpoint Depth (cm)	*Year (AD)*	*Result (VSMOW)*	*Rpt*	*Avg*	*$\delta^{18}O_{lw}$ (‰)*	*5-pt Run Mean*
4 25	1993 25	11 81		11 81	-15.75	-15.75
4 75	1991 35	9 94		9 94	-16.65	-17 57
5 25	1989 36	10 91		10 91	-17 73	-17 59
5 75	1987 29	8 47		8 47	-18 20	-18 22
6 25	1984 97	8 48		8 48	-18 98	-18.64
6 75	1982.16	8 53		8 53	-19 19	-19.16
7 25	1980 00	7 81		7 81	-19 28	-19.12
7 75	1977 50	8 20		8 20	-19 22	-19.14
8 25	1974 32	8 71		8 71	-19 04	-19 19
8 75	1970 47	8 54	8 19	8 37	-19 24	-19.25
9 25	1966.88	7 57		7 57	-18 76	-18 76
9 75	1961 34	10 20		10 20	-18 83	-18 90
10 25	1956 42	8 16		8 16	-17 48	-18 08
10 75	1951 71	11 73		11 73	-18 10	-18.30
11 25	1945 63	8 28		8 28	-18 10	-18 19
11 75	1938 12	8 16		8 16	-19 27	-18.59
12 25	1930 54	8 12		8 12	-19 08	-18.45
12 75	1925 71	8 89		8 89	-19 00	-19 10
13 25	1918 68	8 39		8 39	-18 67	-18 93
13 75	1912 12	9 42	8 89	9 15	-18 91	-18.83
14 25	1906 79	8 15		8 15	-18 73	-18 83
14 75	1899 39	8 95		8 95	-18 83	-18 81
15 25	1893 08	8 85		8 85	-18 50	-18 70
15 75	1886 73	9 16		9 16	-18 78	-18 70
16 25	1878 11	8 07		8 07	-19 00	-18.84
16 75	1872 71	8 19		8 19	-18 98	-18 83
17 25	1866.63	9 20		9 20	-18 54	-18 78
17 75	1859 06	9 44		9.44	-18 40	-18 67
18 25	1852 82	8 62		8 62	-18.20	-18 77
18 75	1845.98	9 74	9 92	9 83	-18.15	-18.43
19 25	1837 99	9 58		9 58	-16 89	-18 22
19 75	1829 59	12 49		12 49	-16 74	-18.13
20.25	1822 79	10 29		10 29	-16 89	-17 38
20 75	1814 65	9 13		9 13	-17 87	-16 97
21 25	1807 08	9 47		9 47	-17 28	-17.14
21 75	1797 57	12 11		12.11	-17 34	-17.32
22 25	1789 71	8 95		8 95	-16.63	-16 83
22 75	1781 57	12 28	11.00	11.64	-17 20	-17 52

23 25	1773 96	10 35		10 35	-16 20	-17 26
23.75	1764 39	12 03		12 03	-17 07	-16 98
24 25	1756 25	8 97		8 97	-16 81	-16 77
24 75	1745 98	11 14		11 14	-18 06	-16.79
25 25	1736 17	8 19		8 19	-18 71	-16 78
25 75	1728 66	6 98		6 98	-19 65	-16 90
26 25	1718 86	8 24		8 24	-19 61	-17 38
26.75	1709 29	8 30		8 30	-19 14	-18 03
27 25	1699 53	8 44		8 44	-19 42	-18 77
27 75	1690 43	7 36		7 36	-18 79	-18 90
28 25	1680 23	10 26		10 26	-19 27	-19 43
28 75	1670 35	6 63	7 24	6 93	-19 24	-19.59
29 25	1655 57	7 46		7 46	-19 95	-18 95
29.75	1648 23	8 07		8 07	-19.86	-19.20
30.25	1636 15	7 23		7 23	-20 08	-19.21
30 75	1627 49	6 78		6 78	-20 32	-19 45
31 25	1617 42	7 33		7 33	-19 89	-19 28
31 75	1607 79	8 54		8 54	-18 89	-20 02
32 25	1598 25	9 87		9 87	-18 25	-20 05
32 75	1587 11	9 30		9 30	-17 39	-20 06
33 25	1576 78	11 21		11 21	-17 52	-19.85
33 75	1566 32	9 28	9 67	9 47	-17 81	-19 50
34 25	1557 67	8 39		8 39	-18 73	-19 10
34 75	1546 52	8 36		8.36	-19 08	-18.24
35 25	1537 00	8 40		8 40	-19 35	-17.82
35 75	1526 04	7 56		7 56	-19 22	-17 55
36 25	1515 19	8 78		8 78	-19 08	-17 90
36 75	1506 16	8 82		8 82	-19 26	-18 13
37 25	1496 39	7 01		7 01	-19 19	-18 82
37 75	1489 12	8 99		8 99	-19.24	-19.28
38 25	1479 31	8 67		8 67	-19 02	-19 17
38 75	1469 49	7 93	7.46	7 70	-19 02	-19.08
39 25	1459 67	8 97		8 97	-18 83	-19 34
39.75	1449 86	9 26		9 26	-18 46	-19 23
40.25	1440 04	8 85		8 85	-18 51	-19 01
40 75	1430 23	8 81		8 81	-18 78	-19 22
41 25	1420 41	8 41		8 41	-18.07	-19 37
41 75	1410 59	11 04		11 04	-18 07	-18 89
42 25	1400 78	8 84		8 84	-17 89	-18 82
42 75	1390 96	8 96		8 96	-18 87	-18 78
43 25	1381 14	8 01		8 01	-19 50	-18 51
43 75	1371.33	6 93	6 88	6 90	-19 75	-18 62
44 25	1361 51	8 17		8 17	-19.12	-18 22
44 75	1351.70	9 97		9 97	-18 57	-18.30
45 25	1341 88	8 60		8 60	-18 62	-18 28
45 75	1332 06	8 00		8 00	-19.16	-18 43

46.25	1322 25	8 31		8 31	-19 15	-18 73
47 75	1302 62	8 64		8 64	-18 49	-19 44
48 25	1292 80	8 86		8 86	-19 02	-19 20
48 75	1282 98	9 46		9 46	-19 88	-19 06
49 25	1273 17	7 85	6 20	7 03	-20 87	-18 79
49 75	1263 35	6 42		6 42	-21 24	-18 86
50 25	1253 53	5 87		5 87	-20 36	-18 77
50 75	1243 72	8 90		8 90	-20 48	-18 99
51 25	1233.90	6 06		6 06	-20 60	-18 82
51 75	1224 09	5 52		5 52	-21 50	-18 97
52 25	1214 27	6 12		6 12	-21 48	-19 26
52 75	1204 45	6 12		6 12	-21 22	-19 74
53.25	1194 64	6 32		6 32	-20.58	-20 24
53 75	1184.82	8 09		8 09	-20.97	-20.17
54 25	1175 01	4 74	5 12	4 93	-20 19	-20 39
54 75	1165 19	8 71		8.71	-19.76	-20.58
55 25	1155 37	9 42		9 42	-18 18	-20 56
55 75	1145 56	9 81		9 81	-18 63	-20 52
56.25	1135 74	7 31		7 31	-19 45	-21 17
56 75	1125 92	6 89		6 89	-20 57	-20 72
57 25	1116 11	6 36		6 36	-19 49	-20 88
57 75	1106 29	10 64		10 64	-19 61	-20 82
58 25	1096 48	6 52		6 52	-18 57	-20 26
58 75	1086 66	9 56		9 56	-19 22	-19 47
59 25	1076 84	8 03	9 25	8 64	-18 18	-19 04
59 75	1067 03	9 73		9 73	-18 08	-18 74
60 25	1057 21	9 87		9 87	-17 33	-19 14
60.75	1047 39	10 95		10 95	-18 30	-19 67
61 25	1037 58	6 75		6 75	-18 52	-19 54
61 75	1027.76	9 19		9 19	-19 73	-20 20
62 25	1017 95	7 22		7 22	-19 33	-19 74
62 75	1008 13	7 98		7 98	-19 11	-19 42
63 25	998 31	9 85		9 85	-18 58	-18 95
63 75	988 50	8 86		8 86	-18 95	-19 03
64 25	978 68	7 18	6 48	6 83	-20.29	-18.33
64.75	968 87	5 73		5 73	-21.15	-18 00
65 25	959 05	6 23		6 23	-20 85	-18.33
65 75	949 23	7 74		7 74	-20 69	-18 67
66 25	939 42	6 22		6 22	-19 63	-19 38
66 75	929 60	9 50		9 50	-19 04	-19 80
67 25	919 78	9 56		9 56	-19 29	-19 54
67 75	909 97	5 43		5 43	-20 11	-19.39
68 25	900 15	6 98		6 98	-21 07	-19 57
68 75	890 34	6 63		6 63	-20 74	-19 21
69 25	880 52	5 94	6 92	6 43	-20.26	-19.85
69 75	870 70	8 46		8 46	-20 04	-21 15

70 25	860 89	7 29		7 29	-20 34	-21 28
70 75	851 07	5 52		5 52	-20 51	-21 48
71 25	841 26	7 95		7 95	-20 33	-20 79
71 75	831 44	7 85		7 85	-19 43	-19 86
72 25	821 62	8 59	7 99	8 29	-19 77	-20 09
72 75	811 81	6 88		6.88	-19 43	-20 30
73 25	801 99	8 91		8 91	-20 15	-20 12
73 75	792 17	6 08		6 08	-20 38	-20 75
74 25	782 36	6 16		6 16	-20 52	-21 48
74 75	772 54	8 48		8 48	-19 77	-18 99
75 25	762 73	8 40		8 40	-19 07	-19 068

GSL1 KB1 and RC1
Date
Cored: 25-Mar-07
Cellulose Inferred Oxygen Isotope Analysis

Midpoint Depth (cm)	*Year (AD)*	*Result (VSMOW)*	*Rpt*	*Avg*	*$\delta^{18}O_{lw}$ (‰)*
0 25	2007 2	17 61		17 61	-10 1029
3 75	1985 9	12 50		12 50	-15 075
6.75	1962.1	10 43	8 96	9 70	-17 804
9 75	1938 5	10 52		10 52	-17 0044
12.75	1894.6	10 21		10 21	-17 3089
16 25	1852 2	10 73		10 73	-16 7996
19 25	1815 0	11 49		11 49	-16 0579
22 25	1779 0	10 30	8 79	9 55	-17 947
31 25	1664 3	8 45	9.13	8 79	-18 687
34 25	1626 6	9 67		9 67	-17 7693
37 25	1588 9	9 73		9 73	-17 0398
40.25	1551 1	9 73		9 73	-16 8551
43 25	1513 4	10 48		10 48	-17 1654
45.75	1482 0	10 67	8 35	9 35	-18 1420
48 75	1444.3	10 35		10 35	-18 6886
51 75	1406 6	9 14		9 14	-18 3906
54 75	1368 9	8 79		8 79	-19 1798
57.25	1337 5	9 09		9 09	-19 2718
60 25	1299 8	8 28	7 42	7 85	-19 6011
63.25	1262 1	8 19		8 19	-20 2018
66 25	1224.4	6 42		6 42	-21 9453
69 25	1186 7	7 23		7 23	-24 1497
72 25	1149 0	5 44		5 44	-20 2181
75 25	1111 3	3 17		3 17	-22 2558
78.25	1073 6	7 22		7 22	-21 1471
81 25	1035.9	5 12		5 12	-21 5548
84.25	998 2	6 26		6 26	-21 5593
87 25	960 4	5 84		5 84	-21 7833
90 25	922 7	5 84		5 84	-22 0677
92 75	891 3	5 61		5 61	-21 3653
96 75	841 0	5 31		5 31	-27 2374
99 75	803 3	6 04		6 04	-27 2374